EDITORIAL STAFF

R. J. McKay, Chairman, Publication Committee

Cecil V. King, Editor

Norman Hackerman, Technical Editor

Ruth G. Sterns, Managing Editor

U. B. Thomas, News Editor

Natalie Michalski, Assistant Editor

Eleanor Blair, Assistant Editor

DIVISIONAL EDITORS

W. C. Vosburgh, Battery

J. E. Draley, Corrosion

John J. Chapman, Electric Insulation

Abner Brenner, Electrodeposition

H. C. Froelich, Electronics

D. H. Baird, Electronics—Semiconductors

Sherlock Swann, Jr., Electro-Organic

John M. Blocher, Jr., Electrothermics and Metallurgy, I

A. U. Seybolt, Electrothermics and Metallurgy, II

W. C. Gardiner, Industrial Electrolytic

C. W. Tobias, Theoretical Electrochemistry

REGIONAL EDITORS

Howard T. Francis, Chicago

Joseph Schulein, Pacific Northwest

J. C. Schumacher, Los Angeles

G. W. Heise, Cleveland

G. H. Fetterley, Niagara Falls

Oliver Osborn, Houston

Earl A. Gulbransen, Pittsburgh

A. C. Holm, Canada

J. W. Cuthbertson, Great Britain

T. L. Rama Char, India

ADVERTISING OFFICE

Jack Bain, Advertising Manager
545 Fifth Avenue, New York 17, N. Y.

ECS OFFICERS

Norman Hackerman, President
University of Texas, Austin, Texas

Sherlock Swann, Jr., Vice-President
University of Illinois, Urbana, Ill.

W. C. Gardiner, Vice-President
Olin Mathieson Chemical Corp., Niagara Falls, N. Y.

R. A. Schaefer, Vice-President
Cleveland Graphite Bronze Div., Clevite Corp., Cleveland, Ohio

Lyle I. Gilbertson, Treasurer
Air Reduction Co., Murray Hill, N. J.

Henry B. Linford, Secretary
Columbia University, New York, N. Y.

Robert K. Shannon, Assistant Secretary
National Headquarters, The ECS, 1860 Broadway, New York 23, N. Y.

Journal of the Electrochemical Society

JUNE 1957 **VOL. 104 • NO. 6**

CONTENTS

Editorial

Inflation 123C

Technical Papers

Some Unusual Effects of Hydrogen in Corrosion Reactions. *J. E. Draley and W. E. Ruther* 329

Kinetics of the Oxidation of Chromium. *E. A. Gulbransen and K. F. Andrew* 334

Anodic Oxidation of Aluminum, Chromium, Hafnium, Niobium, Tantalum, Titanium, Vanadium, and Zirconium at Very Low Current Densities. *H. A. Johansen, G. B. Adams, Jr., and P. Van Rysselberghe* 339

Metal-Water Reactions, IV. Kinetics of the Reaction between Calcium and Water Vapor. *H. J. Svec and C. Apel* 346

Reaction of Zirconium with Water Vapor at Subatmospheric Pressures. *M. W. Mallett, W. M. Albrecht, and R. E. Bennett* 349

A New Commercial Process for Electrowinning Manganese. *M. C. Carosella and R. M. Fowler* 352

Effects of Various Polyvalent Metal Anion Additions to an Alkaline Magnesium Anodizing Bath. *W. McNeill and R. Wick* 356

Electric Moments of Certain Partially Fluorinated Esters. *J. B. Romans and T. D. Callinan* 359

The Thermoluminescence of CaF_2:Mn. *R. J. Ginther and R. D. Kirk* 365

Defect Structure and the Temperature Dependence of Hardness of an Intermetallic Compound. *J. H. Westbrook* 369

Preparation of Thorium Bismuth Dispersions from Electrolytic Thorium. *M. E. Sibert, M. A. Steinberg, and R. J. Teitel* 374

Measurements on Galvanic Cells Involving Solid Electrolytes. *K. Kiukkola and C. Wagner* 379

Technical Notes

Measurement of Ion and Water Transport across Membranes. *J. G. McKelvey, Jr., K. S. Spiegler, and M. R. J. Wyllie* 387

Anodic Behavior of Iron in Acid Solutions. *M. Stern and R. M. Roth* 390

Discussion Section 393

Current Affairs

Annual Report of the Board of Directors for 1956 ..... 125C

Annual Report of the Secretary for 1956 ..... 125C

Section News 126C
New Members 127C
ECS Membership Statistics 128C
Personals 129C
News Items 129C
Letter to the Editor 130C
Announcements from Publishers 132C
Book Reviews 133C
Meetings of Other Organizations 134C
Employment Situations 134C

Published monthly by The Electrochemical Society, Inc., from Manchester, N. H., **Executive Offices, Editorial Office** and **Circulation Dept.** at 1860 Broadway, New York 23, N. Y., **Advertising Office** at 545 Fifth Ave., New York, N. Y., combining the JOURNAL and TRANSACTIONS OF THE ELECTROCHEMICAL SOCIETY. Statements and opinions given in articles and papers in the JOURNAL OF THE ELECTROCHEMICAL SOCIETY are those of the contributors, and The Electrochemical Society assumes no responsibility for them. Nondeductible subscription to members $5.00; subscription to nonmembers $18.00. Single copies $1.25 to members, $1.75 to nonmembers.

Copyright 1957 by The Electrochemical Society, Inc.

Entered as second-class matter at the Post Office at Manchester, N. H., under the act of August 24, 1912.

FUTURE MEETINGS OF
The Electrochemical Society

Buffalo, October 6, 7, 8, 9, and 10, 1957

Headquarters at the Statler Hotel

Sessions will be scheduled on
Batteries, Corrosion, Electrodeposition (symposium on "Metal Powders"),
Electrodeposition–Corrosion (Joint Symposium on
"Corrosion of Electrodeposited Metals"),
Electronics (Semiconductors),
Electro-Organics, Electro-Organics–Theoretical Electrochemistry
(Joint Symposium), and Electrothermics and Metallurgy

★ ★ ★

New York, April 27, 28, 29, 30, and May 1, 1958

Headquarters at the Statler Hotel

Sessions probably will be scheduled on
Electric Insulation, Electronics,
Electrothermics and Metallurgy, Industrial Electrolytics,
and Theoretical Electrochemistry

★ ★ ★

Ottawa, September 28, 29, 30, October 1, and 2, 1958

Headquarters at the Chateau Laurier

★ ★ ★

Philadelphia, Pa., May 3, 4, 5, 6, and 7, 1959

Headquarters at the Sheraton Hotel

★ ★ ★

Papers are now being solicited for the meeting to be held in New York, N. Y., April 27-May 1, 1958. Triplicate copies of each abstract (*not exceeding 75 words in length*) are due at the Secretary's Office, 1860 Broadway, New York 23, N. Y., *not later than January 2, 1958* in order to be included in the program. *Please indicate on abstract for which Division's symposium the paper is to be scheduled.* Complete manuscripts should be sent in triplicate to the Managing Editor of the JOURNAL at 1860 Broadway, New York 23, N. Y.

Editorial

Inflation

INFLATION has been described as "when the schoolteachers get a raise, but it's too late." Perhaps not very good English, but it explains a situation that we fear: rising prices, lagging income, maybe a depression around the corner, with wide-spread destruction of all values. Money saved to send the children to college has become inadequate . . . vacations must be curtailed . . . keep the old car another year.

War invariably brings inflation. This should not be so, because at the end of the war everything has been paid for in terms of life and labor, of "blood, sweat and tears." Not so in terms of money: a huge national debt remains, while money waiting to be spent, and the needs of reconstruction, force prices up. Probably no democratic government could resist the terrific economic pressures during and after a major war. We simply must accept the fact that money invested in insurance, annuities, and the like in the 1930's has less purchasing power in the 1950's.

The creeping inflation we have right now, in the prosperous peacetime economy of 1957, is very disturbing; it could get out of control, wipe out the savings of millions. "Cost of living at all-time high; commodity prices rise another 4% in 3 months . . . Builders predict further increase in cost of housing . . . 52 daily newspapers raise price to 10¢ . . . More colleges raise tuition . . . M.I.T. announces increase in on-campus room and board, student protest demonstration becomes near-riot, 30 arrested, among them an itinerant Yale man . . . Frankfurters ~~2¢~~ 25¢." Such items can be multiplied manyfold.

Inflation and business failure are, to a certain extent, an integral part of our economic system. Mark Twain recognized this fact, when he suggested that a few mills per day was a satisfactory workman's wage in the days of King Arthur. An old problem is illuminating: If 1¢ is invested at 6% interest, compounded annually, how much will it be worth in 10,000 years? The mathematical answer is, at the present price of gold, enough to buy a fantastic ball of gold more than 10^{m} light-years in diameter! Obviously, money cannot be invested continuously at an exponential rate without "inflation" or some other breakdown of values.

Detailed consideration of monetary problems is, of course, outside the province of this editorial page. The subject is one for continuous study by experts in the field, who, it is safe to say, do not understand all the complications which are involved. The fact remains that we are all much concerned about the coming value of our current income and of our savings. We have to look to the national Government to work out systems of checks and balances, and we wonder if the Administration and the Congress have the best of counsel, and are willing to take appropriate measures. Most of us can do little more than to urge our congressmen to study the problem and to act, not to remain completely indifferent, to play the fiddle while Rome burns.

—CVK

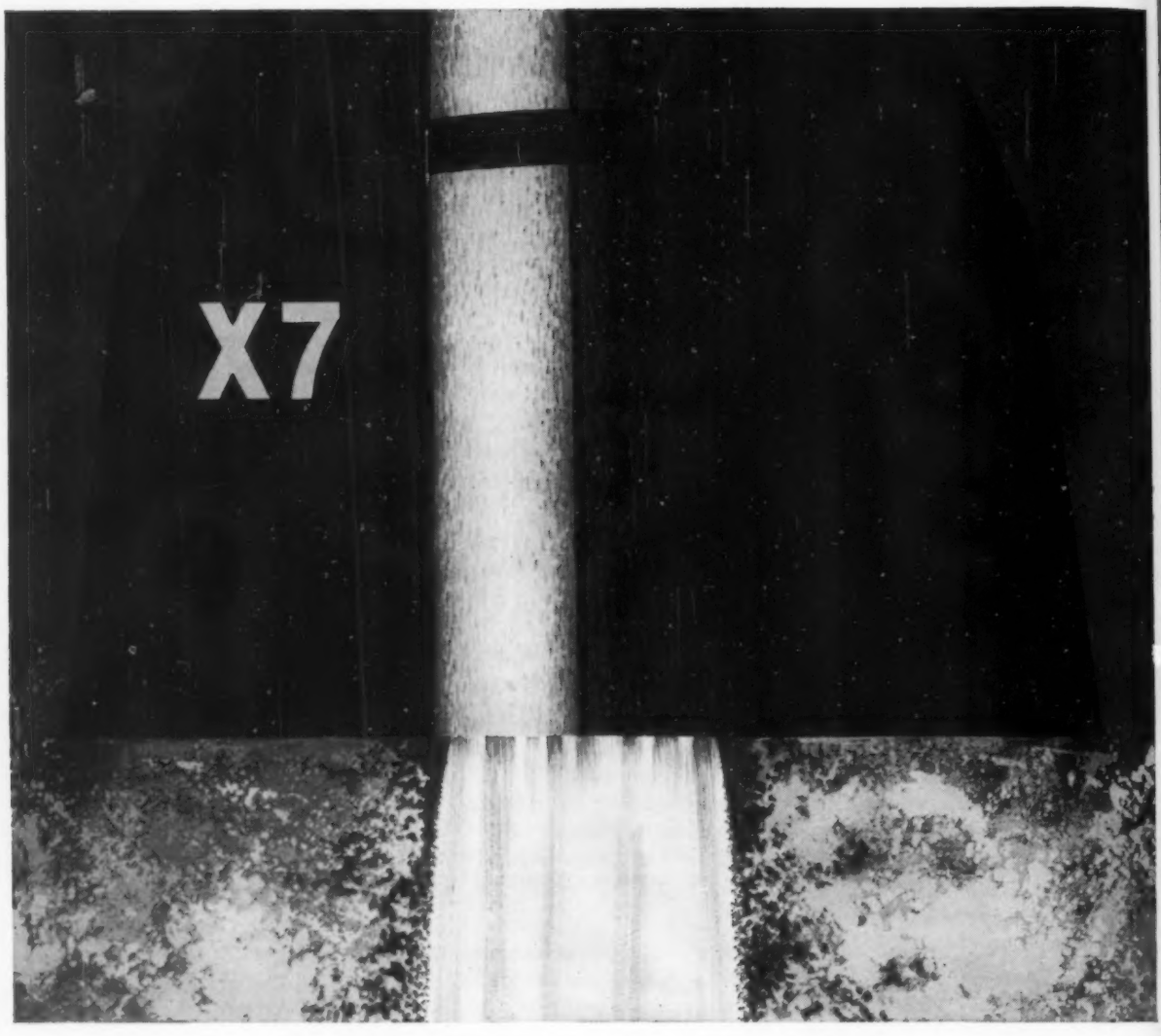

New punch for missile propellants

High heat of reaction, other characteristics point to magnesium for high-energy fuels

Magnesium, in its finely divided form, may well be suitable for new types of rocket fuels. It has long been known that a tremendous amount of chemical energy is locked within the metal. Upon further examination, finely divided magnesium has many significant characteristics that are important to the development of an efficient fuel:

High heat of reaction
Chemically reactive
High energy per unit volume
High theoretical flame temp.
Can be dispersed in various media

Products of combustion are: inert, relatively non-abrasive and present no toxicity problem
Inexhaustible raw material supply

Magnesium's heat of reaction, for example, compares to that of other fuel materials as follows: magnesium, 14,200 B.T.U. per lb. of oxygen required for combustion; aluminum, 13,370; lithium, 10,980; boron 9,670 (all at 2900°K). This plus magnesium's high theoretical flame temperature indicates that magnesium is especially adaptable for short-range applications where high initial thrust is desirable.

In addition, magnesium can also be considered as an intermediate in the manufacture of other metallic and organometallic fuels.

For information about finely divided magnesium, contact your nearest Dow sales office or write THE DOW CHEMICAL COMPANY, Midland, Michigan, Department MA1438QQ.

YOU CAN DEPEND ON DOW

Some Unusual Effects of Hydrogen in Corrosion Reactions

J. E. Draley and W. E. Ruther

Argonne National Laboratory, Lemont, Illinois

ABSTRACT

Consideration of corrosion in the presence of water has led to the postulation of damage by hydrogen produced in the reaction. For cases where the metal surface is covered with a protective layer, it is considered that some hydrogen ions diffuse through the layer and form hydrogen atoms beneath it. The consequence of the production of hydrogen in this location is to decrease corrosion resistance. Three types of harmful effects are illustrated.

Existing theory has left a number of inconsistencies and anomalies in its explanation of corrosion phenomena. The following has been developed in an effort to provide reasonable explanation for some of these cases. This theory has evolved largely as a consequence of studies of the behavior of Al, U, and their alloys. Much of its development during investigation of high temperature aqueous corrosion of Al and its alloys has been reported (1). This paper presents the theory in a more generalized form, and an effort is made to show instances in which it applies. In addition, its applicability is suggested in some cases where the theory might be valuable but for which there is little or no evidence to indicate its validity. It is suspected that the phenomenon (acceleration of corrosion damage by H produced) is more widespread than has hitherto been believed, and it is hoped that the present work will promote more active consideration of its possibility.

The description of the processes is given for corrosion reactions which proceed through a thin continuous protective film on the metal, which is called a "barrier film." Probably the most common type of barrier film is that which is formed as a consequence of the corrosion reaction, most frequently being an oxide. There might be cases in which films with similar properties can be formed prior to the corrosion exposure.

One of the most interesting properties of such films is their adherence to the base metal. At this time the nature of the bonding between the film and the metal is not believed to be well understood. There does seem to be indication that the protective properties of the film and probably its very existence (as a film) require attachment to and support by the metal beneath.

It is not unusual for the barrier film to be covered over with a thicker corrosion product layer. In some cases this thicker layer appears to be a considerably more porous material. It is likely that it is formed by some sort of transformation process from the thinner barrier layer. The nature of this transformation process probably changes from case to case. In some instances the compositions are different and the transformation might consist of an oxidation or a hydration process. In some cases it appears not to be one of these and perhaps represents only a cracking or fragmentation into discrete crystals (the barrier layer is probably under a considerable stress). This type of situation would be expected to lead to a diminishing rate of reaction for an initial period, followed by a constant oxidation or corrosion rate, as the rates of destruction and formation of the protective barrier film became equal. The concept of double layered corrosion product for Al has been developed by Dekker and Urquart (2) and Hunter and Fowle (3), among others.

The present theory will be developed in terms of barrier films but no restriction is intended against other cases such as adsorbed layers. With minor modifications the theory can be adapted to fit these cases.

Description of Corrosion Process

Oxidation probably proceeds through barrier films by ionic migration. For the case of corrosion in environments containing water the important processes are represented in Fig. 1. Migrations are represented as occurring through the bulk of a continuous oxide film. If some of these actually occur by diffusion through breaks or cracks in barrier films it will not alter the general argument. The barrier film is represented as consisting of oxide because this is the most general case. Only small changes in wording would be necessary to allow application of the description to films of other con-

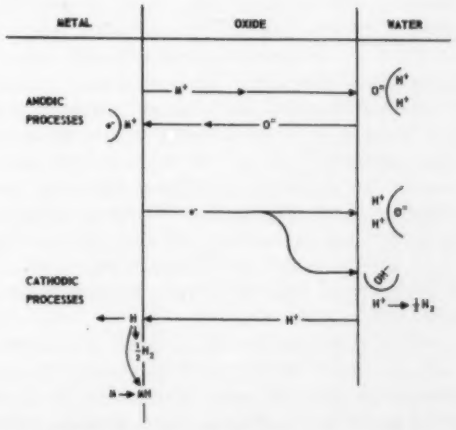

Fig. 1. Schematic representation of corrosion processes

stitution. In those cases where there is a porous solid on the outside of the barrier layer of oxide the water indicated in Fig. 1 should be imagined as being absorbed in the porous layer.

The anodic process can proceed by cation diffusion outward through the oxide or by anion diffusion inward. Both encourage the oxidation of the metal and the formation of new oxide, and this is the reason they are classed as anodic. Also, two types of diffusion are shown for the cathodic process: diffusion of electrons out through the oxide and, the new feature proposed here, inward migration of H ions. Some of the possible reactions forming oxide ion, hydroxide ions, and hydrogen ions from water are shown at the oxide interface. Other possible surface reactions perhaps should have been illustrated, such as the reduction of oxygen and the reduction of cations to form metal.

Probably the H ions in the oxide are combined with oxide ions and diffusion, or migration, proceeds by a series of transfers. They could also be interstitial, of course, with no instantaneous attachment to any particular oxide ion. The so-called hydrated oxides contain hydroxide ions and it is suspected that at least some of the diffusing protons were originally incorporated into the oxide in this form. The driving forces for the diffusion of protons are presumably the potential gradient and a proton concentration gradient through the oxide. It is believed that H is formed beneath the oxide largely as a result of cathodic proton migration rather than anodic hydroxide ion migration. The basic evidence is that the accumulation of corrosion product H in the metal is decreased by anodic polarization and increased by cathodic polarization. The metals for which this is known to have been demonstrated include steels, aluminum, and uranium alloys.

One could also propose that the H is transported through the oxide in the form of atoms rather than ions. There is no known positive refutation of this hypothesis, but it is considered unlikely. First, the H atoms would be considerably larger than the ions; this would make migration through the oxide lattice much more difficult. Second, it appears unlikely that such a neutral atom could exist for very long in an environment such as an oxide, with its very high local electric fields. Third, the driving force for the migration would be considerably lower than for the migration of protons. The potential gradient would not be influential, and the only known driving force leading to a net transfer would be a concentration gradient set up by removal of the H atoms at the metal-oxide interface. In many cases such removal does not occur without a hydrogen (atomic?) pressure to increase the rate.[1] If the diffusion of H atoms occurred through the oxide, no greater pressure of this sort could develop beneath the oxide than existed above it.

The cathodic reduction of H ions produces H atoms at the most active cathode spots, that is, where the electrons are most available. It is not necessarily possible to describe such cathode points in terms of their potential, although the reactions should alter the potential gradients in the oxide and adjacent solution.

Three types of disposal of the hydrogen atoms thus produced beneath the barrier film are illustrated:

(*A*) *Diffusion into the metal.*—It is notable that the same metallurgical factors which characteristically increase local cathodic activity usually also increase permeability to H diffusion. Included among such factors are the presence of inclusions (usually cathodic), porosity, and structural defects. As will be illustrated, the resultant diffusion into the metal can lead to quite harmful effects.

(*B*) *Formation of gaseous* H.—Such gas can rupture the barrier film as its pressure becomes sufficient to do so. This rupturing action would result in increased corrosion, probably localized at any one time. The actual rate of corrosion might be determined by the rate of rupturing. This appears likely if the unbroken film is quite protective and the anodic reaction can take place only very slowly by diffusion or migration through it.

(*C*) *Formation of metal hydride in cases where this reaction is possible.*—The hydride produced would be expected to interfere with the bond between the barrier film and the supporting metal. In this way the barrier film stability would be destroyed, the oxide perhaps recrystallizing, and its highly protective nature would disappear.

The total reaction can be summarized as two sets of competing processes in series. The anodic current will be carried by anion and cation migration, in inverse proportion to the "resistances" of the competing total anode processes. The cathodic current will be carried by electron and proton migrations, in inverse proportion to the "resistances" of these respective total processes. Such processes include the acquisition and incorporation of the diffusing species into the oxide, diffusion, cathodic reduction, and liberation and disposal of the products. Control of the corrosion reaction can be considered to be the sum of the anodic and cathodic resistances (each of which is the parallel sum of two complex "resistances").

Disposal of those H atoms which are produced beneath the oxide will be divided among the three competing processes. All can be expected to reduce corrosion resistance.

Preventing their damaging effects can be accomplished by making the "resistance" of the electron migration process very low compared to that for the proton migration process. Note that the substitution of a more favorable cathodic reaction on the surface of the oxide can be a case of this type, since chemical reduction becomes easier. However, if the electronic resistance of the oxide is high, no diminution in damage by H would be expected to occur as a result of the addition of a typical "cathodic depolarizer" such as oxygen (unless the incorporation of H into the oxide is simultaneously reduced).

Certain otherwise anomalous results can be explained in these terms. In particular, some cases of anodic protection or partial protection and cathodic acceleration of corrosion are logical, as far as is known, for the first time.

[1] Hydrogen overvoltage to liberate gaseous hydrogen or to cause rapid embrittlement.

Illustrations of Effects of Liberated H on Corrosion Behavior

In many of the cases given, proof that it is the H which causes the objectionable acceleration of corrosion damage will appear inconclusive. In some instances good correlation will be demonstrated between behavior and H found in the metal after corrosion (or metal hydride found after corrosion). For the liberation of gas beneath the film, however, no such direct evidence can be obtained and less direct indications must be used.

Diffusion into the metal.—Al alloys form blisters at elevated temperatures in moist air. These are believed to be caused by H_2 accumulating in cavities and rifts in the metal structure to produce the pressure which causes swelling. The phenomenon is observed to increase in intensity as metallurgical factors are added which tend to cause less sound surface structures. Thus surface defects caused by incorporated second phases and from severe working cause more blistering by the opening of the surface texture to allow more rapid diffusion of H into the metal. Such surface blistering can be prevented by dissolving off the surface oxide prior to heating. One effective method of accomplishing this is by immersing Al in brazing flux.

This is perhaps evidence that the barrier film prevents the escape of H formed beneath it. This restriction of its free escape appears to be necessary to cause the H to penetrate a material with a low H diffusion rate. Smith (4) reports the difficulty of diffusing H outward through surface films.

In water at temperatures much above 200°C most common Al alloys suffer rapid corrosive deterioration. The samples in Fig. 2 show appearance typical of the beginning of damaging attack of 1100 Al after about 2 weeks in distilled water at 275°C. At a temperature of 350°C this material is entirely disintegrated and corroded to oxide in a few hours. Analysis has shown a considerable increase in H content of the surface layers of corroding 1100 Al prior to damaging attack. The phenomenon can be prevented up to about 350°C by forming active cathode sites for H combination on the metal surface. Metals of low H overvoltage can be deposited from solution or incorporated into the Al by alloying. It has not been determined whether this method owes most of its effectiveness to its ability to cause combination of the H atoms (beneath the oxide) before they can diffuse into the metal, or whether at such points the cathodic metal protrudes through and above the barrier film of oxide, providing active liberation sites for the H on the outside. The latter possibility can be considered to be a case where the total process involving movement of electrons outward through such places in the oxide is made quite easy. For the purpose of preventing H_2 penetration into Al, Ni is the most effective metal which has received much attention. An alloy, made by the addition of 1% nickel to 1100 Al, shows no measurable increase in H content during corrosion in water at temperatures as high as 350°C, and no corrosion damage other than normal surface attack. This development has been described by Draley and Ruther (1).

Fig. 2. Typical appearance of 1100 Al after about two weeks in distilled water at 275°C.

Metallic U corrodes quite rapidly in water at elevated temperatures. A barrier film oxide can be stabilized by alloying to produce materials of low corrosion rate in the same environment. These alloys are generally observed to fail by cracking or crumbling after prolonged corrosion testing. Such failure has been shown to occur after an accumulation of more than a critical concentration of H in the corrosion sample. In some cases (U-Mo alloys), a second phase has been observed to form at about the same time, dispersed within the metallic matrix (5). This is believed to be a hydride. It is considered that the increase in volume in the formation of the new phase creates quite high local stresses. In another class of U alloys, typically containing small amounts of Nb and Zr, no such second phase has been discovered in normal corroded specimens, although some H accumulation in the metal and mechanical failure occur. It is clear that high local stresses are produced. For both types of alloy, corrosion "lifetime" can be increased materially by adding a Ni salt to the water. As has been shown to occur on Al, this should result in Ni deposits, providing good H liberation sites.

During its corrosion in distilled water at elevated temperatures, Zr produces a thin protective layer of corrosion product. By determining the H content of the metal, Thomas (6) has shown that a significant fraction of the total H produced in the corrosion reaction is absorbed in the metal, some of which ultimately forms zirconium hydride crystals at the surface, and growing into the metal (7). At about the same time the corrosion rate increases, with the formation of crystalline corrosion product (less protective). It has not been determined experimentally whether a critical H concentration in the surface layers of the metal influences the transition in corrosion behavior, so that the evidence to support the present thesis is not conclusive.

The absorption of H in steels during corrosion and especially during pickling or electroplating has been

well known for many years. The most serious result is sometimes severe embrittlement of the steel. Damage of this type is generally postulated to occur in the same fashion as has earlier been mentioned for Al: by the formation of molecular H in pores or open places in the metal structure and the resultant high local stresses produced. This kind of embrittlement of Fe can occur in dry H although it is accelerated by the presence of moisture [shown by Stanley (8)]. Several reviews of the damage of steel by H have been written, for example, Buzzard and Cleaves (9).

The initial presence of H in some U alloys (10) and in Zr (6) accelerates the rate of further H pickup during aqueous corrosion, in the former case leading to higher corrosion rates and early "failure." There have also been a number of instances in which the presence of H in other metals has caused increased corrosion. For example, Berger and Tull (11) observed correlation between the amount of blistering of pure (99.8%) Al in air at 600°C and the formation of deep pits in electrolytic etching. Iwamura and co-authors (12) observed that Al alloys containing H corroded faster in 10% NaOH solution than those which contained little or no H. Smith and Derge (13) have shown that the susceptibility of Pd to attack by etching agents varies in parallel with the avidity with which the metal takes up H_2 from the gas phase. The rate of H_2 uptake was shown to be related to the presence of fissures in the metals.

When metal structures have somewhat borderline H diffusion rates, that is, when a small change in metal structure might be expected to increase the acquisition of H by the metal to an extent which would then be discernible, such metal might be expected to be susceptible to "stress corrosion." In this instance, applying tension should produce a small amount of opening in the metal lattice, resulting in diffusion of H inward at the most susceptible places. The reasoning is supported by the fact that the amount of internal hydride formed during cathodic charging of a U alloy is increased by tension and decreased by compression (5). It is perhaps significant that in nearly all cases of "stress corrosion cracking" it is only the effect of tension which increases corrosion susceptibility (14). This type of reasoning does not seem to explain all stress corrosion cracking, however, because some metals which show the phenomenon (e.g., Al alloys at ordinary temperatures) would not be expected to have "borderline hydrogen diffusion rates." It is not clear whether such reasoning should apply to corrosion fatigue. Experimentally it was shown by Evans and Simnad (15) that small cathodic currents decreased the fatigue life of mild steel (although greater cathodic polarization increased fatigue life).

Formation of gaseous hydrogen.—As previously remarked, there is no known unequivocal evidence as to whether H_2 liberated in the corrosion reaction influences corrosion rates by rupturing protective films. The following discussion on Al can be considered useful only where barrier films will form and determine corrosion rates. This probably restricts attention to cases where corrosion is quite slow and uniform on a gross scale, i.e., where significant local attack does not occur.

Corrosion of Al alloys in distilled water at ordinary temperatures is characterized by the formation of tiny shallow pits. It is proposed that these are the places where H_2 is formed beneath the film and ruptures it. At such areas the corrosion reaction then takes place rapidly for a short but significant period (during which time the areas are, of course, anodes), with the ultimate result of reforming the film there. Note that the "etch pits" are proposed to form at what were originally active cathode sites rather than at sites which differed from the rest of the surface by being intrinsically more reactive anodically. In environments where pitting is observed, the same reasoning might be applicable as providing one kind of pit initiation. That is, pits might start at or about what were originally cathodes. It is clear that once pits are formed and continue to grow, the laws that govern the progress of the corrosion reaction must be different, since barrier films do not form at the pits.

This theory predicts that corrosion rates should be increased by mild cathodic polarization, and decreased by mild anodic polarization. In oxygen-saturated KOH solution (pH 10.5), the corrosion of 1100 Al follows this pattern exactly. As much as 90% reduction in rate was caused by anodic polarization. Unfortunately, the corrosion rate is strongly dependent on pH in this solution, and there is no way of knowing how much of the observed changes were caused by the local pH changes resulting from the induced cathodic and anodic reactions.

Much more valuable evidence would be provided by accurately determining the effects of polarizing current (of both polarities) on the corrosion rate of this metal in distilled water. Published data show that the corrosion rate is minimum in this pH range (at 50°C) (16), so that changing the pH by polarization (in either direction) would be expected to increase the corrosion rate slightly. This work has been started, but it will be a long job because of the requirement of accurate determination of extremely low rates.

In some cases striking increase in metal oxidation rate in gases (such as oxygen, air, carbon dioxide, sulfur, and sulfur-containing gases) is caused by the addition of a little water vapor (17). It is reasonable to propose that this is the result of the formation of H_2 beneath the oxide layer. Only a small amount of H_2 might be sufficient to cause a considerable amount of more rapid oxidation by oxide rupturing.

Formation of metal hydride.—U corrodes in hot distilled water at a rapid rate (300-500 mdd at 100°C), which is constant after a short initial period of slower reaction. The corrosion product is usually a fine granular powder of UO_2. After corrosion test, the corrosion product has been observed to contain UH_3 as well as the oxide, UO_2. Since water converts hydride to the oxide, it is inferred that the hydride is formed on the metal surface. This disrupts an initial film of oxide and prevents its subsequent formation. It is believed that during

continuing corrosion, uranium hydride forms under the oxide and prevents the formation of a barrier film.

At lower temperatures, thin protective oxide films form on the same U, only when there is oxygen in the water. This oxide is also UO_2, although it limits corrosion to quite small rates. Here it is perhaps true that the reduction of oxygen occurs in preference to the formation of H_2 so that there is little hydride formed beneath the barrier film. However, it appears that a small amount of H_2 is produced, for, after protracted testing, oxide breakdown occurs at local spots which then spread and the corrosion becomes much more rapid. Careful diffraction work by Waber (18) has shown the existence of UH_3 in such cases.

Conclusion

It is clear that justified application of the theory of increased corrosion caused by H_2 formation beneath the protective film is not universal. However, it appears to be valuable as an addition to existing theory, in affording understanding of some corrosion phenomena, and in a few cases it has predicted successful means of providing better corrosion resistance.

Manuscript received January 20, 1956. This paper was prepared for delivery before the Pittsburgh Meeting, Oct. 9-13, 1955. Work was performed under the auspices of the Atomic Energy Commission.

Any discussion of this paper will appear in a Discussion Section to be published in the December 1957 JOURNAL.

REFERENCES

1. J. E. Draley and W. E. Ruther, *Proc. Intern. Conf. on Peaceful Uses of Atomic Energy* (Geneva, August 1955); **9**, 391; also J. E. Draley and W. E. Ruther, *Corrosion*, **12**, 480t (1956).
2. A. J. Dekker and H. M. A. Urquart, *Can. J. Research*, **28**, 541 (1950).
3. M. S. Hunter and P. Fowle, *This Journal*, **101**, 481 (1954).
4. D. P. Smith, "Hydrogen in Metals," pp. 192 and 285, University of Chicago Press, Chicago (1948).
5. B. Lustman and D. E. Thomas, Private communication.
6. D. E. Thomas, "Metallurgy of Zirconium," edited by B. Lustman and F. Kerze, p. 621, McGraw-Hill Book Co., New York (1955).
7. C. M. Schwartz, D. A. Vaughan, and G. G. Cocks, BMI-793, "Identification and Growth of Oxide Films on Zirconium in High Temperature Water," Battelle Memorial Institute, Columbus, Ohio.
8. J. K. Stanley, Am. Soc. Metals preprint No. 15W, 10 pp. (1952).
9. R. W. Buzzard and H. E. Cleaves, *National Bureau of Standards Circular 511*, Sept. 24, 1951.
10. S. Greenberg and J. E. Draley, To be published.
11. F. J. Berger and V. F. G. Tull, *Nature*, **172**, 729 (1953).
12. H. Iwamura, T. Chihaya, and M. Suzuki, *J. Japan. Inst. Metals*, **14B**, 22 (1950).
13. D. P. Smith and G. J. Derge, *Trans. Electrochem. Soc.*, **66**, 253 (1934).
14. H. H. Uhlig (Editor), "Corrosion Handbook," p. 569, John Wiley & Sons, Inc., New York (1948).
15. U. R. Evans and M. T. Simnad, *Proc. Roy. Soc.*, **A188**, 372 (1947).
16. J. E. Draley and W. E. Ruther, *Corrosion*, **12**, 441t (1956).
17. O. Kubaschewski and B. E. Hopkins, "Oxidation of Metals and Alloys," pp. 205, 208, 210, 211, Academic Press, New York (1953).
18. J. T. Waber, Private communication.

Kinetics of the Oxidation of Chromium

Earl A. Gulbransen and Kenneth F. Andrew

Research Laboratories, Westinghouse Electric Corporation, Churchill Borough, Pittsburgh, Pennsylvania

ABSTRACT

The oxidation of high purity chromium was studied over the temperature range 700°-1100°C using the vacuum microbalance method. Below 900°C conventional oxidation curves were obtained which can be fitted to the parabolic rate law. Above 900°C and for a film thickness of approximately 4800Å, the rate of oxidation increased in an unusual manner. This increase in the rate of oxidation disappeared on further oxidation. At temperatures of 1050°C and higher a large increase occurred in the rate of oxidation, suggesting that the oxide film was no longer protective for film thicknesses greater than 42,000Å.

A logarithmic plot of the parabolic rate law constant vs. 1/T shows two straight lines separated by a transformation region. This gives 37,500 cal/mole and −15.3 entropy units for heat of activation and entropy of activation between 700° and 900°C and 59,400 cal/mole and +6.2 entropy units for 1000°-1100°C.

The rate of evaporation and the rate of oxidation of Cr are equal at about 950°C. This corresponds to the transformation region between the two mechanisms of oxidation. It is concluded that the failure of Cr in oxidation is closely related to the high vapor pressure of Cr above 900°C.

A preliminary study was made of the oxidation of Cr and the data could be fitted to the parabolic rate law. The heat of activation was reported to be 66,300 cal/mole (1). This paper presents a more complete study of the kinetics of the oxidation of a pure grade of Cr over the temperature range 700°-1100°C and for reaction times of 6 hr.

Since Cr is an important component of oxidation resistant high temperature alloys, one of the objectives of this work was to study the conditions under which Cr fails in oxidation. This failure occurs when a rapid reaction develops in which diffusion processes are no longer rate controlling. Poor adhesion of the oxide to the metal is observed for these conditions. For some metals, this breakdown of the protective oxide film is termed "break-away" corrosion.

Two oxides form on Cr, Cr_2O_3 and CrO_3, the latter under strong oxidizing conditions. Cr_2O_3 exists in more than one phase (2,3). Rhombohedral Cr_2O_3 is formed on oxidizing Cr (4). The resistance to oxidation of alloys containing Cr has been attributed to the formation of Cr_2O_3 or to spinels containing Cr_2O_3 (5-7).

Experimental

The vacuum microbalance method has been described (8-10). In this study a new type of microbalance of low sensitivity for the high temperature reaction range was used. The sensitivity is 0.22 divisions per microgram and one division equals 0.001 cm. The weight change could be estimated to 1.2 μg.

The furnace tube containing the specimen was constructed of mullite (11). This tube was sealed direct to the all-Pyrex glass vacuum system.

To avoid evaporation of Cr at 900°C and higher the specimen and reaction tube were heated rapidly to the reaction temperature in a vacuum of less than 10^{-6} mm Hg. Purified oxygen (8) was added as soon as thermal equilibrium was established.

The reproducibility of the oxidation experiments was about 5-10% above 950°C and 10-20% below 950°C.

Samples.—Table I shows the analyses of the Bureau of Mines grade of Cr used in this study. Strips of 10 mil sheet were sawed to specimens 1 cm wide and 1.6 cm long. Samples had surface areas of 3.5 cm^2 and weighed 0.50 g. Specimens were abraded and cleaned following the procedures used previously (1).

Results and Discussion

The rate curves are shown in Fig. 1 and 2. The weight gain is in $\mu g/cm^2$ and is converted to thickness in Å by multiplying by 60. This is calculated on the basis of the oxide Cr_2O_3 (4) and a surface roughness ratio of unity.

Table I. Analyses of chromium metal (Bureau of Mines)

Metal	Analyses Wt % or ppm	Method
Al	0.01 — 0.1%	Spectroscopic
Si	0.05%	Spectroscopic
Fe	0.001 — 0.01%	Spectroscopic
Cu	0.001 — 0.01%	Spectroscopic
Mg	Less than 0.001%	Spectroscopic
O*	150 ppm	Vacuum fusion
H*	5 ppm	
N*	Less than 10 ppm	
C	0.0032%	

* Ingot material.

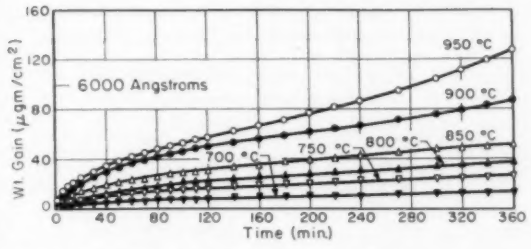

Fig. 1. Oxidation of Cr, 700°-950°C, 7.6 cm Hg of O_2, abraded 1-4/0.

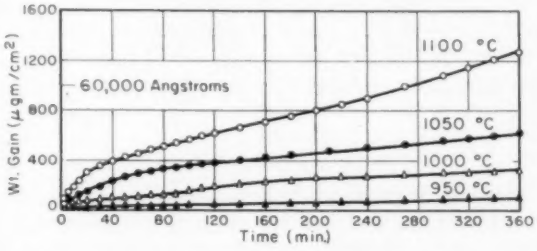

Fig. 2. Oxidation of Cr, 950°-1100°C, 7.6 cm Hg of O_2, abraded 1-4/0.

Time and Temperature

Fig. 1 shows conventional oxidation curves for temperatures of 700°-950°C. A rapid initial rate of oxidation is found, with the rate decreasing as the film thickens. A new phenomenon appears in the 950°C experiment. Here, the rate of oxidation does not decrease continually with time. Instead, at a film thickness of 80 μg/cm² or 4800Å, the rate of oxidation increases. A similar phenomena occurs in oxidation experiments in Fig. 2 at 975°, 1000°, 1025°, and 1050°C for similar film thicknesses. However, for these temperatures, the increase is only temporary and the course of the oxidation again appears to follow a normal behavior.

For oxidation experiments above 1050°C the oxidation curves show a second type of breakdown phenomenon with the rate of oxidation increasing for thicknesses above 700 μg/cm² or 42,000Å. Due to the limitations of the balance it has not been possible to study the end result of this type of breakaway oxidation.

A comparison of the results of this study with that of the older work (1) shows lower oxidation rates. The lower oxidation rates are attributed to the greater purity of the present Cr samples.

Parabolic Rate Law Correlation

The parabolic rate law is of value in studying the mechanism of oxidation, even though deviations may occur, since the law is based on fundamental physical theory. Deviations from the rate law suggest that physical and chemical changes do occur in the oxide film as a function of time, film thickness, and temperature.

The parabolic rate law states that

$$W^2 = At + C$$

Here W is the weight gain, t is the time, and A and C are constants. The constant A includes the diffusion coefficient of the diffusing specie, the number of defects in the lattice, and has an exponential temperature dependence (12).

Fig. 3 to 6 show parabolic rate law plots for the 700°, 900°, 1000°, and 1100°C oxidation experiments. At 700°C the parabolic rate law fitted except for the initial stage of the reaction (Fig. 3). A deviation from the parabolic rate law occurred after 240 min of reaction at 900°C (Fig. 4). Deviation from the parabolic rate law is noted at B (Fig. 5) for the 1000°C oxidation. This was at approximately the same film thickness as found in the 900°C ex-

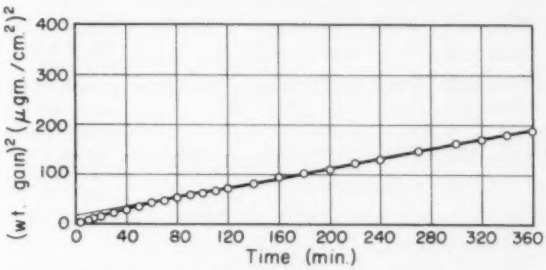

Fig. 3. Oxidation of Cr, 700°C, 7.6 cm Hg of O_2, abraded 1-4/0, parabolic plot A = 8.22 × 10^{-15} $(g/cm^2)^2$/sec.

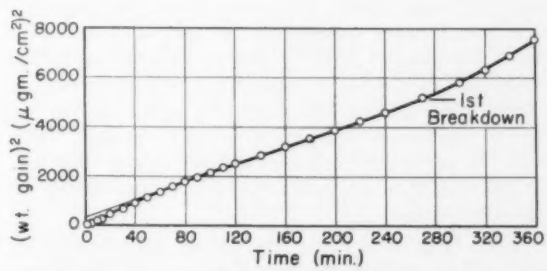

Fig. 4. Oxidation of Cr, 900°C, 7.6 cm Hg of O_2, abraded 1-4/0, parabolic plot A = 2.92 × 10^{-13} $(g/cm^2)^2$/sec.

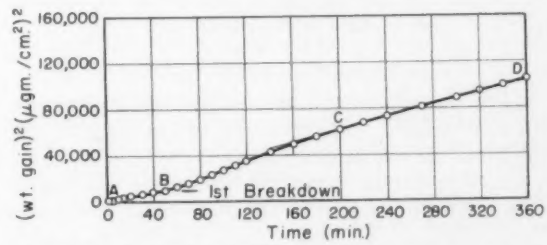

Fig. 5. Oxidation of Cr, 1000°C, 7.6 cm Hg of O_2, abraded 1-4/0, parabolic plot A_{C-D} = 4.51 × 10^{-12} $(g/cm^2)^2/sec^{-1}$.

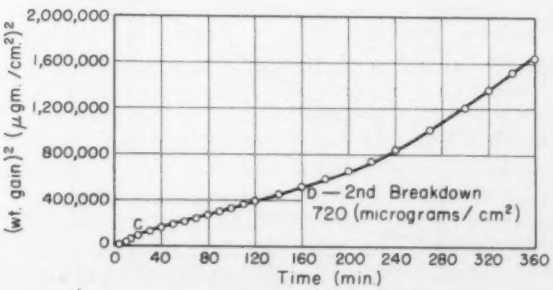

Fig. 6. Oxidation of Cr, 1100°C, 7.6 cm Hg of O_2, abraded 1-4/0, parabolic plot A_{C-D} = 5.28 × 10^{-11} $(g/cm^2)^2$/sec.

Table II. Properties of oxide films on Cr

Temp, °C	Thickness* μgm/cm²	A°	Color	Stability of film to cracking on cooling	Rate law
700	13.7	822	Straw	Stable	Parabolic
750	26.9	1614	Green	Stable	Parabolic
800	38.1	2286	Green	Stable	Parabolic
850	52.5	3150	Green	Stable	Parabolic
900	87	5220	Green	Stable	Parabolic
950	127	7620	Green	Stable	Parabolic
975	228	13680	Gray-green	Stable	Parabolic
1000	324	19440	Gray-green	Stable	Parabolic
1000	346	20760	Gray-green	Stable	Parabolic
1025	516	30960	Gray-green	Stable	Parabolic
1050	640	38400	Dark gray	Stable	Some acceleration of reaction
1075	960	57600	Dark gray	Unstable	Accelerating reaction
1100	1280	76800	Dark gray	Unstable	Accelerating reaction

* 6-hr experiments.

periment. At C the film appears to regain its protective properties. However, the slope C-D is greater than the slope A-B. Deviation from the parabolic rate law is only temporary in nature. Due to the rapid reaction at 1100°C the temporary deviation noted at lower temperatures is not easily observed (Fig. 6). At D for a film thickness of 720 μg/cm² the rate of oxidation deviates in a positive sense from both the parabolic rate law and the linear rate law. On cooling the specimen, the oxide film flaked off from the metal.

Table II gives a summary of the experimentally observed properties of oxide films on Cr. The thickness of the oxide film formed after 6 hr of reaction is tabulated, together with the color of the oxide, its stability to flaking off of the metal on cooling, and the type of rate law correlation.

Comparison with Nickel

Fig. 7 shows a comparison of the oxidation curve of Cr at 1050°C with that for Ni at 1050°C. Cr oxidizes at an appreciably slower rate than Ni (13). In the Ni oxidation experiment the oxide film flaked away from the metal on cooling, while the oxide

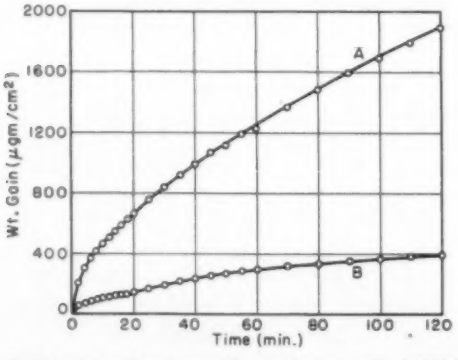

Fig. 7. Oxidation of Ni (curve A) and Cr (curve B), 1050°C, 7.6 cm Hg of O_2, abraded 1-4/0.

Table III. Summary of parabolic rate law constants

Temp, °C	A (g/cm²)² sec⁻¹
700	8.22×10^{-15}
750	3.14×10^{-14}
800	6.95×10^{-14}
850	1.18×10^{-13}
900	3.02×10^{-13}
950	5.50×10^{-13}
975	1.20×10^{-12}
1000	4.51×10^{-12}
1000	4.93×10^{-12}
1025	1.15×10^{-11}
1050	1.81×10^{-11}
1075	3.08×10^{-11}
1100	5.28×10^{-11}

film formed on Cr was near to the unstable condition.

Temperature Dependence

Table III summarizes the parabolic rate law constants over the temperature range. For experiments below 950°C, parabolic rate law constants are calculated for thicknesses below that for the first deviation of the rate law correlation. Above 950°C, parabolic rate law constants are calculated for conditions above the first deviation and below the second deviation noticed at temperatures above 1050°C.

Fig. 8 shows a log A vs. $1/T$ plot. Two straight lines are found to describe the temperature dependence of the parabolic rate law constants. Between the two straight line portions of the plot a transformation region exists. The heat of activation is 37,500 cal/mole between 700° and 950°C and 59,400 cal/mole between 1000° and 1100°C. The existence of this transformation zone suggests that a major change is occurring within the oxide-metal system.

It is concluded that Cr fails in oxidation above 1000°C. The rapid increase in the parabolic rate law

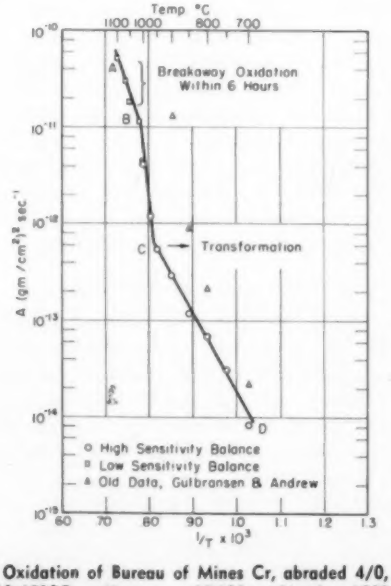

Fig. 8. Oxidation of Bureau of Mines Cr, abraded 4/0, log A vs. $1/T$, 700°-950°C, ΔH_{C-D} = 37,500 cal/mole, 1000°-1100°C, ΔH_{A-B} = 59,420 cal/mole.

constants at 950°-1000°C suggests that this increase is a preliminary symptom of breakdown.

Comparison of Rate of Oxidation with Rate of Evaporation

One property of Cr which plays an important role in oxidation at high temperature is the high vapor pressure of the metal above 900°C (1). To discuss the role of vapor pressure in oxidation, it is essential to review briefly the fundamental principles of oxidation and to indicate that the oxide film formed on metals consists of many small crystallites of variable size.

In the usual oxidation process, only the oxide very close to the metal interface is in equilibrium with the metal. Metal ions are transferred from the metal to the oxide only at locations where the oxide and metal are in intimate contact. The energy barrier for this transport process is usually less than the sublimation energy of the metal. Due to this fact, concentration gradients of Cr occur across the oxide crystallites and oxide film, and diffusion of metal follows. The vapor pressure of the metal for these conditions plays no direct role in the rate-controlling process.

Consider a higher temperature where the rate of evaporation of metal from a free surface approaches that of the rate of metal diffusing through the oxide during oxidation. For these conditions, metal atoms or ions can be transferred to the oxide crystals from the vapor phase as well as at the metal oxide interface, since the oxide film is not continuous, but composed of many oxide crystals. Thus, metal vapor can penetrate through portions of the film and short circuit the normal diffusion processes.

It is of interest therefore to compare for Cr the rate of evaporation with the rate at which metal atoms diffuse through the oxide and react with oxygen. The rate of evaporation data come from an earlier paper (1), while the rate at which Cr atoms diffuse through the oxide is calculated from the 1- to 2-hr oxidation period. Fig. 9 shows a log rate vs. $1/T$ plot of the data.

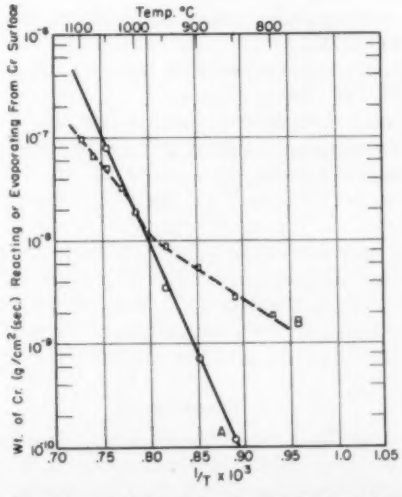

Fig. 9. Comparison rate of evaporation of Cr from clean surface (curve A) with rate of oxidation of Cr (curve B), rate (log scale) vs. $1/T$.

The transformation point (C-B in Fig. 8) corresponds to the condition in Fig. 9 at which the rate of evaporation is equal to the rate of Cr diffusion. Above 1000°C the rate of evaporation is greater than the rate of Cr diffusion. For these conditions (1000°C and higher), the oxide film appears to lose its protective properties after a definite thickness of oxide has formed. The reaction rate increases rapidly with time and the adhesion of the oxide to the metal is very poor.

Thus the high vapor pressure of Cr short circuits the normal diffusion processes and for these conditions a greatly increased rate of reaction results.

Theoretical

The transition rate-theory (1) and the classical expression (12) for the diffusion coefficient as expressed by Zener (14) have been used to interpret the parabolic rate law. Following this treatment, the following equation for the parabolic rate law constant can be derived, assuming a mechanism based on cation vacancy diffusion.

$$A = 2\gamma\nu a^2 e^{\left(\frac{\Delta S^\circ}{8/3} + \Delta S^*\right)/R} e^{-\left(\frac{\Delta H^\circ}{8/3} + \Delta H^*\right)/RT}$$

Here $\frac{\Delta S^\circ}{8/3}$ and $\frac{\Delta H^\circ}{8/3}$ are the entropy and heat of formation of the vacancies, while ΔS^* and ΔH^* are the entropy and heat of activation of diffusion, a is the interatomic distance between diffusion sites, ν is the frequency of vibration along the direction across the saddle configuration, R is the gas constant, T is the temperature, and γ a coefficient determined by the geometry of the atomic jumps. A has the units of $cm^2\ sec^{-1}$.

To evaluate ν and γ it was necessary to assume a particular oxide and a mechanism for diffusion. According to the work of Gulbransen and Hickman (4), rhombohedral Cr_2O_3 is formed on oxidizing Cr.

Details of the application of this equation to Cr_2O_3 have already been discussed (15). From the temperature coefficient of the reaction and the value of A at a given temperature, the value of the heat and entropy terms can be evaluated. These terms have been called heat and entropy of activation, since a rate process is involved.

Table IV shows a summary of the experimental heats, entropies, and free energies of activation for the oxidation of Cr (12). Below 950°C an entropy of activation of -15.3 ± 0.4 cal/mole/°C was calculated from the equation. Above 1025°C an entropy of activation of 6.2 ± 0.3 cal/mole/°C was calculated.

The experimental entropy of activation is made up of two terms (12): (*a*) entropy of formation of vacancies, and (*b*) entropy of activation of diffusion. Zener (14) has shown for the case of metals that the entropy of activation of diffusion should be positive. This has been verified by Gulbransen and Andrew (13) for the oxidation of pure Ni. However, other oxidation reactions have shown negative values for the entropy of activation of diffusion.

The entropy associated with the formation of a lattice vacancy for the Cr_2O_3 lattice is approximately

Table IV. Parabolic rate law constants, entropies, heats, and free energies of activation for the oxidation reaction

t °C	A cm²/sec	ΔH° cal/mole	ΔS° cal/mole/°C	$-T\Delta S°$ cal/mole	ΔF° cal/mole	Comments
700	3.06×10^{-15}	37,500	−15.7	15,300	52,800	
750	1.17×10^{-14}	37,500	−15.0	15,300	52,800	Oxide film adherent, rate of evaporation lower than rate of oxidation.
800	2.59×10^{-14}	37,500	−15.1	16,200	53,700	
850	4.39×10^{-14}	37,500	−15.6	17,500	55,000	
900	1.12×10^{-13}	37,500	−15.2	17,800	55,300	
950	2.05×10^{-13}	37,500	−15.3	18,700	56,200	
1025	4.28×10^{-12}	59,400	5.9	−7700	51,700	Oxide film flakes off on cooling, rate of evaporation higher than rate of oxidation.
1050	6.73×10^{-12}	59,400	5.9	−7800	51,600	
1075	1.15×10^{-11}	59,400	6.2	−8400	51,000	
1100	1.96×10^{-11}	59,400	6.4	−8800	50,600	

−7.5 cal/mole/°C. From this the entropy of activation of diffusion is −8 cal/mole/°C for the temperature range 700°-950°C. Above 1025°C a value of +13.7 cal/mole/°C is calculated.

The positive value of the entropy of activation found for the high temperature range is in agreement with Zener's diffusion picture (14). However, the value appears high when it is compared to the value of +2 found for the oxidation of Ni (13).

The negative value of −7.5 cal/mole/°C for the temperature range 700°-950°C is unexplained, although similar negative values of the entropy of activation are found for a number of metals. The different heat and entropy of activation values found for the two temperature regions suggest that a different reaction mechanism is rate controlling.

Failure of Cr *in Oxidation*

An analyses of the kinetic data show several interesting facts. (*A*) Cr begins to fail in oxidation at a temperature where the rate of evaporation of Cr from a clean surface is equal to the rate of reaction. This suggests that the distribution of defects in the Cr_2O_3 lattice may change greatly at this temperature. (*B*) For oxidation above 1000°C the adhesion of the oxide to the metal depends on the oxide film thickness. This may be related to the fact that at a certain thickness the rate of evaporation approaches or becomes equal to the rate of oxidation. (*C*) The heat and entropy of activation change drastically for oxidation conditions where the metal will ultimately fail at thicker film thicknesses.

Thus, the failure of Cr in oxidation is clearly related to its high vapor pressure at 900°C and higher.

Manuscript received July 9, 1956. This paper was prepared for delivery before the Cleveland Meeting, Sept. 29 to Oct. 3, 1956.

Any discussion of this paper will appear in a Discussion Section to be published in the December 1957 JOURNAL.

REFERENCES

1. E. A. Gulbransen and K. F. Andrew, *This Journal*, **99**, 402 (1952).
2. C. T. Anderson, *J. Am. Chem. Soc.*, **59**, 488 (1937).
3. L. Blanc and G. Chaudron, *Compt. rend.*, **182**, 386 (1926).
4. E. A. Gulbransen and J. W. Hickman, *Trans. Am. Inst. Mining Met. Engrs.*, **171**, 306 (1947).
5. E. Scheil and K. Kiwit, *Arch. Eissenhuttenw.*, **9**, 405 (1936).
6. J. W. Hickman and E. A. Gulbransen, *Trans. Am. Inst. Mining Met. Engrs.*, **180**, 519 (1949).
7. E. A. Gulbransen and W. R. McMillan, *Ind. and Eng. Chem.*, **45**, 1734 (1953).
8. E. A. Gulbransen, *Trans. Electrochem. Soc.*, **81**, 187 (1942).
9. E. A. Gulbransen, *Rev. Sci. Instruments*, **15**, 201 (1944).
10. E. A. Gulbransen, "Advances in Catalysis," Vol. V, p. 119-175, Academic Press, Inc., New York (1953).
11. E. A. Gulbransen and K. F. Andrew, *Ind. Eng. Chem.*, **41**, 2762 (1949).
12. E. A. Gulbransen, *Anals. N. Y. Acad. Sciences*, **58**, 830 (1954).
13. E. A. Gulbransen and K. F. Andrew, *This Journal*, **101**, 128 (1954).
14. C. Zener, *J. Appl. Phys.*, **22**, 372 (1951).
15. E. A. Gulbransen and K. F. Andrew, *This Journal*, **101**, 163 (1954).

Anodic Oxidation of Aluminum, Chromium, Hafnium, Niobium, Tantalum, Titanium, Vanadium, and Zirconium at Very Low Current Densities

Herman A. Johansen,[1] George B. Adams, Jr., and Pierre Van Rysselberghe[2]

Department of Chemistry, University of Oregon, Eugene, Oregon

ABSTRACT

Some aspects of the mode of formation of anodic oxidation films in the potential region below oxygen evolution were examined for a number of metals under as nearly constant experimental conditions as possible. The metals selected were Al, Ti, Hf, V, Nb, Ta, and Cr. Results for Zr were reported in earlier publications. Electrolytic parameters and formation fields were evaluated from the unitary formation rates. Local currents were estimated using the method described previously.

The mode of formation of anodic oxide films on metals is of increasing technical and scientific interest. The technical applications of anodization are well known, and further interest in the subject has derived from its importance from the point of view of the mechanism of electrode processes in general.

The purpose of the present work was to examine the formation of anodic oxide films on certain metals below the potential of oxygen evolution under experimental conditions sufficiently constant to permit comparisons. The metals selected for study were Al, Ti, Hf, V, Nb, Ta, and Cr. Zr had been studied previously (1, 2).

The pioneer work of Güntherschulze and of Güntherschulze and Betz initiated much of the present day interest in oxide film formation, many of the theoretical discussions having been based on their empirical results. The formation of anodic oxide films on Ta was reported by Güntherschulze and Betz (3), and formation of films on the additional metals W, Zr, and Al was discussed (4). Güntherschulze and Keller (5) reported that electrolytically formed oxides had high densities and high dielectric constants corresponding to the properties of fired oxides. Studies of the formation of these films led Güntherschulze and Betz (6) to the conclusion that the ion current forming the films followed an exponential relationship with the electric field. The work of Güntherschulze and Betz has been published in a book on electrolytic capacitors (7).

The general literature on anodization was found to be too extensive for detailed comment; however, references (8) through (33) have been selected as being of interest in connection with anodization of the particular metals examined in this work.

Experimental

The apparatus used consisted of a constant temperature bath containing the anode, cathode, and reference electrode compartments; the potential measuring circuit with potentiometer, galvanometer, and millivoltmeter; the current measuring circuit with sensitive galvanometer (null type) and potentiometer; and the current regulator.

For most of the experiments the galvanometer for the current measuring circuit was an A. C. Brown Electronik null indicator with a sensitivity of 10^{-8} μ amp/mm. For the 1 μ amp current density runs a L&N reflecting-type galvanometer with a sensitivity of 3.7×10^{-4} μ amp/mm was used.

Grounding of the cathode through a large condenser was found to be necessary to avoid fluctuations in millivoltmeter readings due to stray currents. Likewise, all motor and metal parts were systematically grounded, as was the a-c galvanometer.

Test specimens were mounted as follows: The metal specimen was first turned to accurate diameter (usually 1.595 cm, equivalent to 2 cm^2 on the face), bored, tapped, and mounted in plastic, using a standard metallographic plastic mounting powder, heated die, and press technique. The plastic cylinder was then drilled and tapped to take a threaded tube through which a brass rod could be inserted to thread into the backside of the metal specimen, thus establishing a firm electrical connection. This method showed special advantages of speed of preparation and reproducibility of apparent surface area, and provided a convenient holder for abrasion of the metal.

Experimental Procedure

Many experiments were carried out to devise a standard method which would minimize the variations due to the experimental conditions. The tests were all run at 25°C and in the same electrolyte (*see* below). Air was bubbled constantly through the electrolyte to maintain air saturation, and to provide stirring. The same reference electrode,

[1] Present address: Research Labs., Westinghouse Electric Corp., Pittsburgh, Pa.

[2] Present address: Dept. of Chemistry, Stanford University, Stanford, Calif.

saturated mercurous sulfate, was used in all experiments, and all potentials given here are referred to this electrode.

The specimens were abraded dry on either metallographic paper or emery cloth immediately before each test. For Ti, Cr, Ta, V, Nb, and Hf, the abrasion consisted of 100 parallel strokes on 3/0 emery cloth. This was sufficient to remove all visible right angle scratches and yet it was believed not to produce an unduly cold-worked surface. Reproducibility between runs was good. With Al, separate studies were made using 3/0 emery cloth in one case, and 400 metallographic paper in the other. With Al, the formation rate (rate of change of potential with time ($\Delta E/\Delta t$) was found to vary considerably with the degree of abrasion (particularly noticeable on the coarser grits), 25 strokes on 400 paper being found sufficient to expose a new surface and give reproducible results. The 3/0 abrasion produced lower initial and lower constant formation rates, as would be expected on the basis of the greater surface area and consequent lower current density in the case of this coarser abrasion.

After abrasion the specimen was connected to the current regulator and the millivoltmeter and immersed with current switched on. Times from final abrasion to first reading were of the order of 6-10 sec and, depending on the applied current, measurements were carried out over a period of up to 8 hr.

The range of current densities was 0-100 μ amp/cm^2 and the apparent surface area of all specimens was about 2 cm^2.

Each metal was anodized at several current densities up to 100 μ amp. At least three check runs were made at each current density except 0 and 1 μ amp where usually only two runs were made in each case.

Materials

The electrolyte used throughout these experiments was a boric acid-ammonia solution. This electrolyte was selected because of its use by many previous investigators for the anodization of Al, Ta, and Zr. The solution was conveniently made by saturating distilled water with reagent grade boric acid at 25°C, then bubbling in gaseous ammonia to a pH of 8.

The present availability of various rare metals in high purity was one of the reasons for initiating the present work on anodic polarization. Further than the availability of the pure metals, a form suitable for experiment was required. Developments in arc-melting and metal-forming techniques permitted the testing of dense metal, whereas earlier investigators frequently had to work with powders or lumps of relatively impure materials.

The Al was obtained as Hoopes pig, recast to bar, and rotary swaged to approximate size.

The iodide titanium was arc-melted from the crystal bar to the arc-cast button, which was then turned to specimen size. Kroll process Ti was obtained as swaged rod and specimens turned from this rod.

The iodide hafnium was arc-melted from the crystal bar to the arc-cast button, which was then turned to specimen size.

Table I. Experimental metals

Metal	Type	% Metal	Chief impurities %
Al	Hoopes	99.99	Fe, Cu, Si traces
Ti	Kroll	99.6	Fe = 0.2, O = 0.05, Mg = 0.1, N, C, Mn traces
Ti	Iodide	99.9	Fe = 0.02, Al, Mn, C traces
V	Calcium bomb	99.9	O = 0.05, N, C traces
Nb	Fansteel	99.9	Labeled research grade by Fansteel
Ta	Electrolytic	99.9	Fe, C, O traces
Hf	Iodide	96.1	Zr = 3.8, Fe, Si, Al traces
Cr	Ductile	99.95	O = 0.04, Fe, Si traces
Zr	Kroll (not annealed)	99.6	O = 0.16, Fe = 0.06, C = 0.037, Sn = 0.05, Hf = 0.03

Va was obtained as lumps from the Ca bomb reduction process and arc-melted to a button which was turned to specimen size.

Nb was obtained as rolled sheet, cut up, and arc-melted to a button, which was turned to specimen size.

Ta and Cr were obtained as swaged rod.

Zr (Kroll process) was tested in sheet form as reported previously (1, 2).

Table I lists the metals with approximate total metal contents and chief impurities.

The arc-melted buttons were used in the as-cast condition directly without further annealing. The swaged rod materials were annealed by sealing in evacuated Vycor ampoules and heating to 950°C for Cr, Ta, and Ti, and to 500°C for Al.

Experimental Results

Experimental results for the different metals were recorded in the following manner: potential vs. time curves, representing the primary data, were obtained for each metal; from the potential-time data a second series of curves was constructed which show the relationship log ($\Delta E/\Delta t$) vs. log time and also the relationship of the log of the constant rate vs. log current density. Such plots show, for the film formers, how the limiting constant formation rate ($\Delta E/\Delta t$) at constant current density increases with this current density. From the log rate vs. log time and vs. log I plots the local currents were calculated, according to the method developed earlier (1).

If the values for the constant rate of change of potential at a given current density be divided by that current (in microamperes per cm^2) a new value is obtained which has been called the unitary formation rate, $1/I$ ($\Delta E/\Delta t$), or R_I. From the plots of the unitary formation rate vs. log current density, a third series of curves was obtained showing the linear dependence of the unitary rate on the logarithm of the current density. This result is predicted from the empirical law of anodic film growth $I = A_+e^{B_+F}$ where I is the total anodic current, A_+ and B_+ are the electrolytic parameters, and F is the field across the oxide film.

Aluminum.—Fig. 1 shows the potential vs. time curve for annealed Al abraded on 400 paper. The log

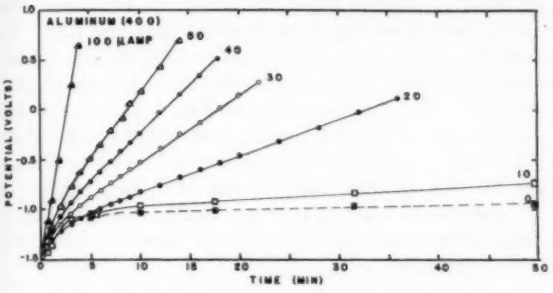

Fig. 1. Potential vs. time for Al abraded on 400 grit paper. Anodized in air-saturated ammonium borate solution at 25°C.

rate vs. log time and log current density curves for Al abraded on 3/0 and 400 are similar in form to that shown for Ta in Fig. 2. Fig. 3 shows the plots of unitary rates vs. log current density. The 400 test as seen from the dotted line shows deviation from linearity. However, for purposes of calculation a straight line was drawn through the intermediate points.

Experimental runs in the region below 10 μ amp were found to give unreproducible results. Indeed, the formation rate at 10 μ amp is seen to be scarcely more than that at zero applied current. Although Al is considered here to be a genuine film former under the conditions of these experiments, the abnormally low film formation rate, which may be due to partial dissolution of the film, did prevent ready discrimination of the results at the lowest current densities, i.e., below 10 μ amp. Reproducibility on the 3/0 emery cloth with Al was found to be very poor. This was attributed to the virtual impossibility of duplicating the degree of abrasion between runs. High purity Al is extremely soft, and consequently very small changes in pressure during abrasion would be expected to cause large variations in the degree of abrasion and, hence, in the real surface area. The increased formation rate of the 400 grit over the 3/0 grit quite probably reflects this difference.

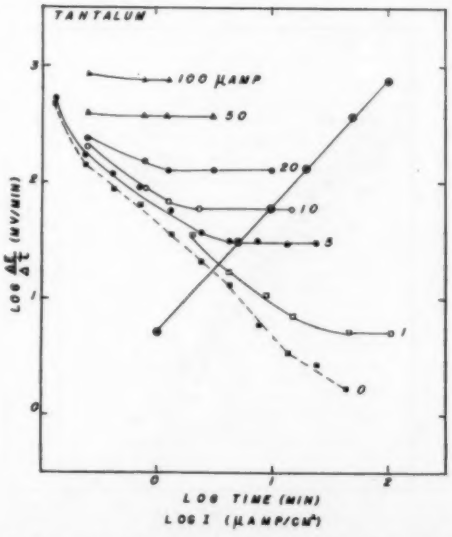

Fig. 2. Log rate of change of potential vs. log time and vs. log current density of Ta in air-saturated ammonium borate solution at 25°C.

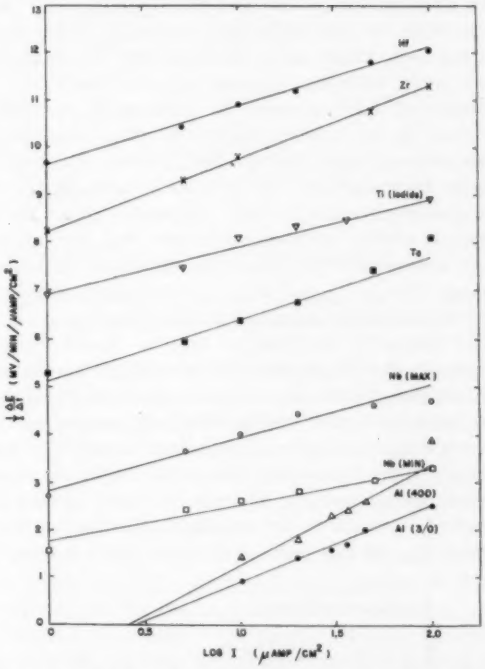

Fig. 3. Comparison of the unitary formation rate vs. the log of the current density for Hf, Zr, iodide titanium, Ta, Nb, and Al. Air-saturated ammonium borate at 25°C.

Since 3/0 was found to be unsuitable, 400 grit paper was used and reproducibility found to be more satisfactory. Despite the improvement noted using 400 grit paper, other variables continued to influence the formation rate. In particular, it was found that the age of the ammonium borate electrolyte had a pronounced effect on the results. A fresh, i.e., previously unused, solution produced formation rate values about 30% lower than those obtained in solutions which had been used repeatedly (a possible indication of solubility of the film in the electrolyte or of discharge of certain anions in the solution, such as chloride).

Attempts to study the effect of cold work on the formation rate for Al were abandoned because of these irregularities.

Titanium.—Ti received the most detailed examination of the metals tested in the present investigation. Iodide titanium was tested because of its relatively higher purity compared with the commercial Kroll process metal.

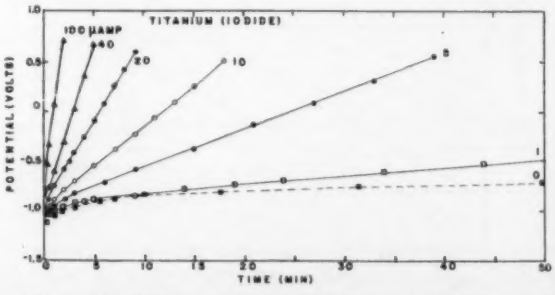

Fig. 4. Potential vs. time for iodide titanium abraded on 3/0 emery. Anodized in air-saturated ammonium borate solution at 25°C.

In addition to iodide and Kroll process Ti (corresponding to two different purities), three series of runs were made using Kroll process Ti which had been given different degrees of cold work. Three cylinders of Kroll process Ti of about ⅝ in. diameter and ½, ½, and ¾ in. in height, respectively, were vacuum annealed at 800°C, then cold pressed axially to reductions of 11%, 24%, and 34% each. The specimen reduced 34% slipped in shear on the diagonal of the pressed cylinder and the slipped plane was made the face of the specimen for anodic testing. The 11% and 24% cold-worked specimens were tested on the original circular faces.

The specimen reduced 11% was found to give values of the formation rate virtually unchanged from annealed material. The specimen reduced 24% gave slightly higher values than the annealed, but of such slight differences as not to be clearly conclusive. The specimen reduced 34%, however, showed quite positive increase. Fig. 4 shows the potential-time curve for iodide Ti. Curves for Kroll process Ti and the 34% cold work were indentical in form but with greater slopes in each case, the cold-worked having greater slope than the Kroll Ti, and the latter more than iodide. It should be noted that the zero applied current curve was nearly identical for the three cases. Fig. 5 shows the log rate vs. log time and log current density for iodide Ti. Fig. 6 shows the dependence of the unitary rate on the log current density for the three types of Ti specimens. Kroll process and the cold-worked specimens gave curves displaced upward from the iodide curves.

Other metals.—Results for iodide Hf are shown in Fig. 7. The log rate vs. log time and log current

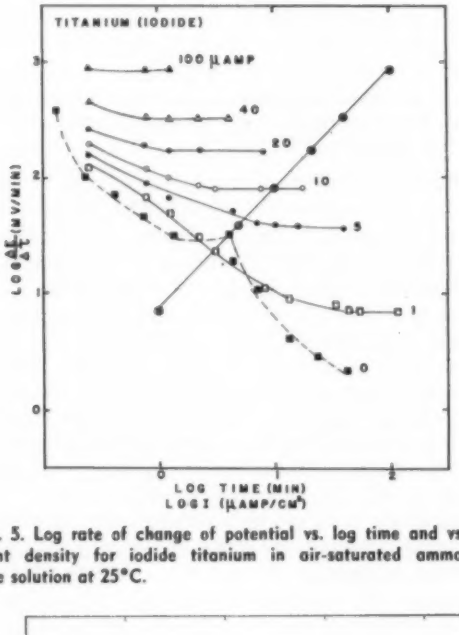

Fig. 5. Log rate of change of potential vs. log time and vs. log current density for iodide titanium in air-saturated ammonium borate solution at 25°C.

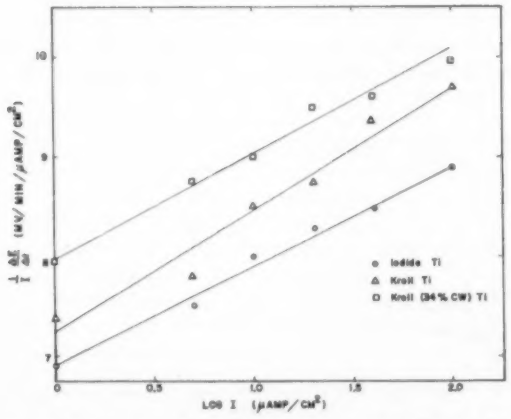

Fig. 6. Unitary formation rate vs. log current density for iodide titanium, Kroll process Ti, and Kroll process, 34% cold-worked Ti. Air-saturated ammonium borate solution at 25°C.

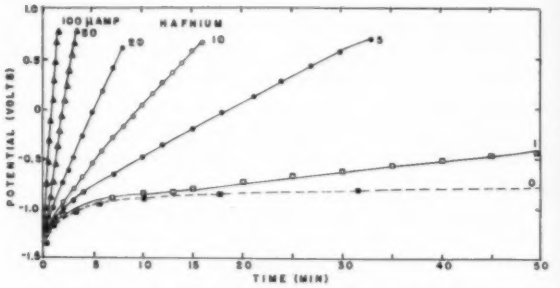

Fig. 7. Potential vs. time for Hf abraded on 3/0 emery. Anodized in air-saturated ammonium borate solution at 25°C.

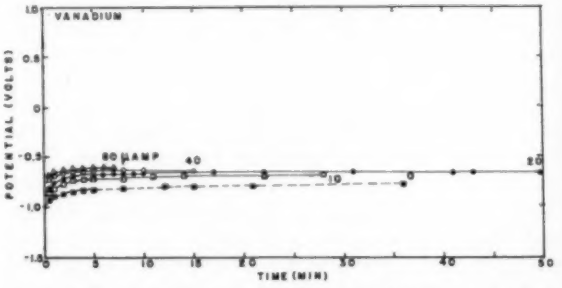

Fig. 8. Potential vs. time for V abraded on 3/0 emery. Anodized in air-saturated ammonium borate solution at 25°C.

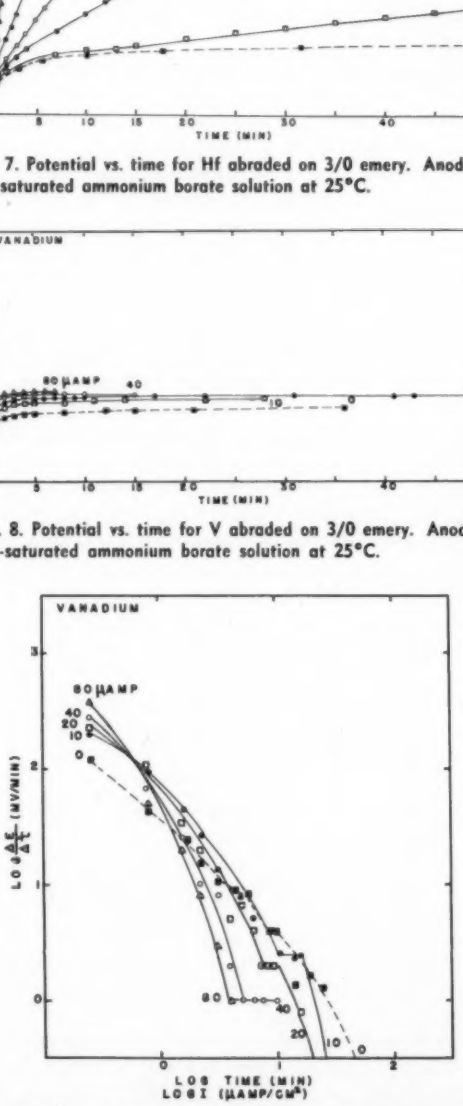

Fig. 9. Log rate of change of potential vs. log time and vs. log current density of V in air-saturated ammonium borate solution at 25°C.

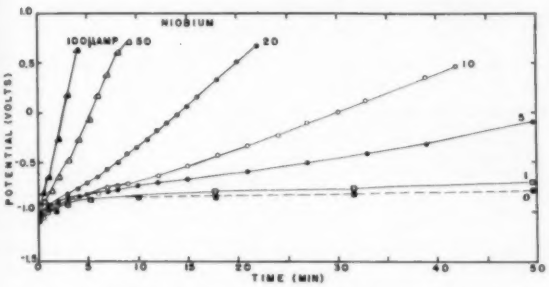

Fig. 10. Potential vs. time for Nb abraded on 3/0 emery. Anodized in air-saturated ammonium borate at 25°C.

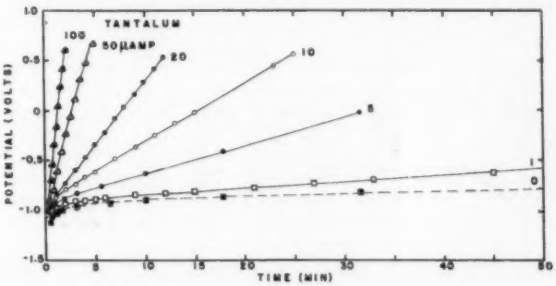

Fig. 12. Potential vs. time for Ta abraded on 3/0 emery. Anodized in air-saturated ammonium borate solution at 25°C.

density curve is again of the same type as shown by Ta, Fig. 2.

Results for V are shown in Fig. 8 and 9.

Results for Nb are shown in Fig. 3, 10, and 11.

Potential vs. time curves for Ta are shown in Fig. 2, 3, and 12.

Results for Cr are shown in Fig. 13. The log rate vs. log time curves are of the same type as shown by V, Fig. 9. Anodization of Cr at high current densities gave a distinctly green dissolution product.

Discussion

Metal Types

The results show that the metals tested under the conditions of these experiments fall roughly into three categories: (*a*) the non film-formers Cr and V; (*b*) the film-formers Al, Ti, Hf, Ta, and Zr; (*c*) an intermediate class containing Nb as a single member.

Examination of the potential-time curves for representative metals of these groups, for example, V, Ta, and Nb, show certain differences. The V potential time curves (Fig. 8) rise rapidly to a nearly constant common value of about minus 0.6 v. This potential is far below that of oxygen evolution. Ta, on the other hand, shows (Fig. 2) a family of curves typical of a film former. Each curve has an initial sharp rise followed by a distinctly linear portion which persists up to the oxygen evolution potential, where the rate falls off suddenly. Increasing current density does not change this characteristic behavior; only the slope of the linear portion of the curve is increased, and the time to reach oxygen evolution potentials is decreased.

Nb (Fig. 10) shows another set of curves. While superficially resembling the performance of the film formers, the behavior is somewhat different. In the potential time plots the expected "linear" portion is not linear, as may be determined by sighting along the curves in the plane of the page.

The differences among the three types are more apparent, however, when the logarithm of the rate of change of potential log ($\Delta E/\Delta t$) is plotted vs. the logarithm of the time. The data for V (Fig. 9), Ta (Fig. 3), and Nb (Fig. 11) may be compared. The non film-former V is seen to give an initial negative slope which rapidly becomes steeper. With the exception of several unexplained arrests at the higher current densities (for both V and Cr), the curves appear to go downward steadily. This type of curve can be explained possibly on the basis of film dissolution, or else on the basis of an extremely porous film structure. In the case of Cr and V the only effect of increasing current density was merely to accelerate the rapid rise of potential to a constant value.

For the typical film-former Ta (Fig. 2) the curves are seen to decrease more or less rapidly to horizontal lines corresponding to the linear region of constant slope of the potential-time plot.

For Nb (Fig. 11), an initial decrease to a minimum followed by a distinct rise to a maximum is observed. This suggests a combination of the non-

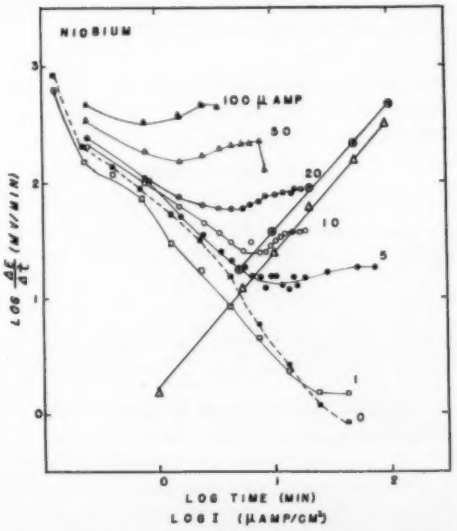

Fig. 11. Log rate of change of potential vs. log time and vs. log current density for Nb in air-saturated ammonium borate solution at 25°C.

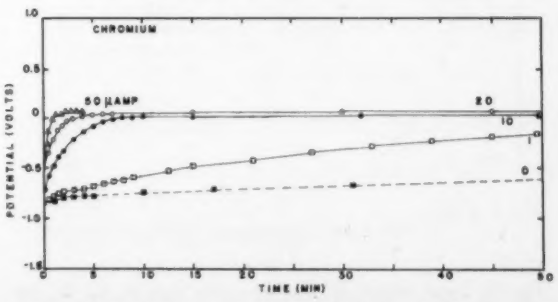

Fig. 13. Potential vs. time for Cr abraded on 3/0 emery. Anodized in air-saturated ammonium borate solution at 25°C.

Table II. Local currents (electrolyte: saturated ammonium borate)

Metal	A mv/min	B slope	(μamp/cm^2) at time Current (min) 0.5	1	5	10	50
Al 3/0	0.355	1.45	36.3	30.2	17.4	9.33	0.925
Al 400	0.447	1.5	67.6	53.7	11.8	5.01	0.977
Ti (iodide)	7.08	1.05	7.94	4.63	2.69	0.895	0.282
Ti (Kroll)	6.61	1.12	7.84	5.41	3.66	0.815	0.38
Ti (Kroll CW)	7.94	1.07	6.50	4.72	1.61	0.65	0.18
Hf (iodide)	10.5	1.03	10.12	8.91	2.09	0.855	0.007
Nb (Max)	3.16	1.06	32.4	17.4	3.31	1.24	0.141
(Min)	1.78	1.12	44.7	25.1	5.19	2.05	0.263
Ta	5.25	1.08	12.3	7.25	1.90	0.899	0.330

film-former and film-former types and hence Nb was considered as belonging to an intermediate type.

Since no distinct horizontal portion of the curve was obtained on the log rate vs. log time plot, the customary plot of log constant rate vs. log current density could not be obtained. However, by assuming either the maxima or minima of the curves to be constant rate portions, a linear relationship was again obtained in both cases. The two straight lines are shown in Fig. 11.

The fact that the potential changes with time, even at zero applied current, has been interpreted as due to a film building process resulting from the passage of local currents between microscopic anodes and cathodes in the surface of the electrode. A method for estimating these local currents at a given time has been developed (1). The rate of change of applied potential with time necessary to maintain a constant current has been found to fit the relationship

$$\Delta E/\Delta t = AI^B \qquad \text{(I)}$$

or

$$\log \Delta E/\Delta t = \log A + B \log I \qquad \text{(II)}$$

where E is the potential, I the current density, and A is the formation rate at unit current density.

Constants A and B are determined from the log rate vs. log I plot and the value of log formation rate at a given time read from the zero applied current curve. From this the local current I at the given time may be calculated. Table II lists the local currents for the various metals at 0.5, 1, 5, 10, and 50 min, respectively, together with the constants A and B. Except for Al, the value of B is seen to be remarkably constant, even among the different metals. The constant A, however, shows a large variation

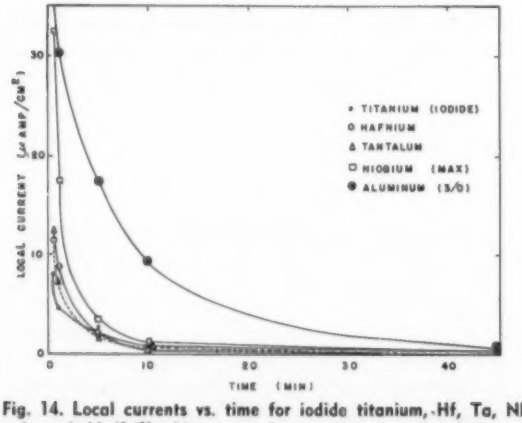

Fig. 14. Local currents vs. time for iodide titanium, Hf, Ta, Nb (max), and Al (3/0). Air-saturated ammonium borate solution at 25°C.

Table III. Unitary formation rates (mv/min/μ amp/cm^2)

Metal	Current Density 1	5	10	20	30	40	50	100
Ti (iodide ann)	6.9	7.4	8.1	8.3		8.4		8.9
Ti (Kroll ann)	7.4	7.8	8.5	8.9		9.35		9.5
Ti (Kroll 34%)	7.95	8.75	9.0	9.5		9.6		9.95
Zr (Kroll ann)	8.2	9.3	9.8				10.8	11.3
Hf (iodide ann)	9.7	10.45	10.9	11.2			11.8	12.05
V				No stable film				
Nb (Max)	2.7	3.6	4.0	4.4			4.6	4.7
(Min)	1.55	2.4	2.6	2.8			3.05	3.3
Ta	5.25	5.95	6.35	6.75			7.4	8.1
Cr				No stable film				
Al (3/0)			0.9	1.4	1.6	1.7	2.0	2.5
Al (400)			1.4	1.8	2.3	2.4	2.6	3.9

among the metals. Two sets of values for Nb are included, reflecting the fact that the local currents are calculated from the maximum or minimum values of the log rate vs. log I plots.

The local current values for Ti, Hf, and Ta are of the same order as those calculated for Zr (1) both in ammonium borate and other electrolytes, i.e., about 10 μ amp/cm^2 at about 0.5 min. For Nb, however, a value between 32 and 44 μ amp/cm^2 was obtained, and for Al, abraded on 400 grit paper, the very large value of 67.6 μ amp/cm^2 was obtained. At 50 min it had diminished to only 1 μ amp/cm^2. Fig. 14 shows a plot of the local currents vs. time for the film-formers. Only Al appears to diverge from the pattern of the other metals.

Unitary Formation Rates

The unitary formation rate, $1/I$ $(\Delta E/\Delta t)$, or R_I, affords some comparison of the behavior of the different metals. Table III gives the values for the metals examined in the present work, plus Zr from other work for comparison.

Table III shows that R_I increases with current density for a given metal. The R_I value is found to increase also with impurity content in Ti and to increase with cold work.

Further, if the metals are arranged according to their places in the periodic table as in Table IV, the R_I values for all current densities show an increase in going from top to bottom and from right to left as shown by the path of the arrows. Values of R_I for 100 μ amp/cm^2 are arranged in Table IV for illustration.

The position of Al is somewhat uncertain, but the very low unitary formation rate does show that it probably belongs to the right in the table.

Electrolytic Parameters

Plots of the unitary formation rate vs. log current density gave linear relationships as predicted from the empirical law of anodic film growth

$$I = A_e e^{B_e F} \qquad \text{(III)}$$

where I is the total anodic current, A_e and B_e are electrolytic parameters, and F is the field across the

Table IV. Trends of R_I with the Periodic Table

Al (2.5) 3/0
(3.9) 400

Ti (8.9) | V (0) Cr (0)
Zr (11.3) | Nb (4.7) max
(3.3) min
Hf (12.05) | Ta (8.1)

Table V. Electrolytic parameters

Metal	Slope	Intercept $\frac{mv}{min}$ $\frac{cm^2}{\mu amp}$	σA_+ $\mu amp/cm^2$	σB_+ cm/v	$F_{100/\sigma}$ v/cm	$B_+ F_{100}$
Ti (iodide)	1.0	6.9	1.23×10^{-7}	6.75×10^{-6}	3.04×10^{6}	20.5
Ti (Kroll)	1.2	7.25	8.91×10^{-7}	5.63×10^{-6}	3.30×10^{6}	18.6
Ti (Kroll 34%)	1.1	8.0	5.37×10^{-8}	6.14×10^{-6}	3.48×10^{6}	21.4
Zr ref. (36)	1.69	7.68	2.9×10^{-5}	4.6×10^{-6}	3.26×10^{6}	15
Hf	1.25	9.6	2.09×10^{-6}	6.2×10^{-6}	3.60×10^{6}	22.3
Nb Max	1.15	2.7	4.47×10^{-5}	7.35×10^{-6}	1.36×10^{6}	10.0
Nb Min	0.75	1.8	3.98×10^{-3}	11.3×10^{-6}	0.89×10^{6}	10.1
Ta	1.28	5.07	1.05×10^{-4}	5.8×10^{-6}	2.38×10^{6}	13.8
Al (3/0)	1.6	—0.7	2.74	3.8×10^{-6}	0.95×10^{6}	3.6
Al (400)	2.12	—0.7	2.14	2.86×10^{-6}	1.34×10^{6}	3.84

oxide film. The Cabrera-Mott theory leads to an equation of the above type (29).

It is possible (2) to calculate A_+ and B_+ using the slope and intercept of the unitary rate vs. log I plot. The values of σA_+ and σB_+ (where σ is the roughness factor), with the slopes and intercepts they are calculated from, are shown in Table V. The dimensionless constant B_+F_{100} for each metal is also shown (where F_{100} is the formation field for a current of 100 μ amp/cm^2).

In addition to the results reported in Table V for Ta, low potential runs were made on the same specimen in 0.1% Na_2SO_4 solution at 48°C, using both mechanically polished and bright-etched surfaces. The average unitary formation rate obtained for 25 different runs was 19.0 $\frac{mv}{min} \frac{cm^2}{\mu amp}$. This corresponds to $F_{100/\sigma} = 6.3 \times 10^6$ v/cm using 8.74 g/cc for the density of tantalum oxide. Formation rates on the polished surfaces were not constant. The time required for the potential to increase by 200 mv was measured over the pre-oxygen evolution potential range. Eighty-three of these measurements were taken in the 25 different runs and averaged to obtain the final average unitary formation rate.

Ta was studied in the high potential range by Vermilyea (14) and by Young (25). Vermilyea obtained a value of $F_{100/\sigma}$ for anodic Ta_2O_5 films on bright-etched Ta of 6.13×10^6 v/cm. These measurements were made at 48°C in 0.1% Na_2SO_4 solution. Young obtained 6.17×10^6 v/cm (interpolated to 48°C) for Ta_2O_5 formed on mechanically polished Ta in 0.5M Na_2SO_4.

The product B_+F_{100} may be used as an estimate of the amount the activation barrier must be lowered by the field in order that a constant current density of 100 μ amp/cm^2 may pass through the oxide film. The higher the zero-field barrier height, the higher the product B_+F_{100} should be for a given metal. (The parameter A_+ should also be a measure of this barrier height; an increase in barrier height would decrease A_+.)

It would also be expected that the local current would decay at increasing rate for increasing barrier height for a given metal.

The foregoing treatment permits an analysis, up to a point, of the kinetics of the film building process. An alternative treatment, more directly based on the methods of electrochemical kinetics, has been developed and will be the object of another communication.

Acknowledgments

The receipt by one of the authors (H.A.J.) of a fellowship from the Alcoa Research Foundation is gratefully acknowledged. The kind assistance received from the personnel of the U. S. Bureau of Mines Station at Albany, Ore., in the preparation and analysis of several specimens, is acknowledged with thanks. The work on Zr, referred to here for comparison, was carried out under contract AT(45-1)-535 between the University of Oregon and the U.S. Atomic Energy Commission.

Manuscript received July 17, 1956. This paper was prepared for delivery at the San Francisco Meeting, April 29 to May 3, 1956. It was taken from the thesis submitted by H. A. Johansen in partial fulfillment of the requirements for the Ph.D. degree.

Any discussion of this paper will appear in a Discussion Section to be published in the December 1957 JOURNAL.

REFERENCES

1. M. Maraghini, G. B. Adams, Jr., and P. Van Rysselberghe, *This Journal*, **101**, 400 (1954).
2. G. B. Adams, Jr., P. Van Rysselberghe, and M. Maraghini, *ibid.*, **102**, 502 (1955).
3. A. Güntherschulze and H. Betz, *Z. Physik*, **68**, 145 (1931).
4. A. Güntherschulze and H. Betz, *Z. Elektrochem.*, **37**, 726 (1931).
5. A. Güntherschulze and F. Keller, *Z. Physik*, **75**, 78 (1932).
6. A. Güntherschulze and H. Betz, *ibid.*, **92**, 367 (1934).
7. A. Güntherschulze and H. Betz, "Elektrolyt-Kondensatoren," M. Krayn, Berlin (1937).
8. R. H. Brown and R. B. Mears, *Trans. Electrochem. Soc.*, **74**, 495 (1938).
9. R. B. Mears, *J. (and Trans.) Electrochem. Soc.*, **95**, 1 (1949).
10. R. B. Mears and R. H. Brown, *This Journal*, **97**, 75 (1950).
11. R. H. Brown, G. C. English, and R. D. Williams, *Corrosion*, **6**, 186 (1950).
12. W. G. Burgers, A. Claasen, and I. Zernike, *Z. Physik*, **74**, 593 (1932).
13. A. Charlesby, *Acta Met.*, **1**, 340 (1953).
14. D. A. Vermilyea, *ibid.*, **1**, 282 (1953).
15. R. B. Mason and C. J. Slunder, *Ind. Eng. Chem.*, **39**, 1602 (1947).

16. A. Charlesby, *Proc. Phys. Soc. (London)*, **B66**, 317 (1953).
17. M. S. Hunter and P. Fowle, *This Journal*, **101**, 481 (1954).
18. C. D. Hall, Jr., and N. Hackerman, *J. Phys. Chem.*, **57**, 262 (1953).
19. R. D. Misch and E. S. Fisher, *This Journal*, **103**, 153 (1956).
20. R. K. McKechnie and A. U. Seybolt, *ibid.*, **97**, 311 (1950).
21. E. Deltombe, N. de Zoubov, and M. Pourbaix, Report 29, "Electrochemical Behavior of Vanadium," *Centre Belge d'Etude de la Corrosion*, Brussels, January (1956).
22. U. Sborgi, *Gazz. chim. ital.*, **42**, II, 331 (1912).
23. G. Schulze, *Ann. Physik*, **25**, 775 (1908).
24. L. Young, *Trans. Faraday Soc.*, **51**, 1250 (1955).
25. L. Young, *ibid.*, **50**, 153 (1954).
26. H. E. Haring, *This Journal*, **99**, 30 (1952).
27. D. A. Vermilyea, *Acta Met.*, **2**, 476 (1954).
28. J. F. Dewald, *ibid.*, **102**, 1 (1955).
29. N. Cabrera and N. Mott, *Rep. Prog. Phy.*, **12**, 163 (1948).
30. R. H. Roberts and W. J. Shutt, *Trans. Faraday Soc.*, **34**, 1455 (1938).
31. I. Issa, I. Ammar, and H. Khalifa, *J. Phys. Chem.*, **59**, 492 (1955).
32. A. Charlesby, Atomic Energy Research Establishment M/R 714, Harwell, Berks, England, May 1951.
33. R. D. Misch and W. E. Ruther, *This Journal*, **100**, 531 (1953).

Metal-Water Reactions

IV. Kinetics of the Reaction between Calcium and Water Vapor

Harry J. Svec and Charles Apel

Institute for Atomic Research and Department of Chemistry, Iowa State College, Ames, Iowa

ABSTRACT

Calcium metal was reacted with water vapor in the temperature range 20°-70°C and at water vapor pressures of 18-93 mm Hg. The experiments indicated that the only products were $Ca(OH)_2$ and H_2 and that the reaction proceeded according to the equation

$$Ca + 2H_2O \rightarrow Ca(OH)_2 + H_2$$

A manometric study of the reaction showed that it followed the logarithmic rate law. The rate constant was observed to be linearly dependent on water vapor pressure below 70°C and to decrease with increasing temperature in the range 20°-50°C. At 70°C the rate constant was observed to be independent of water vapor pressure. The activation energy was found to be —7.52 kcal/mole in the pressure dependent range.

The kinetics of gas-metal reactions involving N_2, O_2, and H_2 have been widely studied and numerous references are available (1). Recently there has been interest in the reactions between metals and water vapor. Svec and Deal have shown that Li (2) and Th (3) both follow the logarithm law when reacted with water vapor.

A study of the rate at which reaction takes place between Ca and water vapor was undertaken in order to compare the reactivity of Ca with that of Li and the other alkaline earth metals. An examination of reaction products showed that the reaction takes place according to the equation

$$Ca + 2H_2O \rightarrow Ca(OH)_2 + H_2 \qquad (I)$$

Because of the nature of the reaction, the rate was followed by observing the evolution of H_2 as a function of time. Conditions of temperature and water vapor pressure were regulated carefully in order to determine their effect on the rate of the reaction.

Experimental

One pound cylinders of cast, redistilled Ca metal were obtained from the Metallurgical Division of the Ames Laboratory. Spectrographic analysis showed that the impurities totalled approximately 0.5%, occurring as a mixture of Al, Ba, Cr, Fe, Mg, Mn, Si, Sr, Y, and Zr. Some of these elements, notably Y and Zr, were probably introduced in trace amounts during the machining of the sample specimens. Rough cylinders, approximately ½ in. in diameter and 2 in. in length, were cut and turned under Na-dried turbine oil on a lathe in the machine shop. They were then finished by machining on a lathe mounted in a controlled atmosphere box containing He. The final machining conditions were carefully duplicated for each cylinder to insure uniform metal surfaces for the entire group of specimens used in this study. Before use, freshly prepared cylindrical specimens were stored under Na-dried turbine oil through which purified He had been bubbled.

Immediately preceding use, dimensions of each cylinder were measured with machinists' calipers. Following this, a stainless steel hook was fastened to the top of the cylinder in order to hang the cylinder in the reaction vessel. The oil in which the Ca had been stored was removed by means of rinses in Na-dried, low boiling petroleum ether, followed by one rinse in Na-dried diethyl ether.

The reactions occurred in apparatus slightly different from the one described in a paper to be published.[1]

During the study, water vapor pressures of 18, 32, 55, 72, and 93 mm Hg were used at reaction temperatures of 20°, 25°, 30°, 35°, 40°, 45°, 50°, 55°, 60°, and 70°C. Water was introduced into the apparatus through the Hg covered serum bottle stopper by means of a hypodermic syringe. As the reaction between water vapor and Ca proceeded, the pressure of the H_2 evolved was continuously followed by means of a recording Hg manometer (4).

Values for the amount of water vapor undergoing reaction per unit area of metal were obtained from H pressures by determining the total volume of the reaction apparatus and the volume and surface areas of the Ca cylinder. The H_2 pressures were obtained by subtracting the water vapor pressure employed in a particular run from the total gas pressures throughout the run. It was assumed that the Ca surface areas obtained from the cylinder dimensions and used in these calculations were minimum areas, but that they were proportional to the true areas by a constant factor. The reproducibility of the experimental results supported this assumption.

Results

Inasmuch as the reaction of Ca with water vapor proceeds with the formation of a surface film, the reaction data are expected to fit one of the gas-solid reaction rate laws. A comparison of the most common of these laws (5,6) is presented in Fig. 1. It is evident that a straight line is followed by the logarithmic treatment of the data, while the linear, parabolic, and cubic plots are curved. Plots of data from water vapor-Ca reactions at other temperatures and pressures corroborate this conclusion.

The value of the constant in the logarithmic equation was set equal to 0.4 by Brodsky and Cubicciotti (7) in silicon-oxygen reaction rate studies. Svec and Deal observed that a value of 0.45 for a fit the data when water vapor was reacted with Li (2) and Th (3). The value 0.45 also fit the data in the present study.

Logarithmic plots were made for each reaction and values of the logarithmic rate constant K were obtained from the slopes of the first 100 min of the curves. Several typical plots are shown (Fig. 2) for reaction data obtained at various temperatures and a water vapor pressure of 32 mm Hg. On extending the data presented in Fig. 2 over longer periods of time, definite changes or breaks were observed in the slopes of the curves. After each of these breaks, the reaction rate became unpredictable.

The temperature dependence of the rate constant K was determined by plotting the values of K obtained at constant water vapor pressure against temperature, as shown in Fig. 3. The rates were found to decrease with increasing temperature until attaining a minimum between 50° and 70°C. The rate then increased with temperature up to 70°C, which was the highest temperature employed in this study. With the exception of the runs at 18 mm Hg, all isobars converge to a K value of about 12 at 70°C.

[1] This Journal, July 1957 issue.

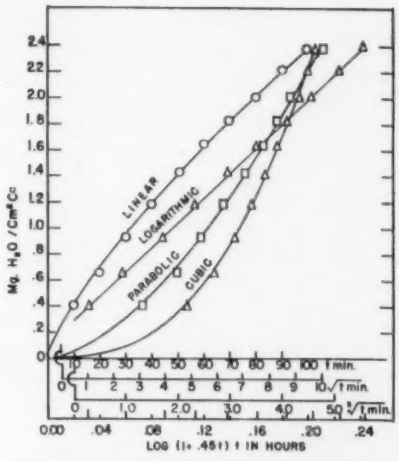

Fig. 1. Comparison of four rate laws for gas-metal reactions using Ca-water vapor data. Temperature, 36°C; water vapor pressure, 32 mm Hg.

Arrhenius plots were made for each isobar over the temperature range in which the reaction rate decreased with increasing temperature, and activation energies were obtained from the slopes of the lines. These were positive (Fig. 4) and were linear within experimental error, indicating negative energies of activation. At the temperatures employed the activation energy appeared to be independent of water vapor pressure and had an average value of -7.52 ± 0.28 kcal/mole.

The dependence of the rate constant on water vapor pressure was determined by plotting the values of K at constant temperature against water vapor pressure. Each isothermal plot was linear and most of them indicated a value of zero for K at a vapor pressure of about 10 mm Hg.

On the basis of the pressure dependence of the rate constant and the activation energy -7.52 ± 0.28 kcal/mole, an empirical equation was derived relating the rate constant K to temperature and water vapor pressure. This equation states that

$$K = A(P - 10)e^{3785/T} \text{ mg } H_2O/cm^2 \text{ Ca surface-log hr} \qquad (II)$$

where A is a constant, P is the water vapor in mm Hg, and T is the absolute temperature. The value 3,785 is the $-Q/R$ of the Arrhenius equation which states that K is proportional to $e^{-Q/RT}$. The constant -10 was taken from the value for P when $K = 0$ from the plots of the rate constant vs. water vapor pressure.[2] This equation applies to the temperature range 20° –60°C in which the minimum values of the rate constant occur as indicated in Fig. 3. In this range the constant A was found to have a value of $(2.57 \pm 0.31) \times 10^{-4}$ mm H_2O/cm^2 Ca mm Hg log hr. Using this value leads to the rate expression

$$W = 2.57 \times 10^{-4}(P - 10)e^{3785/T} \log (1 + 0.45t) \qquad (III)$$

where W is the number of milligrams of water consumed per square centimeter of Ca surface, P is the water vapor pressure in millimeters of mercury,

[2] The authors believe that a different rate law is followed at pressures below 10 mm. No experimental data were obtained, however, due to the limitations of the present method. $K = 0$ only applies here where the logarithmic law holds.

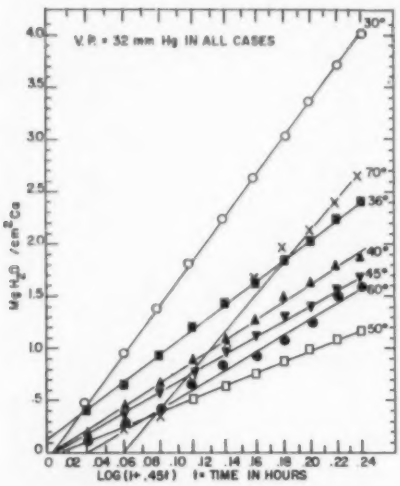

Fig. 2. Logarithmic plot of Ca-water vapor data at 32 mm Hg water vapor pressure and varying temperatures.

T is the absolute temperature, and t is the time in hours. Values of K determined from Eq. (II) compare favorably with the experimental values of K obtained in the water vapor pressure dependent ranges.

The ratio of the molecular volume of $Ca(OH)_2$ to that of Ca metal is 1.20. According to Evans (8) such a ratio should lead to blistering and flaking as the coat thickens. This was found to be true, especially for runs of more than 100-min duration, after which the reaction rate often changed abruptly and fragments of the $Ca(OH)_2$ coat were observed at the bottom of the reaction vessel. Under such conditions, $Ca(OH)_2$ does not form a truly protective coating, but is crazed with minute cracks giving rise to many possible diffusion paths.

Discussion of Results

Inasmuch as a reaction product film separates the two species undergoing reaction, a diffusion process must occur before reaction can take place. Either water molecules must be absorbed and diffuse in-

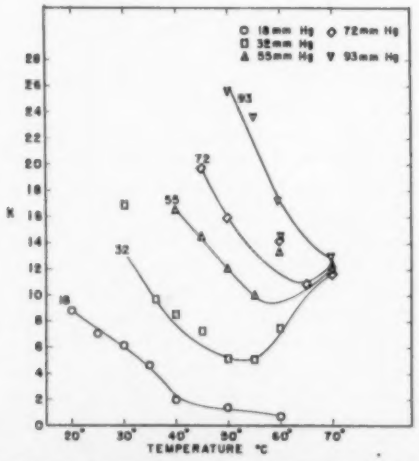

Fig. 3. Effect of temperature on rate constants from Ca-water vapor data. Units of K are mg H_2O/cm^2 Ca.

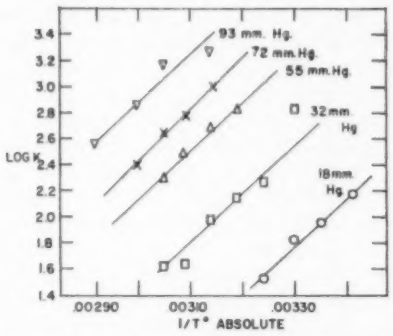

Fig. 4. Log K vs. $1/T$ at different water vapor pressures from Ca-water vapor data. Units of K are mg H_2O/cm^2 Ca. (Naperian logarithms are plotted in this figure.)

ward or Ca ions must diffuse outward. It is possible that a combination of both occurs. The first order dependence of the rate constant on water vapor pressure indicates that, in the temperature range 20°-50°C, the inward diffusion of water molecules through the crazed reaction product coat is probably the rate-controlling step. Further evidence in support of this concept is the decrease of the reaction rate with increasing temperature in this range. To explain this dependence of the reaction rate on temperature and water vapor pressure (9), it should be considered that the number of water molecules striking the $Ca(OH)_2$ surface is directly proportional to the water vapor pressure at a given temperature. Of these, a certain fraction adhere and diffuse inward through the $Ca(OH)_2$ layer. However, as the temperature of the system increases, some of the adhered water molecules atta enough thermal energy to break away from the surface of the specimen and return to the gas phase. This process decreases the number of molecules which can diffuse through the $Ca(OH)_2$ coat and become available for reaction with the Ca, and leads to a reduction in the value of the rate constant. A negative activation energy as a heat of desorption results. At 70°C, the reaction rate becomes independent of the water vapor pressure, probably because of another mechanism becoming dominant, such as the outward diffusion of Ca ions through a coating in which crazing is at a minimum or is absent due to healing of the crystal discontinuities.[3] In this case the Ca ions and electrons reach the $Ca(OH)_2$ gas interface and undergo reaction with all available water molecules before the water molecules receive sufficient thermal energy to escape from the surface. The number of Ca ions diffusing outward then becomes the rate-controlling factor. When this process becomes rate-controlling, the reaction rate should increase with temperature because the rate at which Ca ions diffuse outward increases with increasing temperature. This was found to be true (Fig. 3) inasmuch as

[3] That this is reasonable is indicated by some work in which samples of both $Ca(OH)_2$ and $Ca(OD)_2$ were prepared by the metal-water vapor reaction at room temperature. X-ray data on this materials as it was first prepared were very poor, appearing as extremely diffuse or even spotty powder diagrams. Annealing the material at about 100°C in the presence of water vapor completely eliminated this difficulty, indicating considerable crystal growth by a kind of coalescing of very small crystallites. X-ray diagrams of the $Ca(OH)_2$ coating from reactions at 70°C show considerably sharper lines than do those from material produced at lower temperatures.

the reaction rate was observed to increase with temperature as soon as the pressure dependence disappeared.

The work in this study was limited to the temperature range 20°-70°C. The inward diffusion of water molecules through the $Ca(OH)_2$ coat is primarily responsible for the observed phenomena. Further studies at higher temperatures are complicated by the formation of new or different reaction products. The work of Svec and Gibbs (10) certainly supports this contention. A detailed study at temperatures above 70°C is under way. The results of this new study differ from those reported here and will be reported separately.

Manuscript received August 6, 1956. Work was performed in the Ames Laboratory of the A.E.C. Contribution No. 000.

Any discussion of this paper will appear in a Discussion Section to be published in the December 1957 JOURNAL.

REFERENCES

1. O. Kubaschewski and B. E. Hopkins, "Oxidation of Metals and Alloys," Academic Press Inc., New York (1953).
2. H. J. Svec and B. E. Deal, *J. Am. Chem. Soc.*, **75**, 6173 (1953).
3. B. E. Deal, Ph.D. Thesis, Iowa State College Library, Ames, Iowa (1955).
4. H. J. Svec and D. S. Gibbs, *Rev. Sci. Instr.*, **24**, 202 (1953).
5. N. F. Mott, *Trans. Faraday Soc.*, **36**, 472 (1940).
6. N. B. Pilling and R. E. Bedworth, *J. Inst. Metals*, **29**, 529 (1923).
7. M. Brodsky and D. Cubicciotti, *J. Am. Chem. Soc.*, **73**, 3497 (1951).
8. U. R. Evans, *Trans. Electrochem. Soc.*, **91**, 547 (1947).
9. S. Glasstone, "Textbook of Physical Chemistry," 2nd ed., p. 1118-9, D. Van Nostrand Co., Inc., New York (1946).
10. H. J. Svec and D. S. Gibbs, *J. Am. Chem. Soc.*, **75**, 6052 (1953).

Reaction of Zirconium with Water Vapor at Subatmospheric Pressures

M. W. Mallett, W. M. Albrecht, and R. E. Bennett

Battelle Memorial Institute, Columbus, Ohio

ABSTRACT

The reaction of iodide zirconium with water vapor at 33 mm Hg pressure was investigated in the range 300°-600°C. The rates follow a cubic law. The cubic rate constant in $(\mu g/cm^2)^3/sec$ is $k = 6.71 \times 10^3 \exp(-29{,}700/RT)$ where $29{,}700 \pm 700$ cal/mole is the activation energy. Reaction films of monoclinic ZrO_2 are *N*-type semiconductors. Therefore, it is concluded that the mechanism of film formation is the same as that for the zirconium-oxygen reaction.

The performance of Zr in high-temperature water is of great interest in nuclear reactor technology. Therefore, considerable work has been carried out on this subject. Work on the corrosion of Zr in water at high temperature and pressure has been reviewed (1). No specific rate law was reported for the corrosion reaction, but one could infer from the published data that the cubic law might have been followed.

In the usual corrosion testing it is customary to cool the samples from the experimental temperature periodically, remove them from the pressure vessel, and weigh them at room temperature in order to determine corrosion rates. It is not known what effect this periodic temperature cycling may have on the reaction kinetics. Because of the insensitivity of the technique the initial stage of reaction is often indiscernible and the means by which later rate-controlling conditions are established in the surface film cannot be determined. Therefore, the present study of the reaction of Zr with water vapor was made in a system in which continuous measurement of weight gain data could be obtained. Subatmospheric pressure (33 mm Hg) water vapor was used in order to slow the reaction so that the kinetics during the initial period of reaction could be determined. Also, tests were made to determine some of the mechanisms of formation of the reaction products.

Experimental

Material.—Cylindrical test specimens, 1 cm in diameter by 1 cm long, were machined from arc-melted iodide-zirconium rod. For low temperature runs, some of this rod was fabricated into foil, 0.03 cm thick. Results of spectrographic, chemical, and vacuum-fusion analyses are given in Table I. An accelerated corrosion test of this material in 400°C steam gave a weight gain of 360 mg/dm^2 after 90 hr.

Apparatus.—A Sartorious Electrona Microbalance was used to measure the weight gain of the specimen. Essentially this balance is an electronically controlled null-type instrument. The amount of current necessary to maintain balance is measured on a microammeter which is calibrated directly in micrograms.

The balance was evacuated by a three-stage Hg-diffusion pump, backed by a mechanical vacuum pump. A liquid-N cold trap was placed between the pumping system and the microbalance to prevent

Table I. Analysis of arc-melted iodide zirconium

Element	Amount present, wt %
Fe	0.060
Hf	0.030
Cr	0.010
Al	0.010
Ni	0.005
Si	0.003
Mg	0.002
Pb	0.002
Cu	0.002
Ca	0.002
Mn	<0.001
Sn	<0.001
Ti	<0.001
H_2	0.0004*
N_2	0.003
O_2	0.042

* After degassing.

back diffusion of Hg into the balance section. An ionization gauge between the cold trap and balance was used to measure pressures in the system.

The sample was spot welded to a Pt wire 0.005 in. in diameter and 24 in. long, which suspended the sample from the beam of the balance into the reaction tube. A resistance wound furnace was used to heat the specimen. Temperatures were controlled to ±5°C.

Water vapor was supplied to the specimen through a stainless steel bellows-type vacuum valve from a glass storage bulb, containing deaerated distilled water. This water was previously boiled for 5 min at atmospheric pressure. After it was placed in the storage bulb, the bulb was evacuated to 10 mm Hg and held there for ½ hr to remove any dissolved gases that might have remained in the water.

Method.—Rates of reaction of Zr with water vapor were determined by measuring the rates of weight gain of the specimens. Prior to the rate determinations, the specimens were degassed for 4 hr at 800°C. Then they were abraded with dry 240-, 400-, and 600-grit SiC paper. The specimen was suspended in the reaction tube and heated to temperature in a vacuum of 0.01 μ Hg pressure by a resistance-wound furnace. The reaction was started by adding water vapor at a pressure of 33 ± 2 mm Hg to the furnace section. Rate data were not taken until 1 min after the reaction was started to allow for adsorption of water vapor by the Pt suspension wire and balance beam of the microbalance. Preliminary experiments showed this time to be sufficient to establish equilibrium with the apparatus. Weight gain measurements were made at 2-20 min intervals for 6-24 hr. The original geometric dimensions of the specimens were used to calculate the weight gain per unit surface area.

Approximations based on weight gain of samples indicated that the maximum amount of H_2 that was formed in the reactions was 3 ml STP. For most of the reactions the amount of H_2 produced was much less than this. The partial pressure of H_2O in the system remains constant. Because of mass differences the H_2 product does not noticeably effect the diffusion of water vapor from the reservoir to the specimen. Calculations show that the minimum mole ratio of water vapor to H_2 in the reaction chamber was about 3-1.

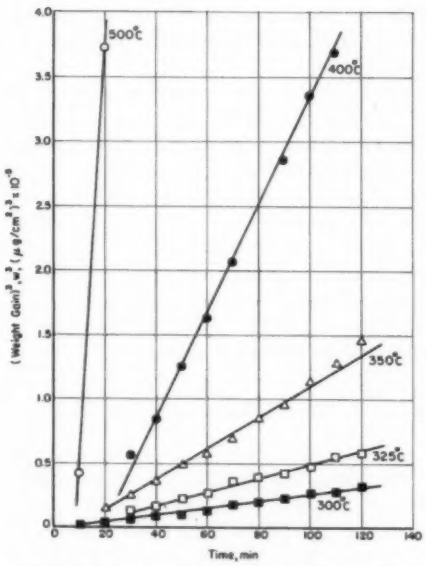

Fig. 1. Reaction of Zr with water vapor at 33 mm Hg pressure

Results

Kinetic data.—Reaction rates of arc-melted iodide zirconium with water vapor at a pressure of 33 mm Hg were measured from 300° to 600°C. The data followed the cubic rate law, $w^3 = kt$, where w is the weight gain in micrograms per square centimeter, t is the time, and k is the cubic rate constant. In Fig. 1, w^3 is plotted against t for several representative experiments. It is seen that the data fall on a straight line. Accordingly a plot of log w vs. log t should give a straight line with a slope of 0.33 if the cubic law is followed exactly. Values of the cubic rate constants, computed from the various plots, and the slopes of the log-log plots are given in Table II. Although the slopes vary somewhat, they agree more closely to the slope for the cubic law than to that for any other simple rate law.

A plot of the cubic rate constants against the reciprocal of the absolute temperature is shown in Fig. 2. The equation for the best straight line through the set of points was calculated by the method of least squares. The Arrhenius equation was used to calculate the energy of activation and frequency factor. In the range 300°-600°C the cu-

Table II. Rate constants for the reaction of arc-melted iodide zirconium with water vapor

Temp, °C	Rate constant, k, in $(\mu g/cm^2)^3/sec$	Slope of log-log plot
300	1.7	0.39
325	9.1	0.35
350	2.8×10	0.41
400	1.2×10^2	0.40
475	1.2×10^3	0.27
500	2.3×10^3	0.39
570	6.7×10^3	0.35
600	2.2×10^4	0.35

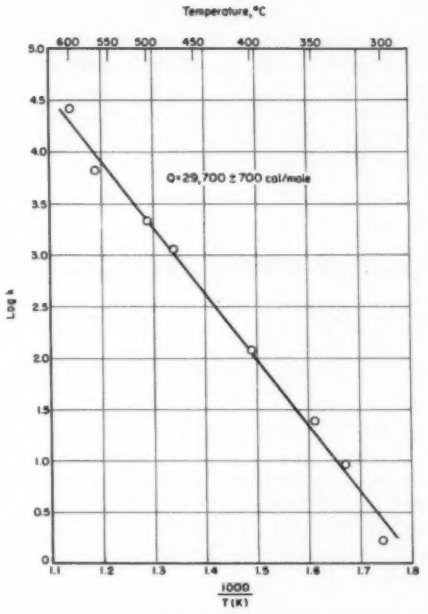

Fig. 2. Temperature dependence of cubic rate constant for reaction of Zr with water vapor.

bic rate constant in $(\mu g/cm^2)^3/sec$ is $k = 6.71 \times 10^8 \exp(-29{,}700/RT)$ where $29{,}700 \pm 700$ cal/mole is the activation energy and the probable error in a calculated k is approximately 2.7%.

Films.—At the end of reaction rate runs, specimens were cooled to room temperature and examined. In all cases, a gray-black film covered the reacted specimens. This film adhered very strongly to the base metal. Metallographic examination showed that the film was a dense single-phased material. A photomicrograph of a film produced on a specimen reacted with water vapor at 400°C for 24 hr is shown in Fig. 3. The film is very thin (about 0.0001 cm) and x-ray analysis showed it to be monoclinic ZrO_2.

Mechanisms.—Experiments were made to determine the mechanisms of the reaction as discussed in a previous study on the oxidation of Zr (2).

A marker experiment was made to determine the diffusing species in the reaction film. The marker was a thin layer of Cr_2O_3 powder (in water) painted on a sheet specimen. The specimen was then reacted with water vapor at 400°C for 1400 hr. At the end of the reaction the Cr_2O_3 marker remained entirely at the film-gas interface indicating that the oxygen ion is diffusing through the film and the ZrO_2 is being produced at the metal-film interface.

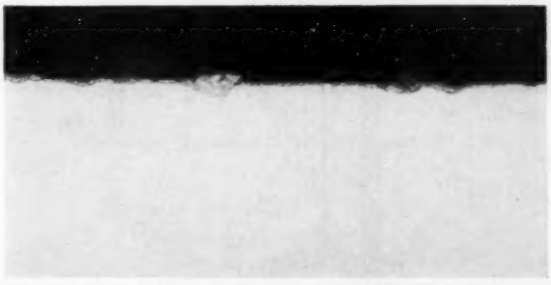

Fig. 3. Zr reacted with water vapor at 400°C for 24 hr. Note thin (0.0001 cm) gray-black film of ZrO_2. Magnification, 1200X.

Thermoelectric power measurements were made to determine the type of electronic conduction through the films. A measurement was made using a hot (700°C) tungsten probe on an oxide film produced on a specimen at 400°C. The sign of the thermoelectric power was found to be negative. Electronic conduction in the films is through excess electrons. Therefore the films are *N*-type semiconductors. Apparently the mechanism of film formation in the reaction of water vapor with Zr is similar to that for the reaction of oxygen with Zr (2).

Specific resistivity measurements made at room temperature on reaction films produced at 400°C gave a value of 4×10^7 ohm-cm. This is considerably lower than the specific resistivity (6×10^{13} ohm-cm) of the films produced in the zirconium-oxygen reaction. This difference in specific resistivity may be caused by H in some form in the film. Vacuum-fusion analysis of an entire reacted specimen (24 hr at 400°C) for H gave 6 ppm by weight. This agrees within the precision of the analysis with 4 ppm obtained on the analysis of the Zr before reaction with water vapor. Therefore, if there is an effect of H on the properties of the film, it is at lower concentrations than could be detected.

Discussion and Conclusions

It was found that in the temperature range 300°-600°C the reaction of Zr with water vapor at 33 mm Hg pressure follows the cubic rate law with an activation energy of 29,700 cal/mole. Thomas (1) in reviewing the various works on the corrosion of Zr in water at high temperature (250°-360°C) and pressure showed that the slope of the plot of log of weight gain against log of time was of the order of 0.3. This indicates that the cubic law was being followed. Thomas reports an activation energy of 11,400 cal/mole which is considerably lower than that from the present study.

The cubic rate law had been found to hold for the reaction of oxygen at 1 atm pressure with Zr (activation energy, 47,200 cal/mole) (3) and with a Zr-1.5 wt % tin alloy (activation energy, 38,400 cal/mole) (2) in the temperature range 500°-900°C. Gulbransen and Andrew (4) in investigating the reaction of Zr with oxygen at low pressures (0.076 to 7.6 cm Hg) in the range 200°-425°C indicated that the reaction may be parabolic. However, their data were replotted (3) and excellent agreement with the cubic law was found for the reaction for which the activation energy is 26,200 cal/mole. This is in fair agreement with the 29,700 cal/mole obtained in the present study. The over-all mechanism of film formation is the same in both cases. This indicates that the controlling steps in reactions of Zr with water vapor and oxygen at low pressures are very similar.

Acknowledgment

The authors wish to acknowledge the assistance of R. K. Willardson who performed the thermoelectric

power and resistivity measurements of the oxide films.

Manuscript received September 14, 1956. Work performed under AEC Contract W-7405-Eng-92.

Any discussion of this paper will appear in a Discussion Section to be published in the December 1957 JOURNAL.

REFERENCES

1. D. E. Thomas, *Nuclear Engineering*, **50**, 16 (1954).
2. M. W. Mallett and W. M. Albrecht, *This Journal*, **102**, 407 (1955).
3. J. Belle and M. W. Mallett, *ibid.*, **101**, 339 (1954).
4. E. A. Gulbransen and K. F. Andrew, *Trans. Am. Inst. Mining Met. Engrs.*, **185**, 515 (1949).

A New Commercial Process for Electrowinning Manganese

M. C. Carosella and R. M. Fowler

Electro Metallurgical Company, A Division of Union Carbide Corporation, Niagara Falls, New York

ABSTRACT

The development of a novel process for the electrowinning of manganese from aqueous solutions is described with emphasis on the raw materials used and the advantages gained thereby. A commercial plant based on this process was built and a description of the methods of quality control, chemical analyses, and characteristics of the metal so produced is given.

Allmand and Campbell (1) reported that they had prepared pure Mn in a coherent form from a Mn $SO_4 \cdot (NH_4)_2 SO_4$ electrolyte in a diaphragm cell, but after a small amount deposited the deposits became loose and scaled off. Shelton (2) and co-workers (3,4) made a number of improvements and developed the first continuous process for producing Mn by electrolysis. The results of these investigations were sufficiently encouraging to justify in 1939 the construction of a commercial plant (5). While this plant started operations in 1941, some process changes had to be introduced so that by 1949 the rather complex process using selected high grade ores was stated to be under close control (6).

Investigation of the process for electrowinning Mn as developed by Shelton, *et al.*, started here in 1938. Also other methods for producing a pure grade of Mn were being investigated with some success. Numerous sources of Mn, including ferromanganese, ores, and slags, were investigated. As a result of these studies, a pilot plant was built to develop a process for electrowinning Mn.

Pilot Plant

The pilot plant was designed to be quite flexible so that it would be suitable for handling various types of starting materials and methods of solution purification.

Processes, based on ferromanganese and several different types of ores, were developed and studied from an economic viewpoint. Some difficulties were experienced in the electrolytic step because the level of impurities in electrolytes derived from some of these source materials was above tolerable limits. Methods of purification as reported by the U. S. Bureau of Mines were not always successful in eliminating all of the deleterious impurities.

After the ore and ferromanganese processes had been demonstrated to be technically feasible, an economic evaluation showed that the cost of Mn in these materials was the largest single factor in the total cost of producing electrolytic Mn. In addition, the methods used to produce an electrolyte of sufficient purity were complex and costly. As a result of these studies, various types of slag, which were available from Mn ore smelting operations, were investigated as source materials for Mn. During these studies it was discovered that the Mn in some of these slags could be extracted with dilute acid solutions, and that the extract liquors were easily purified.

Concurrently an investigation to develop suitable electrolytic cells for this process had been under way. The staff of the Bureau of Mines at Boulder City, Nev., (7) had done considerable experimentation on various types of cells. Their work indicated that a false-bottom-type cell was the best. Although their cell had many inherent advantages, it had the disadvantage of complex design and was difficult to disassemble and clean. Further experimentation here led to the development of a cell (8) which is

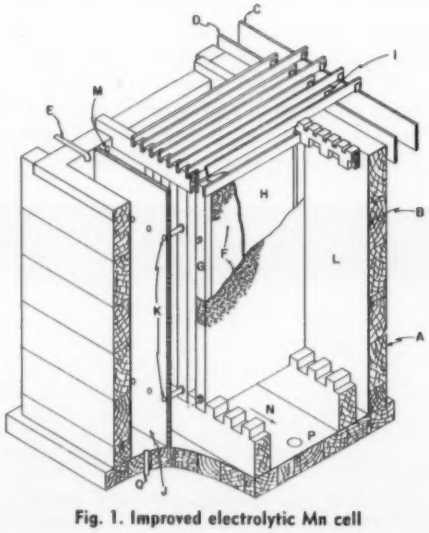

Fig. 1. Improved electrolytic Mn cell

simple in design. Fig. 1 shows the main features of the new cell. Basically, it is a rectangular wooden tank, A, with lead lining, B; C and D are the cathode and anode busbars connected to the Hastelloy alloy cathodes H (9) and 99% lead, 1% silver (10) anodes, I, respectively. Feed is introduced at E into the catholyte header, J, which supplies the individual frames, G, which are covered with canvas or synthetic fiber diaphragms, F. Two outlets, K, are provided on each cathode frame for circulating catholyte to the common header. Hydrogen generated at the cathodes, H, acts as a gas-lift to cause the catholyte to circulate freely, thus resulting in a uniform Mn concentration and pH in all catholyte compartments. The solution passes through the diaphragms, F, into the anolyte compartment, L. The spent anolyte overflows from the cell at M. The anode sludge formed during electrolysis falls freely into the bottom of the anolyte chamber. The bottom of this chamber, N, is sloped to permit flushing the sludge through a valve at P without disassembling the cell. The catholyte header can be readily flushed out, when required, through Q.

Since cathodes for deposition of Mn must be chemically inert, with a surface of such a nature that the electrodeposit adheres but can be easily stripped by flexing or hammering, many corrosion-resistant alloys were tried as cathode materials in the pilot plant. Cathodes made from the Hastelloy alloys performed better than those made from stainless steels because they were more corrosion resistant and required infrequent polishing. In addition any metal which did not strip from the Hastelloy alloy cathodes could be dissolved in anolyte without destroying the polished surface. Stainless steel cathodes had to be polished after each stripping to prevent the next deposit from adhering so tightly that removal was difficult.

Commercial Plant

When an economic analysis of the pilot plant operation showed that the slag process was favorable, a commercial plant was designed and built. In the new process (11), Mn ore was smelted in a submerged arc furnace with coke and a flux, when necessary, to produce standard ferromanganese and a high-manganese slag. As shown in Table I, the slag contains only small amounts of metals which cause trouble in the electrowinning step.

The general flowsheet of the new process is as follows. The manganese silicate slag, milled to −200 mesh in a dry grinding unit, is leached to a pH of 4.4 with anolyte and make-up H_2SO_4. The resulting slurry is next treated with gaseous ammonia to a pH of 6.6 to precipitate most of the impurities. The neutralized slurry is filtered and the residue washed with water to recover the soluble Mn. The filtrate and wash water are treated with a small amount of H_2O_2 to oxidize and precipitate the residual iron. The precipitate is filtered from the solution which is pumped to a cell feed storage tank. SO_2 is added to this solution before it enters the cell circuit. Anolyte produced in the cells is returned to the leaching circuit.

Provisions have been made in the plant to remove Mg from the circuit when necessary. Anolyte is cooled in a continuous vacuum crystallizer and a complex Mg, Mn, $(NH_4)_2SO_4$ crystallized. After removing the salt, the solution is returned to the leaching circuit.

This process is quite different and has less processing steps than either the processes described by Bennett (6) or that developed by the investigators at the Bureau of Mines (7). Typical analyses of the cell feed and anolyte are shown in Table II.

Hastelloy alloy C cathodes, 42- by 24-in. by 16-gauge, are regularly removed from the cells on a 72-hr schedule. They are first dipped in a dilute solution of sodium bichromate to prevent the metal surface from darkening, then washed with water to remove soluble salts, and dried. The brittle cathode deposits are stripped with the aid of a rubber mallet. The cathodes are then soaked in anolyte to dissolve any residual Mn metal. After this treatment, followed by washing with a detergent solution and rinsing with water, they are ready to return to the cells.

The plant is equipped with a buffing machine to restore the polished surface when needed. Under normal operating conditions, cathodes are usually polished aproximately twice each year.

The stripped metal is either packed in drums for shipment or loaded in stainless steel cans which are placed in an electrically heated furnace to remove H.

Quality Control of Electrolytic Mn

One of the major problems in any research program leading to a new product is the development of procedures for determining the quality of the product. Direct estimation of Mn is not a sufficient measure of purity of the product because there is no highly precise method for estimating Mn. The standard bismuthate method (12) in the hands of its developers was not better than one part in a thousand or 0.10% Mn. With improvements that have been incorporated, results still tend to be on the low side because oxidation is never quite complete. The Volhard method is even more empirical and is likewise unsuitable. There is no highly precise gravimetric method for Mn. The classical determination of Mn as $Mn_2P_2O_7$ (13) leaves much to be desired in the way of the composition of precipitate, other elements precipitated, etc., so in all this work the percentage

Table I. Typical analyses of deleterious impurities in slag

	%
Iron	0.14
Molybdenum	0.006
Copper	0.003
Nickel	<0.001
Cobalt	<0.0001

Table II. Analyses of cell solutions, g/l

	Feed	Anolyte
Mn	32 – 34	10 – 12
$(NH_4)_2SO_4$	120 – 140	120 – 140
SO_2	0.30 – 0.50	–
H_2SO_4	–	36 – 44

Table III. Analysis of electrolytic Mn, content in ppm

<10 if present	<10	10-20
Al, B, Cr, Ti, V, Zr	Fe, Cu, Ag, Co, Ni	Pb, Si, Ca, Mg

of Mn was obtained by subtracting the sum of the other elements from 100.

Determination of other metals.—The most satisfactory method for estimating residual metallic elements in electrolytic Mn is by emission spectroscopy. For low concentrations, it is both rapid and precise. Table III lists the results of a quantitative examination of typical electrolytic Mn samples. In the case of the results in this table, excellent agreement was obtained between spectrographic and wet chemical laboratories, and the spectrographic laboratory of an independent research institution to whom samples were submitted. Some of the metals, such as Cu and Pb, can be determined readily with spectrophotometric procedures but for others, for example, Ca, there are no wet procedures with satisfactory sensitivity in the presence of such a preponderance of Mn.

Determination of metalloids.—P, S, and C are of interest to the user of electrolytic Mn. In fact, one advantage of the electrolytic over the electrothermic material is the very low P content of the former. The spectrophotometric method for P (14) is sufficiently sensitive. Using this method, the plant material is consistently below 5 ppm.

Since Mn is deposited from an $(NH_4)_2SO_4$ bath, there is opportunity for S to contaminate the metal. The exact mode of occurrence of S in the metal is not known, although it is probable that under certain conditions some of the complex S compounds in the electrolyte are reduced to sulfides at the active cathode surface. Likewise, any electrolyte trapped in the deposit would contribute to the S present. Initially, it was the practice to determine both sulfide and sulfate sulfur, but it was found that there was no correlation even in successive portions of the same analytical sample. The indications were that it was possible by variations in the rate of solution of a particular sample to alter the percentage of the two forms present. Similar difficulties encountered in the analysis of material containing ferric iron and sulfides (15) can be eliminated by the addition of stannous chloride. Similar tests on electrolytic Mn, while better than without stannous chloride, were not too satisfactory, so it appears that the evolution method has limited utility for the determination of S.

S present in any form would be recovered in the metal when the Mn is used for alloying. Since it is not the form but the amount of S that is important for metallurgical uses, only a determination of total S, by the combustion method that is standard in the steel industry, is now made. A sample is also treated with water to get an estimate of the completeness of the washing of the cathodes for process control. The washer is so operated that no test is obtained for soluble sulfates.

The S content of the Mn has dropped as the process operated and more control was exercised over various factors. At the present time the S is less than 0.030%.

The amount of C present is so small that it is not of importance. The carbon level in the metal has been consistently below 0.005%.

Determination of gaseous elements.—For many metallurgical uses, the content of gaseous elements in electrolytic Mn is important. Since it is deposited from a solution containing large amounts of ammonium ion, N could be present. Fortunately, N can be determined very precisely by the standard method used for steels (17). All the analyses that have been made indicate that the N content is less than 50 ppm although 100-300 ppm may be picked up in the dehydrogenation process. For special purposes, a nitrided grade with about 6% N is produced.

Oxygen is important because it may be an undesirable addition, as for example in Mn-Ti alloys. Also if the Mn is to be determined by difference, a substantial error is introduced in the result for Mn if oxygen is ignored. The only suitable method for oxygen is by vacuum fusion. An apparatus similar to that described by Hamner and Fowler (18) with the sample enclosed in a tin capsule has been found satisfactory. The cells are operated to keep the oxygen content below 0.15%. However, it must always be kept in mind that Mn is a readily oxidizable metal and the oxygen content can be increased by improper handling.

For some purposes, the H content is of interest, and since significant amounts are codeposited, it must be removed by subsequent treatment if low-hydrogen material is desired. As deposited, the Mn metal contains about 0.02% H. Much of this can be removed by treatment at 500°C as was pointed out by Potter, *et al.* (19). Unfortunately they did not start with hydrogen-free material nor did they ever determine the amount of H remaining after their treatments.

Sieverts and Moritz (20) also studied the solubility of H in Mn. Their material was vacuum-distilled on a small scale and equilibrated with H. They measured the changes in H content of the metal by means of the gas evolved and showed that at 400°-600°C there was about 9 ml of H/100 g or 8 ppm in solution. Potter, *et al.* (19) report that about 7 cc of gas/100 g of metal is reabsorbed below 600°C. Sieverts and Moritz found about 35 ml was reabsorbed on cooling in H at 760 mm pressure. Since neither of these investigators analyzed the Mn for H, the results are the differences of two rather large numbers containing considerable variation. It is not possible to decide precisely from their work how much H would remain on heating electrolytic Mn to 500°C and on cooling to room temperature. The indication is that there may be at least 16 ml/100 g or 14 ppm remaining in material so treated.

Since primary interest lies in the total amount of H present and not in checking whether additional H can be driven off, the apparatus described by Potter, *et al.*, is not suitable for the determination of total H in dehydrogenated metal; the only satisfactory procedure is by vacuum fusion. A 100-g

Table IV. Hydrogen in dehydrogenated electrolytic Mn

Sample	Hydrogen obtained in successive treatments			
	600°C ppm	1000°C ppm	1700°C ppm	Total ppm
No. 1	2	–	9	11
	–	3	11, 12	14, 15
	–	–	11, 12	11, 12
No. 2	3	–	18	21
	–	4	11	15
	–	–	13, 15, 20	13, 15, 20

sample was heated to 600°C in an apparatus, similar to that described by Potter, *et al.*, for 30 min at a pressure of 10^{-5} mm Hg and the H collected. The sample was cooled, dry argon admitted, and 20 g removed. The sample was then reheated *in vacuo* to 1000°C for 30 min and the evolved H collected. After cooling, as before, the remainder was then analyzed by the vacuum-fusion procedure (*see* Table IV). Samples of the original material were also analyzed directly by vacuum fusion. The results are in good agreement and show clearly that all the H cannot be removed at 600°C *in vacuo* in a reasonable time. To see if this was a property peculiar to the electrolytic Mn produced by the present process, samples produced and dehydrogenated in other places were analyzed; similar results were obtained. All the evidence points to the necessity of stating the conditions used to obtain the H content. In other words, a specification that the H content of electrolytic Mn is less than a given figure is meaningless unless the analytical method used to obtain that figure is described. If dehydrogenated at 510°C (950°F), all the evidence obtained here indicates that there is about 10-15 ppm remaining. Table V shows the precision that can be obtained by the vacuum fusion procedure. For this test, samples were chosen sized 16 by 48 mesh. Each sample was divided into three portions. The samples were mixed, dried in air at 110°C for 1 hr, then stored in a dessicator. Before they were sent to the laboratory, they were assigned random numbers so that they were analyzed in random fashion by two different chemists. From a statistical study of these data, it was concluded that the precision of the H determination, using vacuum fusion, is of the order of 5 ppm. Factors such as drying and the size of sample used are important.

Sampling electrolytic Mn.—In any quality control program, it is essential that the sample examined in the laboratory represent adequately the lot of material from which it was drawn. The plant procedure for sampling follows.

The material is combined in 42,000-lb lots. When a lot is packed in drums, 500 lb to the drum, 5 lb are taken from each drum by periodically cutting the stream as the drum is filled. Thus a 400-lb gross sample is accumulated. This is broken into small pieces ¼ x ⅛ in., and a sample riffled out for gas analysis. A second portion is rolled to 20 mesh, riffled to 1 lb, and crushed to 100 mesh for the analytical sample.

Table V. Precision of the determination of H in electrolytic Mn

Sample No.	Sample not dried	Dried 110°C for 1 hr, ppm
1	220	192, 204, 195
2	21	13, 15, 21
3	15	10, 11, 13
4	13	10, 11, 14
5	13	10, 10, 10

Table VI. Effect of crushing on oxygen content

Sample preparation	Oxygen, %
Coarse	0.13, 0.14
Coarse (pickled 3% HNO_3)	0.13, 0.14
8 × D	0.15, 0.16
8 × D (dried 1 hr at 110°C)	0.18, 0.18
35 × D	0.17, 0.18
35 × D (dried 1 hr at 110°C)	0.23, 0.23

Since Mn is readily oxidized, the reduction of the gross sample presents problems. Table VI shows some results obtained by crushing to fine sizes. They indicate that substantial oxidation may take place if the metal is reduced from ¼ x ⅛ in. to pass a 35-mesh sieve. The minus 35-mesh material, or even minus 100-mesh material, is much more desirable as a sample. If one is not interested in oxygen, the sample can be reduced to a suitable size by the standard tools used in the ferroalloy industry (21). If the iron content is of interest, it is essential to use only alloy-steel equipment and aliquot a large sample rather than crush to fine sizes, since considerable amounts of adventitious iron can be obtained from ordinary cast iron equipment.

Summary

A plant based on the slag process has been shown to have a simple flowsheet, yet gives a very pure solution amenable to easy electrolysis. Plating difficulties which may be caused by impurities in the solution have never been encountered in the cell room.

The metal produced has been consistently of high quality. The new type of cell has proved to be easy to operate and simple to control. The Hastelloy alloy C cathodes, while higher in initial cost than stainless steel, have been very satisfactory and have justified their higher cost in savings in maintenance and ease of stripping the deposited metal.

With the new process it is possible to smelt a Mn ore to ferromanganese and a slag, then recover the Mn in the slag as electrolytic Mn. In this way nearly all the Mn in an ore is converted into forms suitable for the metallurgical industry, thus conserving Mn resources. This program has made available for the metal industries additional supplies of high-purity Mn metal for the production of better alloys.

Acknowledgments

Any development such as has been described is the work of many minds and hands. Among Electro Metallurgical Co. groups who contributed to this project are the Metals Research Laboratories, the General Engineering Department, the Product and Process Development Department, and the Operating Department. The authors wish to thank the management of Electro Metallurgical Co. for supporting this development and for the opportunity of publishing the results of the work.

Manuscript received July 26, 1956. This paper was prepared for delivery before the San Francisco Meeting, April 29 to May 3, 1956.

Any discussion of this paper will appear in a Discussion Section to be published in the December 1957 JOURNAL.

REFERENCES

1. A. J. Allmand and A. N. Campbell, *Trans. Faraday Soc.*, **19**, 559 (1924).
2. S. M. Shelton, *U. S. Bur. Mines R.I. 3322*, 29 (1936).
3. S. M. Shelton, M. B. Royer, and A. P. Towne, *U. S. Bur. Mines R.I. 3406*, 3 (1938).
4. R. S. Dean, *U. S. Bur. Mines R.I. 3580* (1941).
5. W. L. Hammerquist, *Steel*, **105**, 42 (1939).
6. R. H. Bennett, *Eng. and Mining J.*, **150**, 80 (1949).
7. J. H. Jacobs and Co-workers, U. S. Bur. Mines Bull. 463.
8. M. C. Carosella, (to Union Carbide & Carbon Corp.), U. S. Pat. No. 2,739,116, Mar. 20, 1956.
9. G. D. Bagley and M. C. Carosella (to Union Carbide & Carbon Corp.), U. S. Pat. No. 2,755,241, July 17, 1956.
10. M. C. Carosella (to Union Carbide & Carbon Corp.), U. S. Pat. No. 2,766,198, Oct. 9, 1956.
11. M. C. Carosella (to Union Carbide & Carbon Corp.), U. S. Pat. No. 2,766,197, Oct. 9, 1956.
12. T. R. Cunningham and R. W. Coltman, *Ind. Eng. Chem.*, **16**, 58 (1924).
13. W. F. Hillibrand and G. E. F. Lundell, "Applied Inorganic Analysis," 2nd ed., p. 499, John Wiley & Sons, Inc., New York (1953).
14. *Ibid.*, p. 710.
15. H. A. Bright, *J. Research Nat. Bur. Standards*, **18**, 137 (1937).
16. E. L. Bennet, J. H. Harley, and R. M. Fowler, *Anal. Chem.*, **22**, 445 (1950).
17. ASTM Methods Chemical Analysis Metals, p. 131 (1950).
18. H. L. Hamner and R. M. Fowler, *J. Metals*, **4**, 1313 (1952).
19. E. V. Potter, E. T. Hayes, and H. C. Lukens, *Metals Tech.*, **12**, [4], TP 1809, (June 1945).
20. A. Sieverts and H. Moritz, *Z. physik. Chem.*, **180** (4), 249 (1938).
21. Ref. (17), p. 63.

Effects of Various Polyvalent Metal Anion Additions to an Alkaline Magnesium Anodizing Bath

W. McNeill and R. Wick

Pitman-Dunn Laboratories, Frankford Arsenal, Philadelphia, Pennsylvania

ABSTRACT

The effects of some polyvalent metal anions in magnesium anodizing were compared. Coated panels were exposed to salt spray to determine their corrosion resistance. Hardness and dielectric strength tests were also carried out. Coatings from chromate, stannate, vanadate, tungstate, and manganate baths were compared with those from a bath containing no polyvalent metal anion. Differences in corrosion resistance were noted, with vanadate baths producing the best results. Differences in color were noted also.

Anodic coatings available for magnesium are of two types, those coatings formed at low voltage (under 10 v) and those formed at high voltages (60-320 v).

The low voltage coatings are thin and have low surface roughness in comparison with those coatings formed at high voltages. Low voltage coating formation is probably a simple process, involving only the electrochemical reaction of Mg with the anions in the bath to form an oxide or hydroxide coating. On the other hand, high voltage coatings are formed by a complex process. Sparking, which occurs on the Mg surface during anodizing, results in the formation of very hard deposits which resemble sintered ceramic materials. The chemical reactions which occur in the spark zone are not known, but it is clear that reduction products occur in the coating even when formation is carried out using direct current. The process cannot be electrochemical since oxidation only can occur at an anode. It is more likely, then, that the high voltage anodic coatings are formed by a thermal process which is brought about by electrochemical means. An interesting feature of the baths used for high voltage anodizing is that they usually contain anions such as dichromate or manganate which are reduced, the reduction products appearing in the coating. The use of anions of this type in Mg finishing has been known for many years (1-5), but their value in high voltage anodic baths has been a subject of considerable speculation.

The development of the HAE process (4) afforded an opportunity to investigate the effect of a variety of polyvalent metal anions in alkaline anodizing baths for magnesiums. It was possible to carry out such a study with the HAE bath because anions such as chromate, stannate, etc., could be substituted for manganate and these substitutions were found to have no significant effect on operating conditions necessary for coating formation. With the Cr-22 bath (6), for example, no substitute for chromate has been found which does not adversely affect coating formation.

Early work on substitutes for manganate in the HAE anodic bath gave inconclusive results because

two important variables were not recognized. The first of these was "aging" of the anodic coating. The corrosion resistance of coated panels increased if exposed to the laboratory atmosphere, at ambient temperatures, for several weeks during seasons of high humidity. The same effect could be obtained by placing coated panels in air of approximately 100% relative humidity at about 180°F for several hours. Several acidic post dips were tried also. One of these, an aqueous bifluoride dichromate dip, when combined with humid aging, was found capable of increasing the corrosion resistance of HAE coated panels by several hundred per cent (7).

The second important variable was in the Mg alloy itself. Panels from different production lots gave test differences which were significant and attributable to the alloy stock. These differences appeared repeatedly even after as much as 0.010 in. of surface was removed by acid pickling.

To control variations in the post treatment, all of the panels in a given test are dipped for the same length of time and aged simultaneously. To control the effect of variations in the alloy, stock panels are all cut from the same production lot and randomized before being coated. This procedure gives a measure of control over tests on anodic coatings on Mg which was not obtained formerly. It was necessary, in view of the importance of the above variables, to reinvestigate the role of polyvalent metal anions in Mg coating baths.

Experimental

Mg panels, 4 in. x 6 in. x 0.051 in., were cut from a single lot of FS1 alloy sheet. The Mg was received from the manufacturer with a producer's dichromate pickle and stencilled ink identification marks on one side of each sheet, i.e., the inked side; the opposite side is called here the clear side. The panels were deburred and then numbered on the inked side; they were degreased in acetone prior to anodizing, but were not cleaned otherwise.

A 200-liter stock solution was prepared containing 150g/l USP grade KOH, 30 g/l USP grade (dried gel) Al $(OH)_3$, 35 g/l purified anhydrous KF, 35 g/l technical grade $Na_3PO_4 \cdot 12\ H_2O$, and tap water to make the required volume.

From this solution, five 30-liter baths were prepared, respectively containing chromate, tungstate, vanadate, stannate, and manganate (HAE bath). Each was made 0.086M in the additive. A sixth bath, containing no additive, was used as control.

Anodizing was carried out in a steel tank equipped with a Cu cooling coil. Bath temperature during anodizing varied somewhat, but generally remained within four degrees of 24°C.

Power was supplied to the bath by a 60-cycle, 45-amp unit which maintained bath current constant by automatically varying the voltage as resistance changed. Panels were coated in batches of six at a current density of 15 amp/ft^2, and a treatment time of 90 min. Voltages at the completion of treatment were between 80 and 90 v. After anodizing, the panels were rinsed in cold running water and allowed to stand until dry. After drying the panels were stored in a desiccator over anhydrous magnesium perchlorate to prevent natural aging.

Panels were selected from each bath and two groups of 36 panels each were assembled. One group remained in storage in the desiccator while the other group was dipped and aged. The post treatment consisted of a 45 sec immersion in an aqueous solution consisting of 10% NH_4HF_2 and 2% $Na_2Cr_2O_7 \cdot 2H_2O$.

The dipped panels were allowed to dry without rinsing and were then placed in air of approximately 100% relative humidity for 4 hr at a temperature of from 175° to 180°F. After aging they were removed, wrapped in contact with each other, and stored in the laboratory. Five days later all 72 panels were exposed to the salt spray in accordance with ASTM B-117-44T. The clear side of each panel was exposed with the rack mark down. Observations were made after 48, 120, and 312 hr.

The panels were removed from the salt spray and flushed with tap water (prevailing temperature, 67°F). No brushing was given. The panels were allowed to dry and the number of pits counted. Pits originating on panel edges were not counted. After each observation the panels were replaced in the salt spray cabinet in different order.

Dielectric strength measurements were made in accordance with ASTM test B-110-45, on duplicate samples from each of the six baths. The object of this test was merely to determine whether large differences due to bath composition existed, and no attempt was made to determine the nature of the relationship between bath composition and dielectric properties.

Coating hardness was tested by rubbing a bar of steel of Rockwell C63 hardness over the panels. This test was used only to determine whether any of the coatings were notably deficient in this respect.

Results and Discussion

Appearance.—The appearance of the various coatings was strongly dependent on bath compositions. Texture was not much affected, but, as would be expected, coatings of different colors were obtained. The HAE coated panels were medium brown, while those coated in the chromate and vanadate baths were light green and slate gray, respectively. Panels from the other three baths were all off-white, although those from the stannate bath might be described as light gray. All the coatings had the same type of partly sintered ceramic appearance, when examined under a magnification of 75X. They were all of about the same texture, with the exception of those treated in the no-additive bath. These had a few small white nodules distributed over the surface. It was found that, by adding suitable quantities of chromate and manganate to the no-additive bath, olive drab coatings could be produced which matched the lusterless green No. 3412 (olive drab) of Federal Specification TT-C-595, Jan. 12, 1950.

Whether such a bath could be regulated well enough to be practical was not investigated because it would have required experimental effort beyond the scope of the work reported.

Hardness.—The hardness of all six types of coatings was tested as described in the preceding sec-

Table I. Results of dielectric strength test

Bath type	Mean breakdown voltage	Standard deviation
Stannate	566	48.2
Vanadate	610	50.6
Manganate	581	43.7
Chromate	591	48.0
Tungstate	638	54.0
No-additive	600	51.8

tion. In each case, the coating abraded the steel. There was no noticeable difference between the hardness of the various coatings.

Dielectric strength.—The dielectric strengths of the coatings were measured and the means and standard deviations are shown in Table I.

None of the groups of panels was different from the no-additive group at the 0.95 level of significance.

Corrosion resistance.—In the salt spray tests, each bath composition was represented by two groups of six panels each. One group was post-treated, and the other was not. A summary of the corrosion data in pits per panel is given in Table II.

Nearly all the panels in both groups showed some corrosion, even at 48 hr and this was surprising in view of past experience with some of the coatings in the test. This was believed to be due to the FS1 alloy stock from which the panels were obtained, and does not reflect the maximum corrosion resistance that can be obtained with such coatings. In the case of the post-treated specimens, moreover, further improvement could have been obtained by repeating the post-dipping and aging steps several times, or by increasing the aging time. In an earlier experiment, 16 panels, cut from a different lot of FS1 alloy, were coated in a no-additive bath, dipped in the dichromate-bifluoride solution, aged 22 hr, and exposed to salt spray. After 400 hr exposure the panels averaged 3.6 pits per 4 in. x 6 in. panel, and the standard deviation was 2.3 pits per panel.

With the type of panels included in this test, corrosion usually begins between 48- and 120-hr exposure. In this test corrosion was well underway after 48-hr exposure. Corrosion results for the group of panels coated in the no-additive bath were compared with those for the other coatings. The data were tested for significance using Student's t-test; results are given in Table III.

Table II. Summary of corrosion data

Bath type	Not post treated 48 hr	Not post treated 120 hr	Not post treated 312 hr	Post treated 48 hr	Post treated 120 hr	Post treated 312 hr
Stannate						
Mean	17.8	22.2	23.2	6.5	12.8	14.8
Std dev	8.9	7.4	8.1	5.8	5.3	6.1
Vanadate						
Mean	8.5	13.0	15.5	2.0	6.3	7.7
Std dev	2.7	3.5	3.8	1.7	2.9	3.3
Manganate						
Mean	26.2	56.5	59.0	1.7	12.3	13.5
Std dev	7.1	6.5	7.5	1.9	3.8	3.3
Chromate						
Mean	36.0	52.2	52.3	6.7	10.8	13.7
Std dev	4.0	11.4	12.2	6.9	6.6	7.3
Tungstate						
Mean	48.5	58.5	58.3	8.7	17.0	20.3
Std dev	24.8	16.9	12.4	3.9	7.2	6.0
No-additive						
Mean	46.7	57.7	57.7	3.7	10.3	12.7
Std dev	13.2	11.8	10.1	2.3	2.2	2.2

Table III. Results of significance test

Bath type	Not post treated 48 hr	Not post treated 120 hr	Not post treated 312 hr	Post treated 48 hr	Post treated 120 hr	Post treated 312 hr
Stannate	+3	+3	+3	0	0	0
Vanadate	+3	+3	+3	0	+1	+1
Manganate	+3	0	0	+1	0	0
Chromate	+3	0	0	0	0	0
Tungstate	0	0	0	−1	0	−1

Positive values indicate significantly greater, and negative values indicate significantly less, corrosion resistance than that of the corresponding group of no-additive panels. Numerical values indicate the highest levels at which the differences were significant, and are as follows: 1—0.95 level; 2—0.99 level; 3—0.995 level. Zero values indicate no significant difference at the 0.95 level.

Differences between coatings are much larger at 48-hr exposure than at other exposure times. This is probably because the corrosion at the earlier time was not fully developed at all the potential points of failure. It would appear that the 120-hr exposure was sufficient to produce pits at nearly all of these points since increases in corrosion, from 120 to 312 hr, were small. Probably, then, more reliable conclusions can be drawn from the 120- and 312-hr data. In some cases, fewer pits were counted at 312 hr than at 120 hr. This was not necessarily due to erroneous counting, but occurred when neighboring pits grew so large that they merged. However, no pits over 1/16 in. in diameter were observed on any of the panels. While it is true that this exposes a weakness in pit counting as a method of estimating salt spray corrosion, other methods that might be used have greater shortcomings. An example would be that of estimating the per cent of the area of the panel that was corroded. Here the total area of corrosion per panel is quite small and estimates frequently fail to show differences. The reversals that did occur had little effect on the results of the test, and it was not worthwhile to attempt to refine the technique.

The data show clearly that the post treatment causes a tremendous increase in the corrosion resistance of all the panels. With the exception of vanadate, the effects of bath additives are relatively minor. The non-post-treated vanadate specimens showed almost as much corrosion resistance as most of the post-treated groups, and far more corrosion resistance than any of the other non-post-treated groups.

Conclusions

Protective coatings on FS1 Mg alloy can be obtained by anodizing a bath prepared from potassium hydroxide, aluminum hydroxide, trisodium phosphate, and potassium fluoride. The addition of stannate, vanadate, manganate, chromate, or tung-

state to this bath makes it possible to produce coatings which differ with respect to color and corrosion resistance. The corrosion resistance of all these coatings is greatly improved by a post treatment consisting of immersion in a bifluoride-dichromate solution followed by aging in a hot, humid atmosphere.

The addition of vanadate increases the corrosion resistance of the coating.

All the coatings studied are hard enough to abrade Rockwell C63 steel.

Acknowledgment

This paper describes experimental work supported by the Ordnance Corps and conducted at Frankford Arsenal under Project TB4-302B-5. The authors wish to express their appreciation to the Ordnance Corps for permission to publish this paper.

Manuscript received April 12, 1956. This paper was prepared for delivery before the Cleveland Meeting, Sept. 29 to Oct. 4, 1956.

Any discussion of this paper will appear in a Discussion Section to be published in the December 1957 JOURNAL.

REFERENCES

1. Siemens & Halske, Aktiengesellschaft, British Pat. 459,017, Dec. 31, 1936.
2. L. Renault, French Pat. 815,115, July 7, 1937.
3. R. W. Buzzard, U. S. Pat. 2,314,341, March 23, 1943.
4. H. A. Evangelides, "The HAE Process for Magnesium, I. Introductory Report," Frankford Arsenal Report R-1000, Jan. 1951.
5. H. A. Evangelides, U. S. Pat. 2,723,952, Nov. 1955.
6. W. McNeill, *Metal Finishing*, **53**, 57, December (1955).
7. H. A. Evangelides, *Product Finishing*, (British) p. 54, October (1954).

Electric Moments of Certain Partially Fluorinated Esters

J. B. Romans and T. D. Callinan[1]

U. S. Naval Research Laboratory, Washington, D. C.

ABSTRACT

The electric moments of six partially fluorinated esters have been determined. The materials studied were liquids at room temperature and were known to be chemically inert and thermally stable. All six esters were found to be highly polar compounds exhibiting marked tendencies to associate molecularly; they possessed dipole moments of the order of 2.8 to 3.8 $\times 10^{-18}$ esu-cm. From the experimentally determined permanent electric moments, the most probable molecular configurations were calculated for each of the esters. The predominating structure includes one cis-type configuration. It is evident that the molecules exist, for the most part, in a nonplanar form.

The electrical properties of some partially fluorinated esters have been determined for the purpose of elucidating their molecular configurations. The fluoresters studied (Tables I and Ia) were synthesized by the esterification of partially fluorinated alcohols with unfluorinated acids (1). The straight chain primary alcohols employed were:

1H, 1H, 5H-octafluoropentanol-1 .....
$H(CF_2)_4CH_2OH$ ... ψ'-amyl alcohol
1H, 1H, 7H-dodecafluoroheptanol-1 ...
$H(CF_2)_6CH_2OH$ ... ψ'-heptyl alcohol
1H, 1H, 9H-hexadecafluorononanol-1 ..
$H(CF_2)_8CH_2OH$ ... ψ'-nonyl alcohol

The acids used were 2-ethyl hexanoic acid, glutaric acid, 3-methylglutaric acid, tricarballylic acid, and phthalic acid. In the case of the polybasic acids, only the totally esterified derivatives were prepared. All the materials studied were liquids at room temperature and were known to be chemically inert and thermally stable (1). The density, index of refraction, and molecular weight determined previously (1) are given because they are essential to the calculation of the molar polarization.

The dipole moments of the six partially fluorinated esters were obtained by determining the molar polarization of the material when dissolved in a nonpolar solvent (2), and then calculating the extrapolated value of polarization at infinite dilution. The experimental values obtained and the results of calculations performed are presented in Table II. Solutions of the partially fluorinated esters were prepared in ACS grade benzene. The densities were measured at 20°C with a modified Sprengel-type pycnometer in a constant temperature bath. The dielectric constant data at 1 Mc were obtained at 20°C with a Q meter and cell described previously (3) except that in order to obtain greater precision with this type of apparatus, the main tuning condenser of the Q meter was provided with a detent stop and all tuning was done by means of the vernier condenser. With this arrangement, the dielectric constants of the benzene solutions were determined within ± 0.001.

In determining the molar polarization of the substance at infinite dilution, $P\infty$ graphs were prepared and the required linear extrapolation performed. The dipole moments were then calculated from the values of the polarization at infinite dilution. As shown in Table III, bis(ψ'-amyl) phthalate was found to have the highest dipole moment of the six esters studied (3.8D), while ψ'-nonyl 2-ethylhexanoate had the lowest (2.8D); all are higher than

[1] Present address: International Business Machines Corp., Poughkeepsie, N. Y.

Table I. Formulas and abbreviations (I) of certain partially fluorinated esters

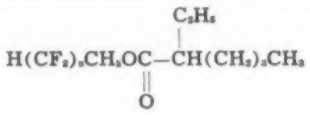

I

ψ′-Nonyl 2-ethylhexanoate
1H,1H,9H-Hexadecafluorononyl
2-ethylhexanoate

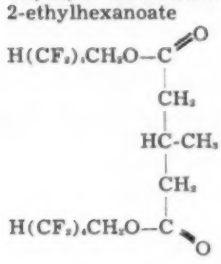

III

Bis(ψ′-amyl) 3-methylglutarate
Bis(1H,1H,5H-octafluoropentyl)
3-methylglutarate

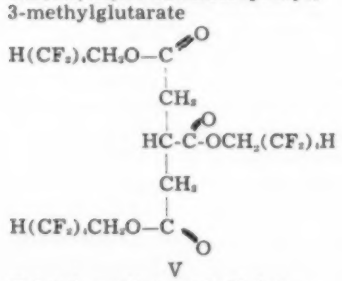

V

Tris(ψ′-amyl) tricarballylate
Tris(1H,1H,5H-octafluoropentyl
tricarballylate

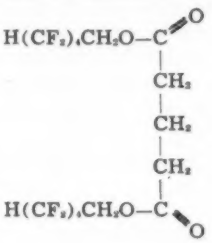

II

Bis(ψ′-amyl) glutarate
Bis(1H,1H,5H-octafluoropentyl)
glutarate

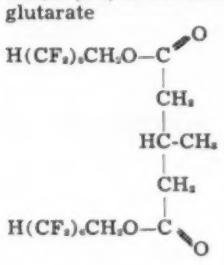

IV

Bis(ψ′-heptyl) 3-methylglutarate
Bis(1H,1H,7H-dodecafluoroheptyl)
3-methylglutarate

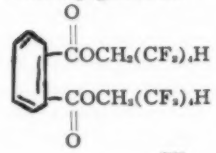

VI

Bis(ψ′-amyl) phthalate
Bis(1H,1H,5H-octafluoropentyl)
phthalate

Table Ia. Physical constants of partially fluorinated esters studied

Substance	Molecular wt (theory)	Density at 20°C (g/cc)	Index of refraction N_D20	Viscosity (cs) 68°F†	Viscosity (cs) 210°F	Flash point (°F)	Freezing* point (°F)
I	558.31	1.4384	1.3555	12	1.44	—	0
II	560.25	1.5980	1.3560	29	2.65	380	−17
III	574.27	1.5570	1.3595	33	2.79	375	−75**
IV	774.31	1.6484	1.3505	66	3.70	440	−30
V	818.32	1.6800	1.3588	240	6.74	—	−30**
VI	594.26	1.6237	1.3990	160	4.80	400	39

† Values interpolated from data.
* The esters supercool readily and are difficult to crystallize.
** Pour point.

water (1.87D), the common alcohols (1.7D) and the esters (1.6D). The effect of introducing the side chain into the acid sector of the ester is to reduce the dipole moment slightly, while the introduction of each CF_2 group in the alcohol chain increases the dipole moment slightly. The high dielectric constants observed arise from the permanent electric moments of these molecules. Values would be higher were it not for molecular association, the arrangement of the molecules being such that the moments cancel each other appreciably.

By determining the polarization of these esters in dilute benzene solution and vectorially adding the polar moments of constituted atomic groups, it is possible to obtain information on the configuration of the molecules. In order to do this the following steps were taken:

1. The dipole moments of the three partially fluorinated alcohols employed in synthesizing the esters were determined.

2. From these dipole moments, the group moments of the $H(CF_2)_4CH_2$-, $H(CF_2)_6CH_2$-, and $H(CF_2)_8CH_2$- radicals were calculated on the assumption that the alcohols were similar in structure to normal aliphatic alcohols and might be considered to have an electric moment arising from the vector addition of two group moments, $\overleftarrow{H(CF_2)CH_2O}$- and $\overrightarrow{HO}$- operating at an angle of 110° (4a).

3. From the group moments thus established, the structures of the partially fluorinated esters which

Table II. Polarization of partially fluorinated esters in benzene at 20°C

Mole fraction	Density (g/cc)	Dielectric constant at 1Mc	Polarization (cc)
	ψ′-Nonyl 2-ethylhexanoate		
0.0022	0.8827	2.301	240
0.0045	0.8878	2.317	232
0.0092	0.8981	2.349	227
1.0000	1.4384	4.66	213
	Bis(ψ′-amyl) glutarate		
0.0045	0.8897	2.340	294
0.0092	0.9015	2.397	291
0.0291	0.9512	2.641	288
1.0000	1.5980	7.48	240
	Bis(ψ′-amyl) 3-methylglutarate		
0.0045	0.8895	2.337	290
0.0092	0.9014	2.399	299
0.0293	0.9493	2.645	283
1.0000	1.5570	7.44	252
	Bis(ψ′-heptyl) 3-methylglutarate		
0.0045	0.8947	2.339	329
0.0093	0.9118	2.399	332
0.0303	0.9811	2.638	325
1.0000	1.6484	5.94	292
	Tris(ψ′-amyl) tricarballylate		
0.0045	0.8962	2.358	394
0.0093	0.9148	2.433	390
0.0304	0.9919	2.787	395
1.0000	1.6800	7.81	340
	Bis(ψ′-amyl) phthalate		
0.0045	0.8907	2.366	381
0.0092	0.9037	2.447	372
0.0292	0.9564	2.804	366
1.0000	1.6237	8.67	263
	Benzene		
1.0000	0.8776	2.283	26.66

were theoretically possible according to known data of stereochemistry were constructed and their dipole moments calculated.

4. The experimentally determined dipole moments were then compared with those theoretically possible.

The dipole moments of the three partially fluorinated alcohols studied were determined by the benzene solution technique outlined previously, the results of which are given in Tables IV and V. Upon dilution with benzene the polarization of all three alcohols increased; the highest values obtained ranged from 198 to 237 cc. The dipole moments of the partially fluorinated alcohols are high (2.88-3.06D) being approximately 90% greater than the dipole moments of the corresponding unsubstituted alcohols. In the liquid state the molecules are highly associated as shown by the relatively low polarization values of the pure compounds.

Table III. Dipole moments of six partially fluorinated esters

$$\mu = 0.219\sqrt{P - R} \times 10^{-18} \text{ esu-cm}$$

Substance	Extrapolated polarization P(cc)	Molar refraction R	Dipole moment* (esu-cm) (±0.04)
ψ′ Nonyl 2-ethylhexanoate	248	84.70	2.80D
Bis(ψ-amyl) glutarate	297	76.60	3.25D
Bis(ψ′-amyl) 3-methylglutarate	281	81.30	3.09D
Bis(ψ′-heptyl) 3-methylglutarate	326	101.2	3.28D
Tris(ψ′-amyl) tricarballylate	398	107.2	3.73D
Bis(ψ′-amyl) phthalate	390	88.53	3.80D

* $D = 1 \times 10^{-18}$ esu-cm.

Table IV. Polarization of partially fluorinated alcohols in benzene at 20°C

Mole fraction	Density (g/cc)	Dielectric constant at 1Mc	Polarization (cc)
	ψ′-Amyl Alcohol		
0.0045	0.8827	2.331	198
0.0180	0.8979	2.471	192
1.0000	1.6647	16.93	117
	ψ′-Heptyl Alcohol		
0.0045	0.8852	2.331	216
0.0182	0.9084	2.468	206
1.0000	1.7532	11.69	148
	ψ′-Nonyl Alcohol		
0.0045	0.8877	2.332	237
0.0185	0.9185	2.466	221

Since the hydroxyl group moment has a known value (4a) of 1.51D and the experimentally determined value of ψ′-amyl alcohol is 2.88D, using the modification of the Law of Cosines for determining the concurrent diagonal,

$$\mu^2_{2.88D} = \mu^2_{1.51D} + \mu^2_x - 2\mu_{1.51D}\,\mu_x \cos 110°$$

the value of the group moment $\overleftarrow{H(CF_2)_4CH_2O}$- was found to be 1.98D and taking 0.74D (4a) as the $\overrightarrow{-C-O-}$ value, the group moment $\overleftarrow{H(CF_2)_4CH_2}$- has a value of 2.72D. By similar reasoning the value of $\overleftarrow{H(CF_2)_6CH_2}$- is 2.81D and that of $\overleftarrow{H(CF_2)_8CH_2}$-, 2.93D.

ψ′-Nonyl 2-ethylhexanoate.—The dipole moments of the planar forms of the aliphatic esters such as amyl, heptyl and nonyl 2-ethylhexanoate were calculated according to the usual methods and found to possess values slightly higher than those of 2-ethylhexanoic acid. The direction of the moment within the ester molecule is, of course, different from that in the acid (4b). Nonyl 2-ethylhexanoate has a value of 1.6D in the cis configuration while the acid has a value of 1.4D in the corresponding planar form. The nonplanar structures calculated on the basis of a 30° tilt (4c) at the C-O-C linkage have dipole moment values of 1.8D for the ester and 1.7D for the acid. A calculated value of 4.4D is obtained for the planar cis form of the ψ′-nonyl 2-ethylhexanoate,

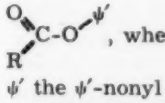

, where R is the 2-ethylhexyl radical and ψ′ the ψ′-nonyl radical. For the nonplanar cis form in which the plane of the ψ′O chain is at an angle of 30° with the plane of the 2-ethylhexanoate group, the calculated dipole moment is 3.8D. This differs from the experimentally determined value of 2.8D. On the other hand, the planar trans form of the 2-

Table V. Dipole moments of the partially fluorinated alcohols

Substance	Extrapolated polarization P(cc)	Molar refraction R	Dipole moment* (esu-cm) (±0.04)
ψ′-Amyl alcohol	200	27.48	2.88D
ψ′-Heptyl alcohol	219	37.34	2.95D
ψ′-Nonyl alcohol	243	47.20	3.06D

* $D = 1 \times 10^{-18}$ esu-cm.

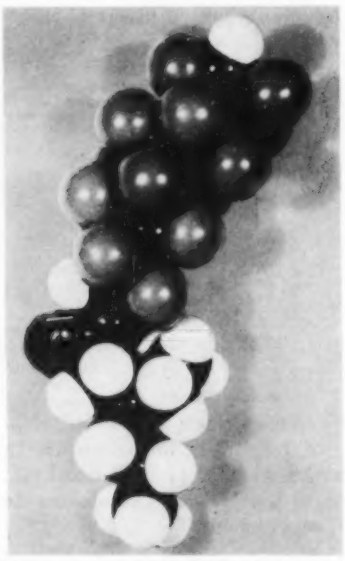

Fig. 1. Probable structure of ψ'-nonyl 2-ethylhexanoate (nonplanar cis form).

ethylhexanoic acid has a calculated dipole moment of 3.9D and the value for the planar trans form of the corresponding nonyl ester 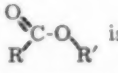 is 3.5D. The calculated value of the dipole moment of the ψ'-nonyl 2-ethylhexanoate in the planar trans form is 0.4D, a value one-seventh that observed experimentally. For these reasons it is probable that the structure of the ψ'-nonyl 2-ethylhexanoate shown in Fig. 1, corresponding to the nonplanar cis form, predominates.

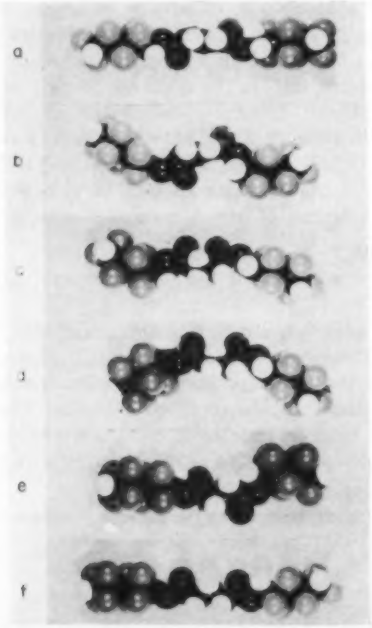

Fig. 2. Planar molecular structure of bis (ψ'-amyl) glutarate: (a) Cis-cis form with carbonyl oxygens opposed; (b) Trans-trans form with carbonyl oxygens opposed; (c) Trans-trans form with carbonyl oxygens adjacent; (d) Cis-trans form with carbonyl oxygens adjacent; (e) Cis-trans form with carbonyl oxygens opposed; (f) Cis-cis form with carbonyl oxygens adjacent.

Bis(ψ'-amyl) glutarate.—Bis(ψ'-amyl) glutarate may be considered for the purposes of structural analysis to be composed of eight electric vectors which give rise to six planar structures, the dipole moments of which can be calculated from the group moments previously established. Two of these structures arise from the cis-cis configurations of the two ester groups, two from the trans-trans configurations and two from combined cis-trans configurations (Fig. 2). Two of the electrically symmetrical planar structures ($\mu=0$), one consisting of a cis-cis form (Fig. 2a) and the other of a trans-trans form (Fig. 2b) are coupled oppositely through the glutaric acid chain; neither of these configurations are thought to be present in the actual material since the latter has an observed dipole moment of 3.2D. By coupling two trans configurations in a plane through the glutaric acid carbon chain and having the carbonyl oxygens on the same side of the molecule (Fig. 2c), an electrically unsymmetrical molecule having a calculated dipole moment of 0.1D results. This value differs appreciably from that observed experimentally and could be present in the material only in very small quantities. Another possible electrically unsymmetrical structure consists of a coupled array of one cis and one trans configuration with both carbonyl oxygens on the same side of the molecule (Fig. 2d). Such a structure has a calculated dipole moment of 3.7D, a value 0.5D greater than that observed experimentally. When either the cis or the trans configuration is rotated through 180°, an unsymmetrical molecule is obtained (Fig. 2e) which has a dipole moment of 3.7D also. Finally by coupling two cis configurations in a plane through the glutaric acid chain, and arranging the carbonyl groups on the same side of the molecule as shown in Fig. 2f, a structure having a calculated dipole moment of 2.6D is obtained.

The observed electric moment of 3.2D, which is intermediate between the two cis-trans configurations (Fig. 2d and 2e) and the cis-cis oxygens adjacent configuration (Fig. 2f), suggests that if the material is planar, it consists of a mixture of all three structures, possibly in the proportions of 50% cis-cis oxygens adjacent, 25% cis-trans oxygens adjacent, and 25% oxygens opposed.

If it is assumed that the molecule is not planar, but rather that the C-O-C atoms form an angle of 30° with the plane of the glutaric acid chain (4c), then it is possible to derive configurations in space having an electric moment approaching 3.2D and structures possessing some of the characteristics of all three planar configurations. As an example, consider the effect of rotating each of the ψ'-O groups in the cis-cis oxygens adjacent configuration (Fig. 2f) (the most abundant planar form) in such a way that each is incident to the same side of the glutaric acid plane at an angle of 30°; the theoretical electric moment is 3.3D. Such a configuration is shown in Fig. 3. No change in the dipole moment would have occurred if the rotation of the ψ'-O groups had been such that both made 30° angles with the glutaric acid chain from opposite sides.

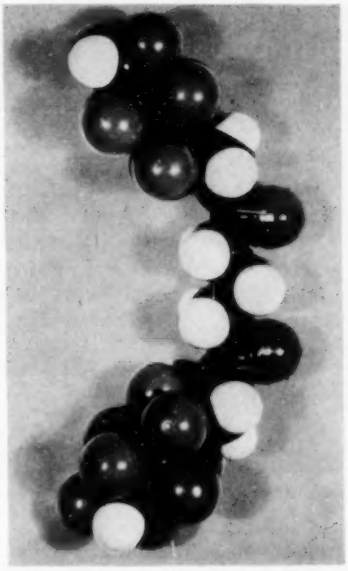

Fig. 3. Probable structure of bis (ψ'-amyl) glutarate (nonplanar cis-cis form with carbonyl oxygens adjacent).

Bis(ψ'-amyl) 3-methylglutarate.—The electrical fields in bis(ψ-amyl) 3-methylglutarate resemble those in bis(ψ'-amyl) glutarate and may be considered to arise from nine electric vectors, four associated with the carbonyl groups, four with the partially fluorinated alkoxy groups, and a small one arising from the 3-methyl group. The latter group causes the slight but measurable difference in the dipole moment of the bis(ψ'-amyl) 3-methylglutarate from that of the bis(ψ'-amyl) glutarate. While the introduction of the 3-methyl group in a planar structure might be thought at first to raise the number of possible structures to twelve, studies made using Stuart-Briegleb atom models indicate that because of steric hindrance only eight structures are likely.

Two cis configurations of ester chains, or two trans configurations coupled oppositely through the 3-methylglutaric acid chain result in structures having dipole moments of 0.4D. A cis configuration coupled to a trans structure with the carbonyl oxygens on the same side of the molecule gives rise to a dipole moment of 3.9D when the 3-methyl group is near the trans carboxyl group and 3.6D when it is near the cis carboxyl group. Two trans configurations with the 3-methyl group on the same side as the adjacent carbonyl oxygens result in a calculated dipole moment of 0.5D, while rotation of the 3-methyl group 180° around the glutaric acid chain results in a calculated value of 0.3D; these values are much lower than that observed experimentally (3.1D). Two cis configurations with the 3-methyl on the same side as the adjacent carbonyl oxygens give rise in a planar structure to a dipole moment of 2.2D. Rotating the 3-methyl group through 180° raises the calculated moment to 3.0D. If the bis(ψ'-amyl) 3-methylglutarate is thus considered to exist in the planar form, the cis-cis configuration with carbonyl oxygens adjacent would seem to predominate. If it is assumed that the molecule is not planar but rather

Fig. 4. Probable structure of bis (ψ'-amyl) 3-methylglutarate (nonplanar cis-cis form with carbonyl oxygens adjacent).

that each ψ'-O group is tilted 30° from the same side of the plane of the 3-methylglutaric acid chain, the dipole moment would approach the value determined experimentally. Such a configuration is shown in Fig. 4.

Bis(ψ'-heptyl) 3-methylglutarate.—Bis(ψ'-heptyl) 3-methylglutarate (3.3D) differs from bis(ψ'-amyl) 3-methylglutarate in that the value of the electric moment associated with the partially fluorinated heptyl group (2.8D) is higher than that associated with the corresponding amyl group (2.7D). The effect of adding vectorially the increment of 0.1D to each of the possible structures results in only small changes in the calculated values from those previously discussed. Thus two cis configurations of ester chains or two trans configurations coupled oppositely through the 3-methyl glutaric acid chain result in structures having dipole moments of 0.4D. A trans-trans configuration with the carbonyl oxygens adjacent and with the 3-methyl group on the same side has a calculated dipole moment of 0.6D, while rotation of the 3-methyl group through 180° around the glutaric acid chain results in a calculated value of 0.2D; these values are much lower than that observed.

A cis-trans configuration with carbonyl oxygens adjacent gives rise to a dipole moment of 3.7D when the 3-methyl group lies near the adjacent oxygens. When it is rotated through 180°, the moment rises to 4.0D. A similar configuration but with the carbonyl oxygens opposed gives rise to a dipole moment of 3.8-4.0D depending on the position of the 3-methyl group. A cis-cis configuration with the 3-methyl group on the same side of the molecule as the carbonyl oxygens gives rise to a dipole moment of 2.2D, while rotating the 3-methyl group through 180° raises the calculated moment to 3.0D.

If it is assumed that the bis(ψ'-heptyl) 3-methylglutarate molecule is not planar but that the ψ'-O

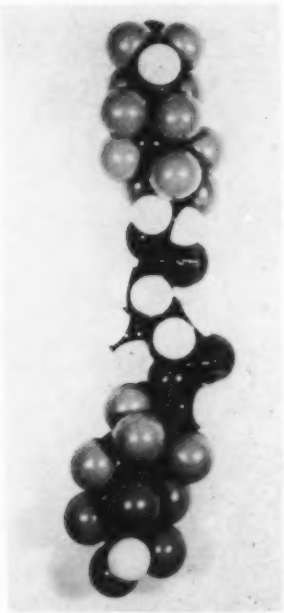

Fig. 5. Probable structure of bis (ψ'-heptyl) 3-methylglutarate (nonplanar cis-cis form with carbonyl oxygens adjacent).

groups are tilted from the same side of the plane of the 3-methylglutaric acid chain, the dipole moment would approach the observed value of 3.3D. Such a structure is shown in Fig. 5.

Tris(ψ'-amyl) tricarballylate.—The tris(ψ'-amyl) tricarballylate molecule (3.7D) may be thought of as being a bis(ψ'-amyl) 3-methylglutarate molecule in which a -C(O)Oψ' group has been substituted for the 3-methyl group. This suggests the possibility of molecular configurations in the form of a T. If the groups are aligned in this way in a plane, there are five combinations of cis and trans configurations possible which lead to electrically unsymmetrical models having permanent moments in the range 0.2-4.7D. Thus the model consisting of two trans groups in the cross-bar of the T and one cis group as the center post (trans-cis-trans) has a calculated moment of 4.0D, while a cis-trans-cis configuration has a moment of 2.4D. Furthermore, a cis-cis-cis configuration has a calculated moment of 4.7D and a trans-trans-trans configuration a moment of 0.2D. Finally, the cis-trans-trans configuration has a calculated moment of 3.6D. All the foregoing are theoretical planar structures; when assembled from Stuart-Briegleb atom models, however, none appear likely because of steric hindrance. Rather, it appears more likely that the actual configuration is nonplanar. One such structure which appears likely is that shown in Fig. 6; the center post of the T is a cis configuration having its vector in the plane perpendicular to the paper; the cross-bar consists of two cis configurations which have been tilted down out of the plane of the paper. The calculated moment of such a molecule is 3.7D when the angle between the cross-bar vector and the center-post vector is 114°.

Bis(ψ'-amyl) phthalate.—The observed electric moment of bis(ψ'-amyl) phthalate is 3.8D, the highest value of the esters studied. In establishing the structure of the ortho-substituted benzene derivatives, the assumption is made that the benzene ring is planar and that the groups exert electric forces at an angle of 80° (5). Assuming this, a trans-trans oxygens adjacent configuration

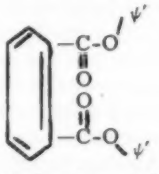

results in a calculated value of 0.3D, while a value of 0.3D is also obtained from a trans-trans oxygens opposed configuration

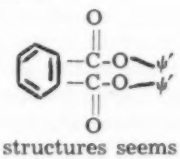

Neither of these structures seems likely. A configuration having cis-trans oxygens opposed has a value of 3.9D while, cis-trans oxygens adjacent results in a value of 4.0D. Both of these values are close to that observed experimentally. Finally, a cis-cis oxygens opposed structure has a calculated moment of 3.9D, while the cis-cis oxygens adjacent structure has a value of 7.3D. From results obtained, it thus appears that one of three planar structures is possible; from Stuart-Briegleb atom models, however, none seems probable; actually, a number of nonplanar configurations containing at least one cis structure possess dipole moments in the range of 3.9D, but due to the limitations of the dipole analysis technique, the exact nonplanar structure is not deducible.

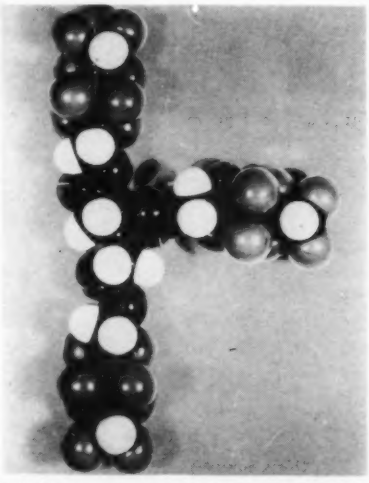

Fig. 6. Probable structure of tris (ψ'-amyl) tricarballylate (tri-cis form).

Conclusions

The dipole moments of the partially fluorinated esters were found to be higher than that of water, the common alcohols, and unhalogenated esters. The introduction of a side chain into the acid sector of the ester tends to reduce the dipole moment slightly. The introduction of each CF_2 group increases the dipole moment slightly. The high dielectric constants of the esters arise from the permanent mo-

ments and would be even higher were it not for molecular association.

A study of the molecular structure of the esters has indicated that several possible structures may exist for each compound, but experimental data limits these possible structures to ones which contain a cis form. It is also concluded that the molecules exist for the most part in a nonplanar form.

Acknowledgments

The authors wish to thank W. A. Zisman for suggesting this investigation and P. D. Faurote, C. M. Murphy, and J. G. O'Rear for making available the samples of partially fluorinated alcohols and esters used in these studies.

Manuscript received November 5, 1956. This paper was prepared for delivery before the Washington Meeting, May 12-16, 1957.

Any discussion of this paper will appear in a Discussion Section to be published in the December 1957 JOURNAL.

REFERENCES

1. P. D. Faurote, C. M. Henderson, C. M. Murphy, J. G. O'Rear, and H. Ravner, *Ind. Eng. Chem.*, **48**, 445 (1956).
2. C. P. Smyth, "Determination of Dipole Moments" in "Physical Methods of Organic Chemistry—II," A. Weissberger, Editor, p. 994, Interscience Publishing Co., New York (1946).
3. T. D. Callinan, J. B. Romans, and R. M. Roe, U. S. Naval Research Laboratory Report 4488, Feb. 17, 1955.
4. C. P. Smyth, "Dielectric Behavior and Structure," (*a*) p. 301, (*b*) p. 306, (*c*) p. 307, McGraw-Hill Book Co., New York (1955).
5. R. J. W. LeFevre, "Dipole Moments," 2nd ed., p. 66, Methuen & Co., Ltd., London (1948).

The Thermoluminescence of CaF_2:Mn

Robert J. Ginther and Russell D. Kirk

United States Naval Research Laboratory, Washington, D. C.

ABSTRACT

The thermoluminescence of manganese-activated calcium fluoride has been found to be dependent on both its manganese content and the presence of other foreign ions. Sodium and oxygen promote high temperature glow peaks, whereas the addition of trivalent cations causes the thermoluminescence of oxygen-containing material to occur at lower temperatures. Thermoluminescence may be excited by x-rays, by mechanical handling, or by irradiation with blue light. Glow peak positions are independent of the method of excitation.

In a current investigation of the application of thermoluminescence to the dosimetry of high energy radiation, one of the most efficient materials found was CaF_2:Mn. The preparation of this phosphor and its sensitization by Ce have been described previously (1). In the present paper, the dependence of the thermoluminescence of this phosphor on both its Mn content and on the effect of substituents are presented. Its application as a thermoluminescent dosimeter will be described elsewhere.

Among the most important characteristics required of a thermoluminescent dosimeter material is freedom from low temperature glow peaks which would enable thermal radiation to free trapped electrons at low temperatures and erase the effect of the high energy radiation (2). It is therefore the search for materials having only high temperature thermoluminescence and the study of the effect of compositional variation on glow peak position which were the principal subjects of the investigation. Consequently, only thermoluminescence above room temperature was of interest.

Consideration of calcium fluoride as a possible dosimeter material was occasioned by the observation of an intense thermally stimulated emission following the x-irradiation of a mineral sample from Franklin, N. J. Wick (3) has studied the thermoluminescence of both synthetic and natural fluorite containing manganese. In her work, glow curves were not obtained, and some low temperature ($<100°C$) thermoluminescence was observed with every sample.

Experimental

Synthetic samples of Mn-activated calcium fluoride were prepared by the technique described earlier (1).

For the thermoluminescence measurements, ½ in. diameter powder plaques were pressed into the recess of either a brass or Al holder. After irradiation, samples were heated at a rate of 10°C/min in a light-tight container. The light output of the phosphor was detected by a 1P21 photomultiplier tube, and amplified by a sensitive d-c amplifier. The phosphor temperature was detected by a thermocouple. The phototube and thermocouple signals were simultaneously recorded with an X-Y recorder yielding a direct plot of thermoluminescence vs. temperature.

A Corning No. 9780 filter was employed in the phototube housing to minimize the signal contributed by black body radiation at high temperatures. In the case of weak thermoluminescent emissions, the red light emitted by the hot sample and surroundings can exceed the thermoluminescence signal and limit the sensitivity of measurement. Use of

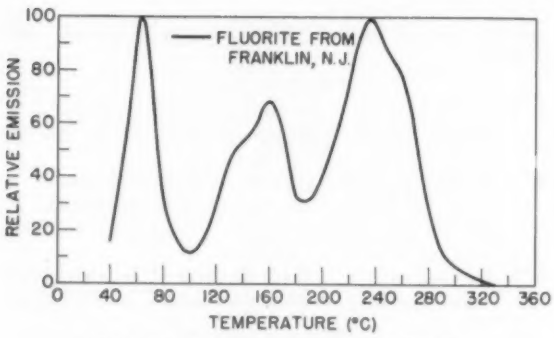

Fig. 1. Thermoluminescence of natural fluorite

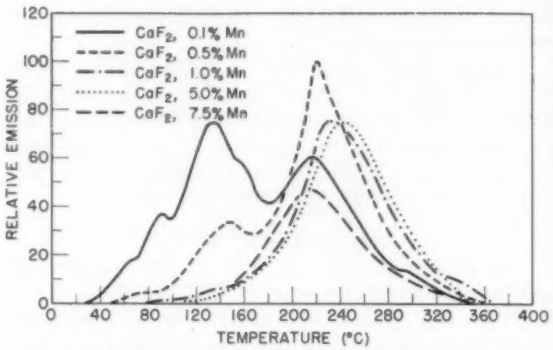

Fig. 2. Thermoluminescence of synthetic CaF_2:Mn as a function of Mn content.

the 9780 filter which transmits the green emission of the phosphor, but absorbs in large measure the red thermal radiation, permits the employment of the amplifier at its full sensitivity (0.001 μa for full scale meter deflection). At this high sensitivity the signal from the thermal radiation is evident from an increasing phototube signal beginning at a temperature of about 340°C. Since the thermoluminescence of CaF_2:Mn is almost completely exhausted at this temperature, an increasing signal at 340°C does not interfere with the measurement.

For the measurement of very low thermoluminescent emission a second apparatus employing a 5819 phototube was constructed. This apparatus was designed to employ powder plaques 1½ in. in diameter rather than the ½ in. diameter plaques used in the earlier model. The larger plaques together with the greater cathode area of the 5819 compared to that of the 1P21 tube gave a sensitivity increase of about a factor of five. The new unit employed the same circuitry and did not differ in principle from the earlier apparatus.

For the determination of the effect of composition on the glow spectrum or on relative sensitivity, samples were exposed to 40 KVP x-rays from a Bucky Therapy Unit[1] employing a Machlett tungsten target, Be window tube.

Thermoluminescence as a Function of Composition

The glow curve for the sample of fluorite from Franklin, N. J., is shown in Fig. 1. This material has a large proportion of its emission at temperatures below 200°C. The mineral has a high temperature peak at 235°C, however; its thermoluminescent yield to the given x-ray exposure placed it among the most sensitive materials the authors have observed. Its green emission suggested the presence of a Mn activator, and it therefore seemed of interest to determine the thermoluminescent properties of Mn-activated CaF_2.

The first series of synthetic samples measured were those containing from 0.10 to 7.50 mole % Mn. Their thermoluminescence following equal exposure to 40 KVP x-rays is shown in Fig. 2. With the two lowest Mn concentrations strong low temperature thermoluminescence is obtained. There is evidence of low temperature peaks at about 90° and 140°C in the glow curve for the 1.0% Mn sample, but samples of 5.0% and 7.5% have but a single glow peak. Apparently 7.5% of Mn exceeds the optimum activator content with respect to both the thermoluminescent yield and the position of the glow peak.

Samples having Mn contents of 2, 3, and 4% were then prepared. Their glow curves are shown in Fig. 3 along with those of the 1.0 and 5.0% samples for comparison. The optimum Mn content appears to be 3.0%. Of the samples containing no vestiges of the low temperature glow peaks it is the most efficient, and its peak is at the highest temperature, 255°C. However, since a number of samples containing 5.0% of Mn together with additions of other foreign ions were already available, this higher concentration was used for further investigation of the thermoluminescence of the system.

It was known that the emission spectrum of calcium fluoride varied with its Mn content, and a correlation of the glow peak position with Mn concentration at first appeared plausible. However, it will be shown that freedom from low temperature thermoluminescence is a function of more than simply the Mn content, so that a correlation of the glow curves with the emission spectra is not warranted.

The above samples had been prepared from calcium fluoride precipitated from $CaCO_3$ with dilute HF. This precipitation technique yielded a coarse grained product which is resistant to hydrolysis on drying and believed to contain a minimum of hydrolyzed products such as $Ca(OH)_2$. Use of commercially available CaF_2 known to contain either $Ca(OH)_2$ or $CaCO_3$ yielded phosphors with very inefficient thermoluminescence. It was therefore of interest to determine the effect of employing a CaF_2

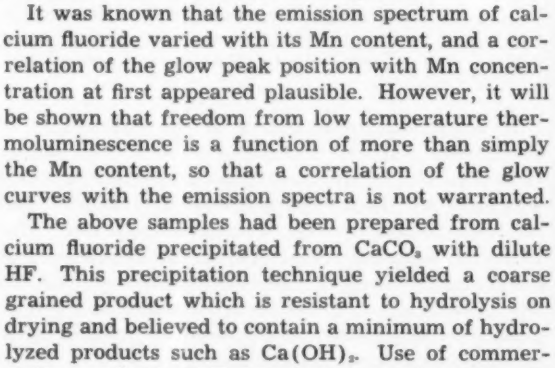

Fig. 3. Thermoluminescence of synthetic CaF_2:Mn as a function of Mn content.

[1] X-ray Manufacturing Corp.

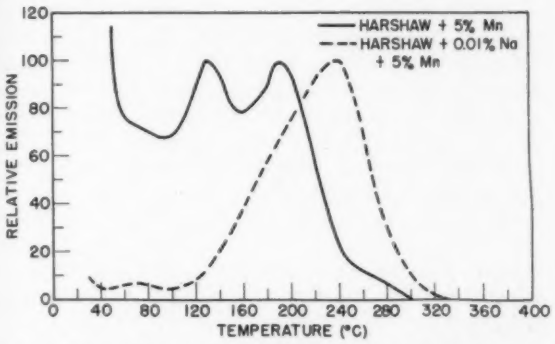

Fig. 4. Thermoluminescence of CaF_2:Mn prepared from Harshaw CaF_2.

raw material with the lowest available oxygen content. Such a source presumably is optical quality crystals, either synthetic or natural. Accordingly samples were prepared from both Harshaw and Optovac synthetic calcium fluoride, as well as from a clear, colorless mineral sample. The glow curve of a CaF_2, 5% Mn sample prepared from Harshaw calcium fluoride is shown in Fig. 4. There is a large proportion of the thermoluminescence below 100°C, and none of the predominant glow peaks are at temperatures above 200°C. Phosphors made from Optovac and natural fluorite gave similar, but not perfectly identical glow curves. Minor variations in the height of the glow peaks were obtained depending on the raw material source, but in every case the glow curve consisted of three approximately equal peaks at 190°, 130°, and in the neighborhood of 40°-60°C. With none of these raw material sources was a strong glow peak above 200°C observed. Spectrographic analysis of the single crystal sources of calcium fluoride indicated that they were all relatively pure. Traces of only B, Mg, and Sr were found in the synthetic crystals. The natural crystal contained in addition faint traces (ca 0.0001%) of Fe and Na.

Addition of 0.01% Na to this formulation by incorporating ground single crystal NaF in the batch composition did produce a phosphor having a glow curve showing mainly high temperature thermoluminescence, but the glow peak obtained was much broader than that of samples prepared from precipitated calcium fluoride with the same Mn concentration. Moreover, as shown in Fig. 4, with 0.01% Na there is still evidence of low temperature peaks. Spectrographic analysis of the precipitated CaF_2 revealed much less than 0.01% of any alkali ion, so the high temperature characteristic associated with use of precipitated CaF_2 is not due to alkali impurity. Inclusion of Na in samples prepared with precipitated CaF_2 did not influence the glow peak position, but produced a loss of efficiency.

It was found that the incorporation of oxygen in Harshaw CaF_2 produced CaF_2:Mn phosphors with a high temperature thermoluminescence similar to that of samples made with precipitated CaF_2. Oxygen may be effectively incorporated by preheating the CaF_2 in a moist atmosphere or by refiring finished phosphors in a dry atmosphere with $CaCO_3$. Experiments performed to date do not distinguish

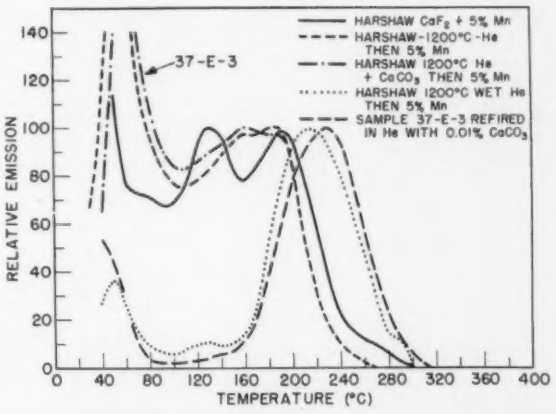
HARSHAW CaF_2 + 5% Mn
HARSHAW-1200°C-He THEN 5% Mn
HARSHAW 1200°C He + $CaCO_3$ THEN 5% Mn
HARSHAW 1200°C WET He THEN 5% Mn
SAMPLE 37-E-3 REFIRED IN He WITH 0.01% $CaCO_3$
37-E-3
RELATIVE EMISSION
TEMPERATURE (°C)

Fig. 5. Effect of oxygen upon thermoluminescence of CaF_2:Mn prepared from Harshaw CaF_2.

whether the oxygen is combined as O^{2-} or OH^- ion.

In Fig. 5 are reproduced the glow curves of some samples prepared with oxygen additions to Harshaw CaF_2. Included in this figure for comparison is the glow curve of the 5% Mn sample with no oxygen addition. When Harshaw CaF_2 was first fired at 1200°C in wet He, and then this partially hydrolyzed material was employed in the synthesis of a 5.0% Mn phosphor, a glow curve having its main peak at 215°C was obtained. Presumably the wet He firing effected the incorporation of oxide or hydroxide ion. Insofar as the authors are aware, neither the existence of a calcium oxyfluoride nor the solubility of O^{2-} or OH^- ions in CaF_2 have been reported, so the mechanism of oxygen incorporation is unclear.

An attempt was made to clarify this situation by preparing a sample from Harshaw CaF_2 in which O^{2-} ion was introduced in a dry atmosphere by prefiring the fluoride with $CaCO_3$ in dry He. As shown in Fig. 5 the variation of the glow curve produced by this synthesis procedure is very different from that obtained by hydrolysis. Moreover, the variation observed is in no way connected with the addition of oxygen as shown by the glow curve of a sample prepared in the same way except that $CaCO_3$ was omitted in the dry He firing. However, if any of the three phosphors shown to have low temperature thermoluminescence in Fig. 5 is refired with 0.10% $CaCO_3$, a phosphor with high temperature thermoluminescence is obtained.

From the above experiments it is observed that the order in which the oxygen and the Mn are incorporated in CaF_2 is important. For the hydrolysis procedure, the CaF_2 must first be fired in wet He and then refired with the source of Mn in a dry atmosphere to produce the phosphor. Experiments in which Mn-containing fluorite was fired in wet He led to oxidation of Mn and a dark brown, weakly luminescent product. The required order in which oxygen and Mn must be introduced when $CaCO_3$ is the source of oxygen is more difficult to understand. In this case the oxygen must be incorporated after the Mn has been combined in the calcium fluoride. From these experiments it has been concluded that the impurity responsible for the thermoluminescence

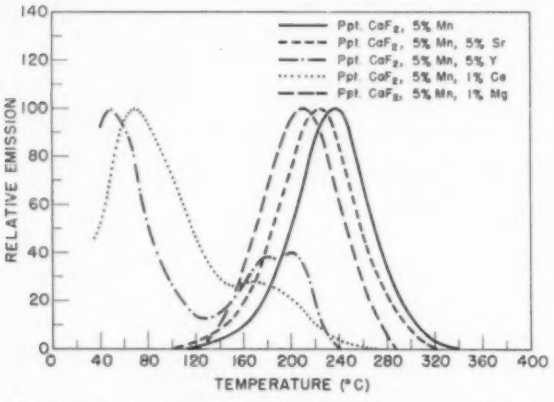

Fig. 6. Effect of substituents on the thermoluminescence of CaF_2: Mn.

characteristics of phosphors prepared from precipitated CaF_2 is oxygen. While some low temperature emission was observed from samples prepared from Harshaw calcium fluoride with oxygen additions, the high temperature glow peak of these materials is similar in breadth to that of phosphors made with precipitated CaF_2.

In a further attempt to confirm that oxygen is the impurity responsible for the thermoluminescence characteristic of phosphors prepared from precipitated calcium fluoride, attempts were made to process the precipitated material in order to remove the contained oxygen and to demonstrate that phosphors prepared from such material have low temperature thermoluminescence. To date such attempts have been unsuccessful. Firing phosphor samples with either ammonium fluoride or bifluoride had no effect upon their glow curves. Incorporation of PbF_2 in the formula, a technique employed by Stockbarger and Blanchard (4) to deoxidize fluoride melts, shifted the glow peak only about ten degrees to lower temperature. Apparently the ammonium fluoride volatilizes before reaction can occur and PbF_2 is ineffective at 1200°C. The minor shift produced by PbF_2 is probably associated with the presence of Pb^{++} ion rather than the removal of oxygen.

Low temperature thermoluminescence may be obtained by incorporating certain foreign ions in Mn-activated calcium fluoride prepared from precipitated material. Fig. 6 illustrates the glow curves obtained with some of these additives. Sr and Mg are shown to provide rather minor shifts of the glow peaks to lower temperature. Ce and Y suppress the high temperature thermoluminescence and produce strong low temperature peaks. No addition was found which would either intensify the high temperature glow peak of phosphors made with precipitated CaF_2 or shift this peak to even higher temperatures.

The above observations were obtained with x-ray excitation of the phosphor. The material may also be excited by γ-rays, by visible light, and by mechanical treatment to produce the same glow peaks. Observation of thermoluminescence following the grinding of glass and of fluorite was made by Nyswander and Cohn (5) who named the phenomenon tribothermoluminescence. Wick observed tribothermoluminescence in Mn-activated fluorite. The 5.0% Mn samples employed in the current investigation exhibited this property. The extreme sensitivity of this material to mechanical handling is illustrated by the following sequence of experiments. Instead of pressing the sample into a plaque, the phosphor was cemented in with sodium silicate and a glow curve measurement was made. A thermoluminescence excited by the grinding of the fired sample cake was observed. Without disturbing the apparatus in any way, the glow curve measurement was repeated. No thermoluminescence was recorded, indicating that the heating of the previous run had exhausted the phosphor. The sample holder was then removed from the apparatus and replaced in complete darkness, and a third glow curve was measured. Approximately one-half of the original thermoluminescence was recorded. The same results were obtained regardless of whether the glow curves were obtained by heating the samples in air, in He, or in vacuum.

The thermoluminescence excited by visible light is very weak, and is best observed only after the mechanically stimulated emission is removed. If a sample is not removed from the apparatus after a thermoluminescence measurement, but is irradiated with white light, a glow curve is obtained upon reheating the sample. Some irradiations made with filters showed that blue light produced the effect but that red light did not. Blue light is absorbed in a 4000A Mn absorption band. This absorption band was first detected by excitation measurements on powdered samples (1). Garlick (6) has recently confirmed its existence by absorption measurements on clear crystals.

Conclusions

The high temperature glow peak of CaF_2:Mn has been shown to be a function of both its Mn content and the presence of either alkali or oxygen impurity. The simplest explanation of the effect of alkali or oxygen in producing a distinct glow peak is that these ions produce local deficiencies of positive charge (7) which are compensated by the production of either negative ion vacancies or interstitial positive ions. The compensating defects provide deep electron traps resulting in high temperature thermoluminescence. Addition of trivalent ions to oxygen-bearing fluorite suppresses the positive charge deficiency and diminishes the high temperature thermoluminescence.

Results obtained by blue light excitation are not easily accounted for by the above explanation. Blue light is absorbed in a discrete Mn absorption band and would not be expected to produce free electrons. In the light of this observation the influence of the impurity must be attributed to a direct effect upon the Mn activator.

Acknowledgment

The authors wish to thank Phillip Pizzolato who assembled the apparatus and made many of the thermoluminescence measurements.

Manuscript received November 1, 1956. This paper was prepared for delivery before the San Francisco Meeting, April 29 to May 3, 1956.

Any discussion of this paper will appear in a Discussion Section to be published in the December 1957 JOURNAL.

REFERENCES

1. R. J. Ginther, *This Journal*, **101**, 248 (1954).
2. F. Daniels and W. P. Reiman, University of Wisconsin, Final Report "The Thermoluminescence Dosimeter," Chemical Procurement Agency, Contract No. DA-18-108-CML3069, Feb. 16, 1954.
3. F. Wick, *J. Opt. Soc. Amer.* **27**, 275 (1937).
4. D. C. Stockbarger and A. A. Blanchard, U. S. Pat. 2,498,186, Feb. 21, 1950.
5. R. E. Nyswander and B. E. Cohn, *Phys. Rev.*, **36**, 1257 (1930).
6. G. F. J. Garlick, Private communication.
7. J. H. Schulman, R. J. Ginther, and R. D. Kirk, *J. Chem. Phys.*, **20**, 1966 (1952).

Defect Structure and the Temperature Dependence of Hardness of an Intermetallic Compound

J. H. Westbrook

Research Laboratory, General Electric Company, Schenectady, New York

ABSTRACT

The temperature dependence of hardness of the intermetallic compound AgMg was studied from —190°C to the solidus temperature over the entire homogeneity range. The effect of structure on hardness at high homologous temperatures differs radically from that at low temperatures. These results, over virtually the full homologous temperature range, appear to rationalize previously contradictory studies of the effect of defect structure on the room temperature strength of intermetallic compounds.

Numerous studies have confirmed the importance of defect structure in determining mechanical properties of intermetallic and interstitial compounds. Experimental results are contradictory, however, some plots of strength vs. composition showing minima, others maxima. Kornilov (1) has suggested that time and temperature might also affect mechanical properties of a compound. Moreover, it was found recently (2) that iron group aluminides containing either vacancy or substitutional defects were considerably harder than the corresponding defect-free stoichiometric compositions, although the magnitude of this effect diminished with increasing temperature. Since in that study the effec of defect structure could not be examined at temperatures higher than about 0.6 of the melting point, the experiments were repeated using AgMg, a stable compound which melts congruently at a substantially lower temperature (820°C) and which exists over a broad homogeneity range. It has the ordered BCC or CsCl structure, as did the previously studied aluminides. This compound permitted testing of the suggestion arising from the earlier work that, at sufficiently high homologous temperatures, lattice defects have a softening effect even with short times of loading.

The Silver-Magnesium System

Although the Ag-Mg system has been investigated many times, no single investigator has done a thorough job over the whole range of the diagram. The main features of the diagram were first delineated by Zemczuzny (3) and later refined and supplemented by other investigators (4-12). The early findings of Saeftel and Sachs (13) are by now completely discredited. Fig. 1 is a composite of what appear to be the most accurate portions of the previously cited works.

Solubility limits of the compound AgMg or β phase are deserving of special mention, not only because of their importance to the present investigation, but also because this is one of the most serious areas of disagreement among investigators. Zemczuzny (3) on the basis of his thermal analyses set the maximum solubility limits at 37.4 and 65.43 A/o Mg. Smirnov and Kurnakov (4), working with specimens annealed at 400°C, claimed confirmation of Zemczuzny's figures, but their actual hardness and resistivity data would seem to indicate limits at 400°C more like 40.0 and 58.2 A/o Mg. X-ray and metallographic studies by Ageev and Kuznetzov (7) on specimens annealed at and quenched from a series of temperatures show somewhat narrower

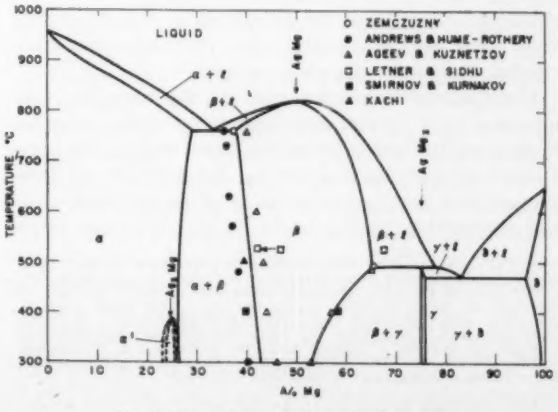

Fig. 1. Phase diagram of the Ag-Mg system

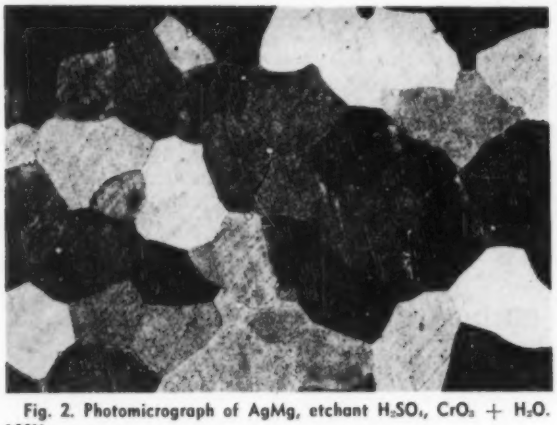

Fig. 2. Photomicrograph of AgMg, etchant H_2SO_4, CrO_3 + H_2O. 100X.

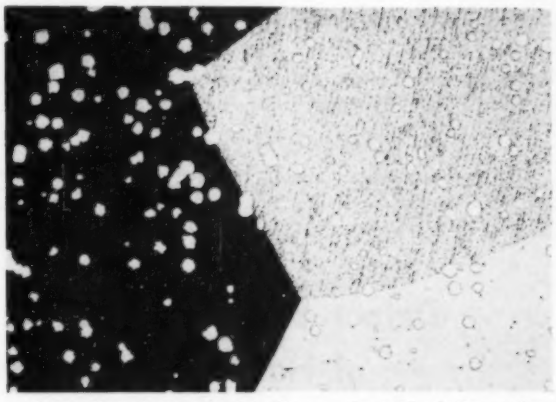

Fig. 3. Photomicrograph of AgMg + α-Ag solid solution, etchant H_2SO_4, CrO_3, + H_2O. 100X.

solubility limits on both sides, as well as a significant temperature dependence of solubility. Andrews and Hume-Rothery (9) determined the limit only on the Ag-rich side. Their results agree only approximately with those of Zemczuzny (3) and Smirnov and Kurnakov (4). Letner and Sidhu (10) claimed the limits at 525°C to be 47.0 and 67.5 A/o Mg, but their lattice parameter data indicate that 42.0 A/o Mg is more likely for the Ag-rich limit. The emf data of Kachi (12) at 500°C define the same limit as just under 40 A/o Mg. Consideration of all these results, as well as the findings of the present study,[1] indicate that the probable boundaries of the β phase lie as shown in Fig. 1.

Experimental

Preparation of samples.—Approximately 500 g heats of several different β phase alloys were induction melted in a graphite crucible and cast into a 1 in. diameter split graphite mold. The Mg[2] and Ag[3] used were both 99.99% pure. Cl gas was bubbled through the melt continuously and maintained as a cover during pouring to protect the metal from oxidation. The ingots were then homogenized 8 hr at a temperature 50°-100° below the supposed melting point. Early in the program, laboratory dry H was used for the heat treating atmosphere. However, variations in dew point at times resulted in serious oxidation of samples. Therefore, most of the heat treatments were carried out in Vycor tubes filled with dry A at approximately 0.5 atm; Ti chips separated from the sample by a plug of quartz wool were used as a getter. This technique was successful even with Mg-rich samples.

Metallographic preparation of the samples was impeded by a pronounced tendency for the material to flow badly during polishing, resulting in the production of structural artifacts. Satisfactory surface preparation was achieved only with extreme care and repeated polishing and etching. Representative photomicrographs of structures obtained are shown in Fig. 2-4. Fig. 2 is typical of those alloys near the middle of the homogeneity range, i.e., a simple, single phase of equi-axed grain structure. Fig. 3 and 4 are typical of alloys, single phase at high temperature, which have precipitated Ag and $AgMg_3$, respectively, on cooling due to decreasing solubility, as shown in Fig. 1. The homogeneity of each ingot was checked metallographically, following which a hardness test specimen approximately ½ in. high and 1 in. in diameter was cut from the ingot. Drilled chips were then removed from an immediately adjacent portion of the ingot for chemical analysis. These fine particles oxidized quite rapidly so that it was necessary to weigh the sample immediately after obtaining it. Ag was determined by electrodeposition from alkaline cyanide solution. In most cases, the balance of the ingot was remelted to make other compositions. Analysis confirmed that usually a small but significant amount of Mg was lost on melting. Therefore, all compositions noted herein are analyzed rather than intended values.

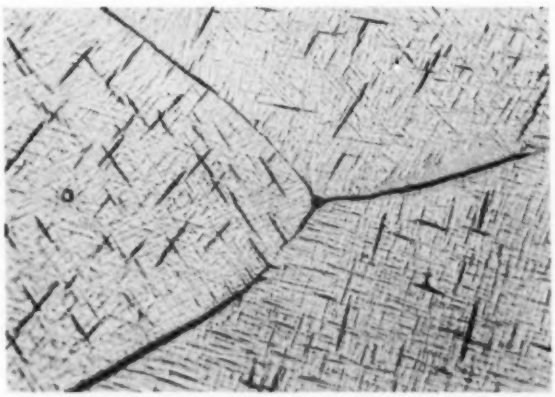

Fig. 4. Photomicrograph of AgMg + γ-$AgMg_3$, etchant HNO_3, Hac + H_2O. 250X.

Hardness tests.—Indentation hardness measurements were made on all samples[4] with a Vickers diamond indenter and a 200 g load. From room tem-

[1] A 38.8 A/o Mg alloy was found to be two phase at 700°C and below. A 65.8 A/o Mg alloy showed no evidence for peritectic formation of γ phase when quenched from 475° or 500°C but only a characteristic Widmanstatten precipitate of γ from solid solution. The same alloy quenched from 525°C showed evidence of liquid phase formation. The inability to retain the solid solution condition at least for the 500°C quench must be attributed to insufficient rapidity of quench. This could perhaps have been circumvented had a vacuum quenching furnace been available.

[2] Dow Chemical Co.

[3] Handy and Harman.

[4] The 38.8 A/o Mg alloy was tested even though a very small amount of second phase was present. It is believed that the occurrence of this second phase in the amount and distribution present did not significantly affect the results. However, fine precipitate present in the 65.8 A/o Mg sample as in Fig. 4 did affect the results; consequently, data for this composition were excluded from further consideration.

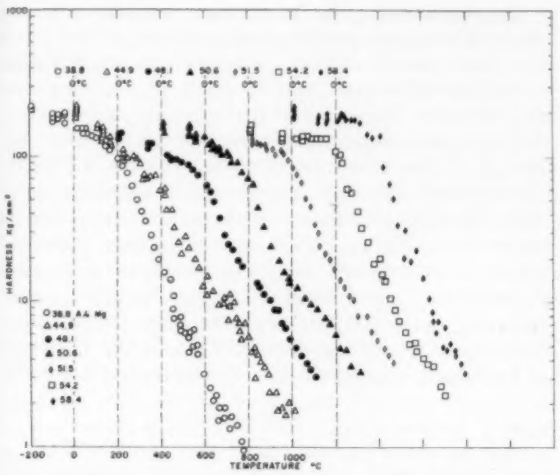

Fig. 5. Temperature dependence of hardness of several AgMg compositions.

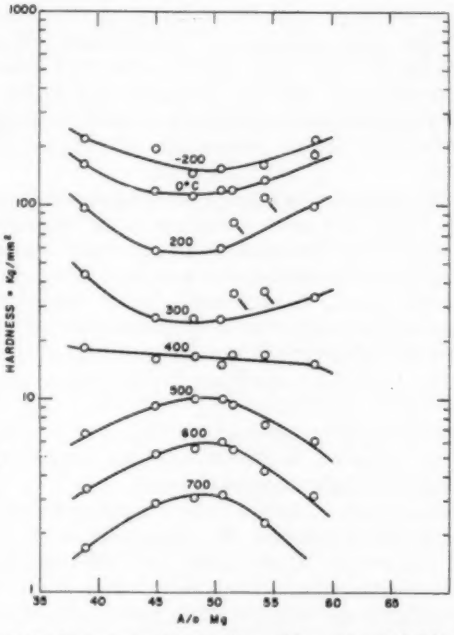

Fig. 6. Hardness-composition isotherms for a series of AgMg alloys

perature to the melting point a micro hot hardness tester of modified Bergh design was used (14). The instrument and testing procedure were identical to those previously employed (2), except that a positive pressure of argon was used as an atmosphere rather than vacuum in order to minimize volatilization of Mg at high temperatures. Argon was purified before introduction into the testing chamber by passage over hot Mg chips (500°C). For tests below room temperature, a Tukon micro hardness tester was used together with cooling baths of liquid N, Freon-12, or dry ice-acetone. Room temperature points determined with both instruments were found to agree satisfactorily. Hardness-temperature curves were run at least twice on each sample to insure that surface work hardening effects had been eliminated (2). The reduced data were finally plotted for convenience on a semi-logarithmic scale (14,15). All of

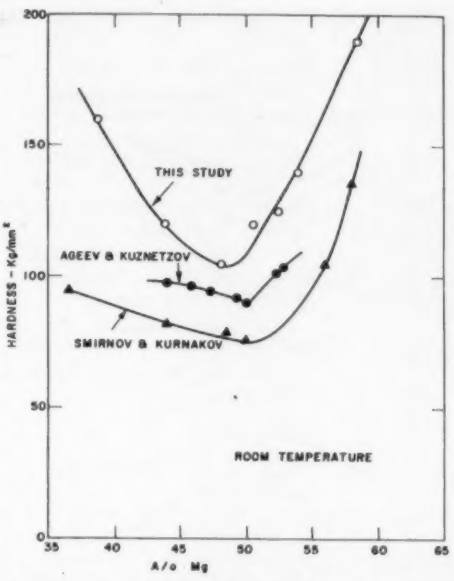

Fig. 7. Comparison of the effect of composition on room temperature hardness of AgMg according to different investigators.

these data are given in Fig. 5. The origins for compositions of successively higher Mg content have each been shifted 200°C higher than the previous curve, to prevent confusion of points.

Discussion

The curves of Fig. 5 are similar in their general features to those previously observed (2,14,15) in that on these semi-logarithmic coordinates the curves are comprised of two approximately linear segments which cross at about 0.5 of the melting point. In this case, however, certain regular and reproducible deviations from true linearity were observed in the high temperature segment of all curves except that for the most Ag-rich alloy. Careful consideration of and testing for possible sources of this anomaly have thus far failed to disclose any unequivocal explanation for this behavior (16).

The effects of defect structure on hardness are most readily perceived from hardness-composition isotherms. The data of Fig. 5 have been cross plotted in this manner in Fig. 6. Here it will be observed that hardness minima are located near the stoichiometric composition at low temperatures. As the temperature increases, these minima flatten and ultimately reverse to become maxima at very high temperatures. The room temperature hardness data by Smirnov and Kurnakov (4) and by Ageev and Kuznetzov (7) are compared with the results of the present study in Fig. 7.[5,6] In view of the differences in testing technique (Smirnov and Kurnahov-Brinell 5.6 mm ball, 50 kg load; Ageev and Kuznetzov unknown), agreement is considered satisfactory. The x-ray studies of Ageev and Kuznetzov (7) and of Letner and Sidhu (10) and the thermodynamic

[5] Ageev and Kuznetzov present their data normalized to a value of 1.00 at 50.0 A/o Mg. Therefore, it was necessary to choose some real hardness for this composition for purposes of comparison. A value of 90 kg/mm² was assumed.

[6] The minimum in the curve as drawn deviates slightly from the stoichiometric value of 50 A/o. It is believed that the data are inadequate for this to be significant.

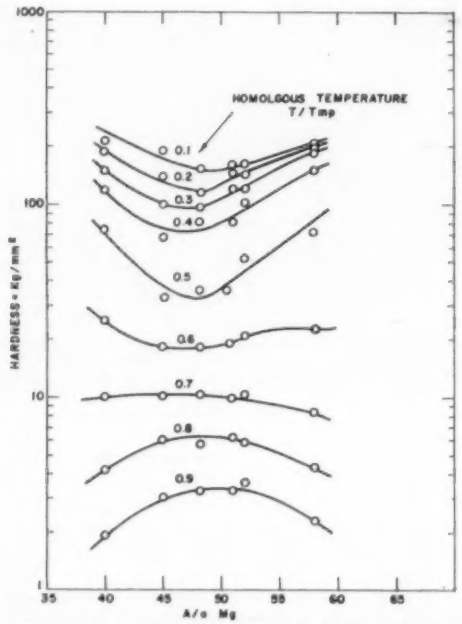

Fig. 8. Hardness-composition isohomologs for a series of AgMg alloys

investigations of Kachi (12) show that AgMg is most perfectly ordered at the stoichiometric composition and has a substitutional defect structure on both sides of stoichiometry. The hardness minima found at low temperatures are therefore in agreement with the previously established effects of defect structure (2).

In rationalizing the high temperature behavior of AgMg, one might wonder whether the lower hardness of compositions near the solubility limits is a result of closer approach to the melting point as has been discussed for other systems by Westbrook and Nisbet (17). To assess this possibility, experimental data are plotted in Fig. 8 as isohomologous temperature curves, i.e., the hardness values on any one curve represent data for different actual temperatures, but for the same ratio of test temperature and solidus temperature. This method of plotting has only altered the shapes of the curves slightly as compared to Fig. 6; the curves become flat at about 0.6 of the melting point and definite maxima still exist above a homologous temperature of about 0.8. This result indicates that the apparent softening is truly an effect of defect structure and not of variations in melting point.

The need for consideration of possible effects of a temperature dependent defect concentration has been obviated by the thermodynamic studies of Kachi (12). Kachi deduced from emf measurements that the degree of disorder of AgMg in the neighborhood of 500°C is 10^{-4}, a value about 100 times as small as that usually experienced for 3/2 electron compounds.[7] These data also permit calculation of a hypothetical disordering temperature of 1500°K, far above the actual melting point of the compound, a result which is indicative of the high stability of AgMg.

On the basis of the foregoing results a tentative general postulate can be advanced that, at low temperatures, lattice defects—substitutional or vacancy—are strengthening factors, while at temperatures substantially above 0.5 of the melting point, lattice defects are weakening factors. Of those cases reported in the literature, Cu_3Au (18), CuAu (18), MgCd (19), and PbTl (20,21) all show minima at stoichiometry and all were tested at temperatures below about 0.6 T_{mp}.[8] Two cases have been reported which show maxima near the stoichiometric composition Bi_5Tl_3 (22) and TiO (23). In the former instance, room temperature (the only temperature studied) is slightly above 0.6 T_{mp} and the duration of loading is long (30 min). The observed behavior thus conforms with that postulated for high (homologous) temperatures. TiO is a particularly interesting case since Ehrlich (24) found that, contrary to the usual case, the maximum number of defects is located at the stoichiometric composition and that each sub-lattice becomes more perfect as the composition becomes enriched in its particular component.[9] The low (homologous) temperature hardness results on TiO, although superficially similar to the high temperature behavior of AgMg and Bi_5Tl_3, actually are consistent with the observed low temperature behavior of all compounds of variable composition.

All the observed behaviors of compounds of variable composition are consistent with the above postulate. The physical basis for the observed high temperature behavior is also apparent, at least in a crude sense. If high temperature deformation is diffusion-controlled as is supposed (26-28), then any factor tending to increase the diffusion coefficients will tend to increase the amount of deformation for a given load and time. Both substitutional and vacancy defects have been shown (29) to enhance diffusion coefficients in an isomorphous compound at high temperatures.

Similar effects of lattice defects may explain some long puzzling anomalies. For example, it has been found that certain Al-Zn alloys have an abnormally high plasticity, greater even than either of the two pure components, at both room and elevated temperatures (30-32). The nature of the solidus curve is such that the behavior cannot be accounted for by a "melting point effect" (17). However, Ellwood (33) has shown that the Al-Zn solid solution has a surprisingly high concentration of lattice vacancies and room temperature for this system is about 0.5 T_{mp}.

The effects of radiation on the creep strength of metals have been apparently conflicting. Radiation has been found to raise, to lower, and to have no effect on the resistance to creep (34). Since the principal effect of radiation is to produce a higher than normal concentration of defects in the lattice, one might expect from the present results that radiation would increase creep strength at low (homologous) temperatures, decrease it at high (homologous) temperatures, and have no significant effect at inter-

[7] A similar study by Trzebiatowski and Terpilowski (35) published since the completion of this manuscript shows a disorder value of 0.03. Their data are believed by the present author to be less accurate than those of Kachi (12).

[8] T_{mp} = temperature of melting.

[9] Rostoker (25) has shown how this peculiar structural behavior may be rationalized from the viewpoint of preserving a critical electron concentration per unit cell.

mediate temperatures. Such consideration would seem to rationalize the observations of the effect of radiation on creep.

Summary

Hardness-temperature studies of six alloys in the compound AgMg or β phase show that lattice defects are a strengthening factor at low homologous temperatures ($<0.5\ T_{mp}$) and a weakening factor at high homologous temperatures ($>0.7\ T_{mp}$). The effects at high homologous temperatures are thought to be a result of the effect of defect structure on diffusion rates. These results appear to rationalize previous studies of the effects of defect structure on the room temperature strength of intermetallic compounds.

Acknowledgment

The author is pleased to acknowledge the many substantial contributions of A. J. Peat to the experimental work. J. E. Burke and R. C. DeVries read and criticized the manuscript.

Manuscript received June 26, 1956. This paper was prepared for delivery before the San Francisco Meeting, April 29 to May 3, 1956.

Any discussion of this paper will appear in a Discussion Section to be published in the December 1957 JOURNAL.

REFERENCES

1. I. I. Kornilov, *Doklady Akad. Nauk S.S.S.R.*, **86**, 721 (1952).
2. J. H. Westbrook, *This Journal*, **103**, 54 (1956).
3. S. F. Zemczuzny, *Z. anorg. u. allgem. chem.*, **49**, 400 (1906).
4. W. Smirnov and N. Kurnakov, *ibid.*, **72**, 31 (1911).
5. R. J. M. Payne and J. L. Haughton, *J. Inst. Metals*, **60**, 351 (1937).
6. W. Hume-Rothery and E. Butchers, *ibid.*, **60**, 345 (1937).
7. N. V. Ageev and V. G. Kuznetsov, *Bull. acad. sci., U.R.S.S.*, **1937**, 289.
8. H. H. George, Master's Thesis, University of Pittsburgh (1939).
9. K. W. Andrews and W. Hume-Rothery, *J. Inst. Metals*, **69**, 485 (1943).
10. H. R. Letner and S. S. Sidhu, *J. Appl. Phys.*, **18**, 833 (1947).
11. L. M. Clarebrough and J. F. Nichols, *Australian J. Sci. Research*, **3A**, 284 (1950).
12. S. Kachi, *Science Repts. Research Insts. Tohoku Univ., Ser. A*, **1**, 351 (1955).
13. F. Saeftel and G. Sachs, *Z. Metallkunde*, **17**, 258 (1925).
14. J. H. Westbrook, *Proc. ASTM*, To be published.
15. J. H. Westbrook, *Trans. Am. Soc. Metals*, **45**, 221 (1953).
16. A. J. Peat and J. H. Westbrook, Unpublished data.
17. J. H. Westbrook and J. D. Nisbet, G. E. Research Lab. Rpt. RL 687, June (1952).
18. N. Kurnakov, S. Zemczuzny, and M. Zasedatelev, *J. Inst. Metals*, **40**, 305 (1916).
19. G. G. Urasov, *Z. anorg. Chem.*, **73**, 31 (1912).
20. N. Kurnakov and S. Zemczuzny, *Z. anorg. u. allgem. Chem.*, **64**, 149 (1909).
21. V. P. Shishokin and V. A. Ageev, *Tsvetnye Metal.*, **1932**, 119.
22. N. Kurnakov, S. Zemczuzny, and V. Takarin, *Z. anorg. u. allgem. Chem.*, **83**, 200 (1913).
23. W. J. Kramers, *et al.*, Atomic Weapons Research Establishment Aldermaston, Berks., Rpt. #0-15/55, May (1955).
24. P. Erhlich, *Z. Elektrochem.*, **45**, 362 (1939).
25. W. Rostoker, *J. Metals*, **4**, 981 (1952).
26. I. Dekhtar, *Doklady Akad. Nauk S.S.S.R.*, **73**, 303 (1950).
27. N. F. Mott, *Proc. Phys. Soc.*, **64B**, 729 (1951).
28. O. D. Sherby, *et. al.*, *Trans. Am. Inst. Mining Met. Engrs.*, **200**, 71 (1954).
29. A. E. Berkowitz, F. E. Jaumot, and F. C. Nix, American Physical Society Meeting paper, March (1954).
30. A. A. Bochvar and Z. A. Sviderskaya, *Bull. acad. sci. U.R.S.S.*, Classe sci. tech., **1945**, 821.
31. A. A. Bochvar, *ibid.*, **1946**, 743.
32. A. A. Bochvar and Z. A. Sviderskaya, *ibid.*, **1946**, 1001.
33. E. C. Ellwood, *J. Inst. Metals*, **80**, 217 (1951-2).
34. S. Glasstone, "Principles of Nuclear Reactor Engineering," p. 477, D. Van Nostrand Co., Inc., New York (1955).
35. W. Trzebiatowski and J. Terpilowski, *Bull. acad. polon. sci.*, Classe III, **3**, 391 (1955).

Preparation of Thorium Bismuth Dispersions from Electrolytic Thorium

M. E. Sibert and M. A. Steinberg

Metallurgical Department, Horizons Incorporated, Cleveland, Ohio

and

R. J. Teitel

Dow Chemical Company, Midland, Michigan

ABSTRACT

The preparation of Th_2Bi_5 dispersions in liquid Bi utilizing electrolytic Th has been investigated by three techniques. These materials are potentially useful as fuels for liquid metal reactors. Dispersions have been prepared successfully in desired concentration, particle size, and shape by addition of crushed Th cathode deposits to Bi, addition of as-deposited cathode to Bi in the cell, and by electrolysis of $ThCl_4$ using a liquid Bi cathode. Procedures, conditions, and results are fully described.

In recent years a variety of reactor types have been proposed as potential nuclear power production systems. Among the more interesting of these reactors is the liquid metal fuel reactor (LMFR).

The basic principle behind such reactors is that they employ low melting alloys for transport of fissionable material in and out of the reactor in place of the usual solid fuel elements. This concept has been extended to include the breeding of fissionable material in the same or secondary liquid metal circuit.

All designs of liquid metal fuel reactors (1,2,4) require a blanket to breed fissile fuel from Th. Since the solubility of Th in low melting alloys is low, the use of dispersions has been considered. One proposed dispersion is that of a thorium bismuthide in Bi. This paper is concerned with the preparation of that particular dispersion.

A liquid metal fuel dispersion such as Th_2Bi_5 in Bi must meet certain requirements to be a satisfactory material. The particle size and shape of the Th_2Bi_5 are of prime importance. If particles are too large or not equiaxed, clogging of pumps, filters, and lines could occur. Large particles would also tend to promote excessive settling of the dispersion. Some pertinent properties are shown in Table I and the liquid Bi solubilities of Th and U in Fig. 1.

It is seen that density and melting point of the dispersion are no particular problem. The main considerations taken into account in preparation of the material are particle size and shape. Small particles ($<50\mu$) of equiaxed shape are desired.

These dispersions may be prepared in at least three ways:

1. Precipitation of Th_2Bi_5 from solution by cooling from 1200°C where the Th would be dissolved. However, large platelets form, so this is not a useful procedure.

2. Exfoliation of Th chips or powder in the Bi melt. Use of powder may give added control over ultimate Th_2Bi_5 particle size. Powder can be produced by: (*a*) hydriding of Th followed by decomposition, and (*b*) fusion electrolysis.

3. Direct electrodeposition of Th from a fused salt bath into liquid Bi cathode.

Th precipitated from solution (method 1) forms undesirable, large platelets. Other methods have

Table I. Properties involved in Th_2Bi_5 system

Material	mp, °C	d(s) g/cc	d(l) g/cc	Solubility in Bi(l)	Neutron absorbtion cross section Barns/atom
Bi	271.3	10.00	9.80	—	0.032
Th	1690±10	11.7	—	0.006%-350°C	7.0
Th_2Bi_5	—	~10.4	—	0.006%-350°C	—

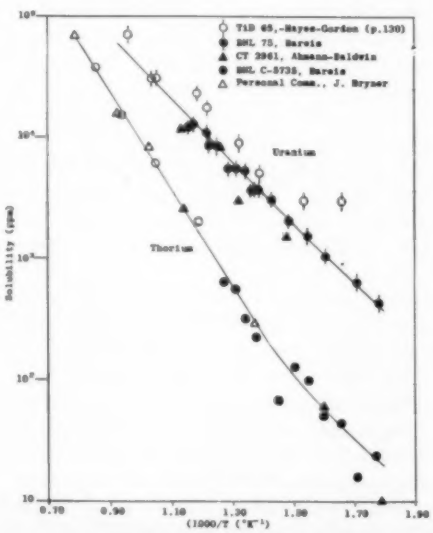

Fig. 1. Solubility of Th and U in liquid Bi

Fig. 2. Typical Th cathode deposit prepared by electrolysis of $ThCl_4$-NaCl system.

an advantage in that stable equiaxed particles are produced by the exfoliation of the compound from Th metal at low temperatures.

This work is concerned primarily with the methods utilizing electrolytic Th powder. It is thought that electrolytic methods could be carried out more economically as a result of the basic economy of electrolytic methods and also because the Th would not have to be recovered as metal prior to formation of the alloy.

Numerous examples of alloy and intermetallic preparation by fused salt electrolysis exist in the literature. At least 3 general methods are used:

1. Deposition of one metal in a liquid metal cathode (5-9).
2. Codeposition of 2 or more metal powders.
3. Deposition of one metal on a solid metal (cathode) to form a liquid alloy eutectic.

The third process type has been carried out here. Intermetallics of Zr-Ni, Ti-Fe, etc., have been prepared by deposition of Zr, Ti, etc., from fused fluoride-chloride melts on a solid base metal cathode. A eutectic forms, drips off, and collects in a pool on the cell bottom.

The basic Th metal powder preparation employed in this work has been described (10); $ThCl_4$ in NaCl or similar halide melt is electrolyzed in an inert atmosphere graphite lined cell. The cathode deposit particle size may be varied by changes in electrolysis conditions.

A typical Th deposit containing 40-50% metal is shown in Fig. 2.

The work described below involves the use of this technique and also the direct electrodeposition of Th in a molten Bi cathode.

Experimental

The experimental program included a systematic investigation of all possible methods involving the electrolytic cell. It has been demonstrated (11) that powder produced by electrolytic methods can be used to produce dispersions with desirable properties. The first set of experiments omitted the aqueous leaching steps and the crushed comminuted deposit was added directly to molten Bi. In the second group, the cathode removal and crushing steps were eliminated and the Th deposit simply mixed into a molten Bi bath on the bottom of the cell. In the last series, Th was deposited directly into a molten Bi cathode.

In all cases the goal of the work was the application of suitable conditions to yield a dispersion of fine particle size ($<50\mu$) containing equiaxed particles and 5-10% by weight Th (12.5-25% Th_3Bi_5). Th content and particle size were determined metallographically.

Mechanical Dispersion Preparation

Initially prepared dispersions of Th_3Bi_5 in Bi were made by the addition of comminuted, screened as-produced (not leached) electrolytic Th deposits to liquid Bi. Conditions of time, temperature, and agitation were controlled.

The following factors were briefly studied in this phase of the work: dispersion time; temperature; effect of deposit mesh size; effect of salt addition to cathode mix (e.g., $MgCl_2$).

This work indicated that unleached cathode deposits could not be used to form the dispersions and was thus abandoned in favor of the more direct methods described below.

Mechanical Preparation within the Cell

The second approach involved the omission of cathode removal and comminution steps as well as the leaching operation. The Th electrodeposit was first prepared by electrolysis of $ThCl_4$ and then dropped into a pool of molten Bi contained within the cell.

Equipment used for this procedure has been described previously (10). All internal parts are of graphite including the crucible. The crucible is supported on a graphite topped Ni post which also serves as the anode connection. Cathode entry is through the port in the removable head. Steel-tipped Ni rods were used as cathodes. The cell is heated by a machined graphite resistance element. Lampblack is employed as an insulating material. The Bi was contained in a porcelain cup on the crucible bottom.

The heating current was supplied by a 7.5 kva transformer coupled with a powerstat. The d-c source was a 200 amp Se rectifier.

Conditions of the electrolysis were adjusted to give a fine particle size deposit, i.e., high current density, lower temperature, and relatively high Th concentration in the melt.

When the melt had been exhausted essentially of Th content, the cell was shut down and the cathode support rod tapped so that the deposit slipped off into the Bi. The mixture was then vigorously stirred 1-1½ hr. Proper stirring is essential in achieving complete reaction and obtaining a homogeneous dispersion.

Data from several runs of this type are summarized in Table II. This was the most consistently successful procedure of the three approaches tried.

Table II. Mechanical dispersion preparation in cell

Melt wt. %	Temp, °C	C.D. amp/dm²	% Th_3Bi_5 in Bi	Th_3Bi_5 character, particle size—μ
37.7 NaCl·$ThCl_4$ 33.5 NaCl 28.8 KCl	650	250	20	Fine grained equiaxed, 9-35 μ
19.0 NaCl·$ThCl_4$ 44.5 NaCl 36.5 KCl	650	250	50	Equiaxed, 42 μ
Like (406-12)	635	250	50	Equiaxed, 42 μ
26.4 NaCl·$ThCl_4$ 16.8 NaCl 56.8 $CaCl_2$	540	250	60	Equiaxed, fine

Note: All melts—5-10% Th by wt, 500 g, Bi pool; all melts agitated using motor-driven stirrer with graphite or stainless steel paddle after deposit dropped.

Dispersions containing up to 60% Th_3Bi_5 were prepared.

The following conditions are important to the successful use of this procedure:

1. The electrolysis of $ThCl_4$ must be carried out under conditions to yield a fine particle size Th powder; temperature, 550°-650°C; Th concentrations 5-10 w/o; ccd, 200-300 amp/dm².
2. Efficient mechanical agitation must be carried out during addition of the deposit to the Bi and for a period of time afterward.
3. Longer stirring periods tend to reduce particle size of the Th_3Bi_5.

Direct Electrodeposition

Direct electrodeposition of Th from a fused $ThCl_4$-MCl_x system using a liquid Bi cathode was carried out in cells, whose design is essentially a closed Ni-lined stainless steel tube heated externally by nichrome wound resistors. The head is a gasketed, water-cooled Ni-lined steel plate with openings for cathode, anode, and stirrer. The melt container was a porcelain beaker inserted in a graphite crucible as a safety measure in case of breakage. Electrolysis was carried out in an A atmosphere using a graphite anode. A graphite tipped Ni rod served as a contact to the molten Bi cathode in the bottom of the porcelain crucible.The cathode contact was insulated from the melt by a quartz sleeve. In earlier runs, stirring was attempted by bubbling A gas through the cathode contact. Later mechanical stirring was used, with a graphite paddle immersed in the cathode; this was more successful. Crucibles, electrodes, and stirrer are illustrated in Fig. 3. The cell was operated through a West controller using a thermocouple in the crucible wall. Temperature was controlled to ±10°C. A 100-amp Se rectifier acted as a d-c source for the unit.

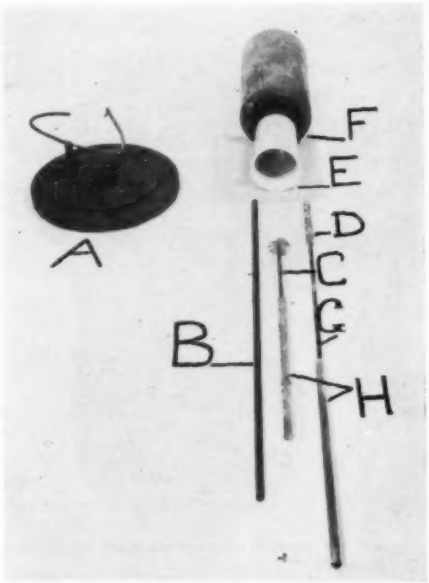

Fig. 3. Component parts of cell used in liquid Bi cathode electrolysis. A, Ni lined steel, water-cooled cell head; B, graphite anode; C, steel stirrer; D, graphite tip, cathode contact; E, porcelain crucible; F, graphite outer crucible; G, Ni shaft of cathode contact; H, quartz sleeves.

The $ThCl_4$ used was prepared in this laboratory from $ThOCO_3$ by procedures previously described (10). Other salts were of reagent grade and care was taken to exclude air, moisture, and other contaminants from the system. In many runs, the melt was first sparged with HCl for further purification.

Electrolysis was generally carried out for a sufficient number of ampere hours to yield a Th_3Bi_5-Bi ingot containing 25% Th_3Bi_5 (10% Th) based on a 50% current efficiency.

Table III. Electrodeposition of Th in liquid Bi

Run	Melt	Temp, °C	% Th melt	Wt Bi g	C.D. amp/dm²	Agitation	% Th_3Bi_5 in Bi	Th_3Bi_5 character; avg. particle size
368–5	NaCl-KCl (1:1)	730	5	150	22	None	2	Small—at grain boundaries 9 μ
368–11	NaCl-KCl(1:1)	755	10	100	140	None	16	Large, long rectang. plates—630 x 42 μ
368–6	NaCl-KCl(1:1)	725	25	150	18	None	11	Massive clusters—10 μ
368–14	NaCl-$CaCl_2$	625	10	150	28	None	0.8	Small amt.—top of ingot—40 μ
368–22	NaCl-$CaCl_2$	625	21	150	160	None	1	Small amt. equiaxed—particles—7 μ
368–25	LiCl-KCl	425	10	150	18	Bubble	2.5	Massive needle like—12 μ
368–24	LiCl-KCl	405	25	150	18	Bubble	1.5	Small amt. large—26 μ
368–34	$MgCl_2$-NaCl-KCl	405	12	150	50	Mech.	5	Small amt. equiaxed—14 μ
368–36	$MgCl_2$-NaCl-KCl	600	12	150	50	Mech.	20	Equiaxed—39 μ
368–38	$MgCl_2$-NaCl-KCl	600	17	500	100	Mech.	30	Equiaxed, some plates

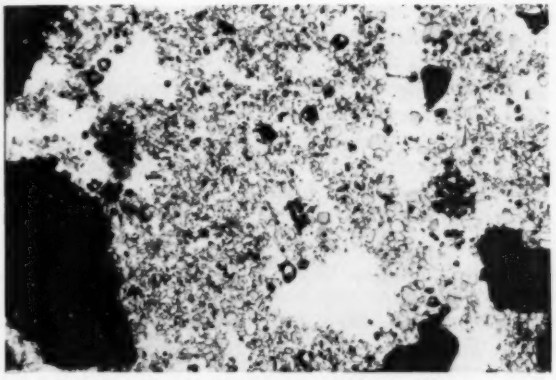

Fig. 4. Button obtained by dropping technique. Middle of specimen. Magnification, 150X before reduction for publication.

Melts were allowed to cool within the cell. The ingot was easily separated from the salt and then sectioned for examination.

Initial runs were of a survey nature in order to establish conditions required to deposit Th in a liquid Bi cathode. Variations were effected in temperature, current density, Th concentration in the melt, and agitation at the cathode.

In order to investigate a range of temperatures from 400°-700°C various alkali and alkaline earth chloride eutectics were employed as melts. Current density variation was from 20-160 amp/dm^2, and melt Th concentration from 5-25% by weight.

Data from several electrolytic runs are summarized in Table III. The following general observations were gained from this work.

1. Runs employing no agitation or bubble agitation generally gave low concentration dispersions with a large amount of residual unreacted Th powder in the vicinity of the cathode.
2. Mechanical agitation of the cathode produced completely reacted dispersions of maximum concentration and more uniform particle size and homogeneity.
3. Bath concentrations of around 10% by weight Th gave the best results from the standpoint of uniform equiaxed particles.
4. Low current densities (<50 amp/dm^2) generally produced inferior results.
5. Bath composition other than Th content has little if any effect on the resulting dispersion.

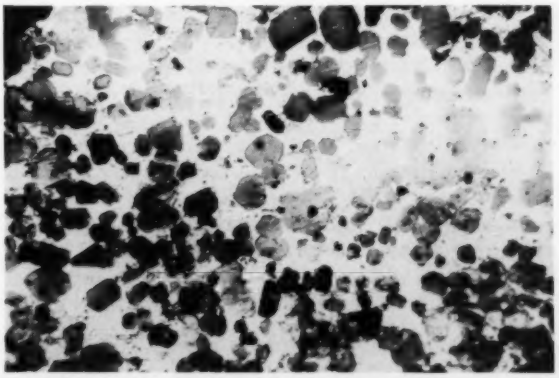

Fig. 5. Top of button in Fig. 4. High magnification. Particles 9-35 μ in size. Magnification, 500X before reduction for publication.

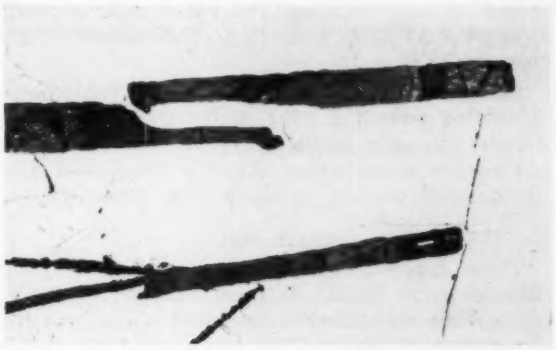

Fig. 6. Electrolytic Th deposited in Bi. Large rectangular plates of Th_3Bi_5. 630 × 42 μ. Magnification, 75X before reduction for publication.

6. Better mixing was obtained using 500 g cathodes as opposed to 100-150 g (in 350-g melts).
7. Stirring is effective in breaking up and/or hindering formation of clusters and large plates of Th_3Bi_5.
8. Temperatures of 600°-700°C are preferred to 400°-500°C from a resulting particle size standpoint.

Evaluation

Metallographic techniques were employed both for particle size analysis and for estimating Th_3Bi_5 content of the dispersion ingots prepared.

All ingots were first washed to remove any surface salts. This produced some surface oxidation, since Th_3Bi_5 reacts readily with moisture. The samples were sectioned for examination, so this did not interfere. All cutting and polishing operations were done under CCl_4 to prevent tarnishing of the specimen surfaces. Bakelite mountings were employed. Plane surfaces were obtained in a grinding belt, and polishing was done on a slow lapping wheel with either 1 μ diamond powder or Linde levigated alumina (B 5125). Specimens were stored under CCl_4.

Particle size determinations were made by use of a Filer eye piece, taking the average of 6 or more readings. Concentrations of the dispersion was estimated by surface area of Th_3Bi_5 particles.

Several specimens produced by the electrolytic methods employed are shown in Fig. 4-7.

The ingots in Fig. 4 and 5 were prepared by the *in situ* addition method. Fig. 4 is a typical middle

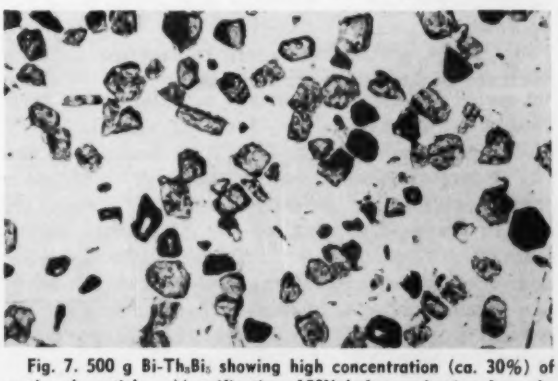

Fig. 7. 500 g Bi-Th_3Bi_5 showing high concentration (ca. 30%) of equiaxed particles. Magnification, 150X before reduction for publication.

section of such an ingot, and Fig. 5 is a specimen containing about 50% Th_3Bi_5 with an average particle size of 42 μ.

Fig. 6 and 7 were prepared by the direct electrodeposition technique. Fig. 6 illustrates the large platelet formation which can occur where stirring is not used or is ineffective. Fig. 7 is the desired type of equiaxed particle in about 30% concentration.

Conclusions

Three approaches to the preparation of Th_3Bi_5 dispersions in liquid Bi have been investigated. These three methods have amounted to a progressive elimination of steps in the recovery of Th metal powder from fusion electrolysis cathode deposits. Dispersions satisfactory in both particle size and shape characteristics have been prepared using comminuted deposits, as-deposited cathodes, and also by direct electrodeposition in Bi.

The particular method suitable for a given practical use would depend largely on the economics involved with respect to the required quantity of dispersion. For laboratory quantities, the use of Th powder or comminuted deposit would be simpler. For small scale commercial amounts, the *in situ* preparation would seem desirable. If large quantities were required, the direct electrolytic procedure would probably offer the most economical preparation. Use of a flowing Bi cathode would enable preparation of the dispersion on a continuous basis.

The more important considerations pertinent to successful preparation of a dispersion suitable for use as a liquid reactor fuel as indicated by this investigation, are summarized below:

1. Th metal powder utilized should be of fine particle size and as uniform as possible. Conditions of high current density, minimum temperature, and high Th melt concentration should be used whether Th is directly deposited in Bi or Th deposit is prepared first.

2. Vigorous mechanical stirring is required during and following mixing of Th with Bi regardless of procedure used. This promotes formation of Th_3Bi_5 and also serves to reduce final particle size and platelet formation.

3. Particle size of Th_3Bi_5 in general decreases with increased temperature, although in the direct electrolysis the tendency of increased temperature to produce larger Th particles minimized the effect somewhat.

4. Th_3Bi_5 particle size tends to decrease with an increase of dispersion or stirring time.

5. Other salts have little effect either as constituents of an electrolytic melt or added to a mechanical mixture.

6. Dispersions may be prepared containing up to 50% Th_3Bi_5 depending on conditions employed. Particle size may range from 5-1000 μ dependent on the Th metal used and on dispersion conditions. Th_3Bi_5 may be prepared as platelets or as equiaxed particles.

This initial investigation has demonstrated adequately the feasibility of preparing liquid metal fuel dispersions, and in particular, Th_3Bi_5-Bi, using electrolytic Th. It is not necessary to remove Th from its salt matrix prior to reaction with the Bi. It also may be directly deposited in an agitated Bi cathode to form the desired dispersion.

Acknowledgment

Acknowledgment is given to the Brookhaven National Laboratory for their sponsorship of this work and permission to publish these results. The assistance of the following staff members of Horizons Incorporated in carrying out this work is also acknowledged: R. Baskey, K. P. Chatham, A. L. Cunningham, and T. S. Liu.

Manuscript received August 13, 1956. This paper was prepared for delivery before the San Francisco Meeting, April 29 to May 3, 1956.

Any discussion of this paper will appear in a Discussion Section to be published in the December 1957 JOURNAL.

REFERENCES

1. R. J. Teitel, D. H. Gurinsky, and J. S. Bryner, *Chem. Engr. Progr. Symposium Ser.*, **50** [13], 11 (1954).
2. C. Williams and F. T. Miles, *Nucleonics*, **12** [7], 11 (1954); R. J. Teitel, D. H. Gurinsky, and J. S. Bryner, *ibid.*, **12** [7], 14 (1954).
3. R. J. Teitel, Reprint No. 34, Nuclear Eng. and Sci. Congress, Cleveland (1955).
4. O. E. Dwyer, D. H. Gurinsky, and R. J. Weeks, Preprint No. 50, Nuclear Eng. and Sci. Congress, Cleveland (1955).
5. H. Fischer and K. Dorsch, German Pat. 615,951, March 18, 1933.
6. J. Smolinski, J. C. Hannan, and A. L. Leach, Report Met. 80, Oct. 1954, Royal Aircraft Estab., Farnsborough, Hauts, England.
7. N. N. Gratsianskii and A. P. Vovkogon, *Zapiski Inst. Khim. Akad. Nauk U.R.S.R.*, **7**, 174 (1940).
8. S. C. Pyk, U. S. Pat. 2,558,627, June 26, 1951.
9. V. A. Plotnikov and E. T. Kirichenko, *Mem. Inst. Chem. Acad. Sci. Ukr. S.S.R.*, **6** [1], 3 (1939).
10. B. C. Raynes, J. C. Bleiweiss, M. E. Sibert, and M. A. Steinberg, To be published.
11. R. J. Teitel, Private communication.

Measurements on Galvanic Cells Involving Solid Electrolytes

Kalevi Kiukkola[1] and Carl Wagner

Department of Metallurgy, Massachusetts Institute of Technology, Cambridge, Massachusetts

ABSTRACT

Electromotive force measurements on galvanic cells involving solid electrolytes have been made in order to obtain the standard molar free energy of formation of CoO, NiO, Cu_2O, Ag_2S, Ag_2Se, PbS, and several phases of the system Ag-Te at elevated temperatures.

Haber and Tolloczko (1), Katayama (2), Reinhold (3, 4), Treadwell, Ammann, and Zürrer (5), Croatto and Bruno (6), Rose, Davis, and Ellingham (7), Sator (8), and others have shown that emf measurements on galvanic cells involving solid electrolytes may yield valuable thermodynamic data. The following investigations have been made in order to show new potentialities of emf measurements on galvanic cells involving solid electrolytes for the determination of the standard molar free energy of formation of oxides, sulfides, selenides, and tellurides at elevated temperatures.

Oxide Cells

General

In order to obtain the standard molar free energy of formation of CoO, NiO, and Cu_2O, cells of type

$$\text{A, A(O)} \mid \text{electrolyte} \mid \text{B, B(O)} \qquad \text{(I)}$$

involving oxides A(O) and B(O) of metals A and B have been investigated. The electrolyte was a solid solution of ZrO_2 and CaO involving oxygen ion vacancies according to Hund (9). Electrical conduction due to migration of oxygen ions via vacancies has been ascertained by tests described below. Analogous solid oxide solutions were tested but found to be less satisfactory.

For predominant ionic conduction due to migration of oxygen ions in the electrolyte, the virtual cell reaction may be expressed in terms of oxygen transfer from the right-hand to the left-hand electrode. Hence the emf E of cell (I) is

$$E = \left[(\bar{F}_{O_2}'' - F_{O_2}^\circ) - (\bar{F}_{O_2}' - F_{O_2}^\circ) \right] / 4F \qquad [1]$$

where $\bar{F}_{O_2}'$ and $\bar{F}_{O_2}''$, respectively, are the partial molar free energies of oxygen on the left-hand and the right-hand side of cell (I), $F_{O_2}^\circ$ is the standard molar free energy of oxygen, and F is the Faraday constant.

In most experiments reported below, a mixture of iron and wüstite was used on the left-hand side of cell (I). Upon combining values of the CO_2/CO ratio over iron and wüstite according to Darken and Gurry (10) and standard molar free energies of formation for CO and CO_2 according to Coughlin (11), values for the relative partial molar free energy $\bar{F}_{O_2} - F_{O_2}^\circ$ over iron and wüstite have been calculated and are listed in Table I. Upon substituting these values and experimental values of E in Eq. [1], values of $\bar{F}_{O_2} - F_{O_2}^\circ$ over metal B and oxide B(O) and the standard molar free energy of formation of oxide B(O) have been calculated for B = Co, Ni, Cu.

Table I. Free energy values for the system iron-oxygen from gas equilibrium measurements

Temp, °C	Iron + Wüstite p_{CO_2}/p_{CO}	Iron + Wüstite $\bar{F}_{O_2} - F_{O_2}^\circ$, kcal	Wüstite + Magnetite p_{CO_2}/p_{CO}	Wüstite + Magnetite $\bar{F}_{O_2} - F_{O_2}^\circ$, kcal
800	0.532	−93.00	2.56	−86.30
900	0.460	−89.76	3.47	−80.34
1000	0.396	−86.68	4.62	−74.26
1100	0.355	−82.52	6.12	——

In some runs, a mixture of wüstite and magnetite was used on the left-hand side of the cell in order to define the oxygen potential. For the evaluation of these experiments, values of $\bar{F}_{O_2} - F_{O_2}^\circ$ over wüstite and magnetite have been calculated and are also listed in Table I.

Preparation of the Electrolytes

The following solid solutions were prepared according to Hund (9, 12),

A: $0.85\ ThO_2 + 0.15\ LaO_{1.5}$
B: $0.75\ ThO_2 + 0.25\ LaO_{1.5}$
C: $0.85\ ThO_2 + 0.15\ CaO$
D: $0.85\ ZrO_2 + 0.15\ CaO$
E: $0.60\ ZrO_2 + 0.40\ CaO$

To prepare electrolytes A and B, a solution of $Th(NO_3)_4$ and La_2O_3 in dilute nitric acid was precipitated with ammonia. The coprecipitated hydroxides were converted into oxides as is described below for ZrO_2-CaO. Electrolyte C was prepared by evaporating a solution of $Th(NO_3)_4$ and $CaCO_3$ in dilute nitric acid. Similarly, to prepare electrolytes D and E, zirconyl nitrate was dissolved in boiling concentrated nitric acid and calcium carbonate was dissolved in dilute nitric acid. A mixture of these solutions was evaporated in a porcelain dish to dryness on a water bath. The remaining solid material was dried overnight at 120°C, ground in an agate mortar, decomposed at about 500°C, and fired 12 hr at

[1] Present address: Ratakatu 5 B 18, Helsinki, Finland.

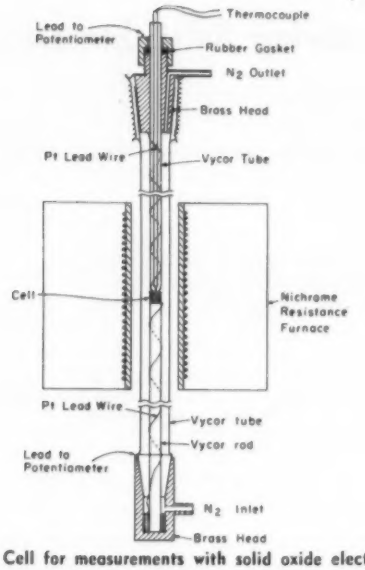

Fig. 1. Cell for measurements with solid oxide electrolyte

1000°C and 12 hr at 1250°C in a Pt boat with grinding after each firing. The powder was pressed into tablets 0.5 cm in diameter and about 0.2 cm thick at a pressure of about 10 tons/cm^2. The tablets were finally sintered overnight in a Pt boat under air at 1400°-1450°C.

When the powder was fired at a temperature below 1250°C, it was too voluminous and not suitable for pressing tablets. On the other hand, when the powder was fired at higher temperatures, it was not sufficiently reactive to yield dense tablets during the final sintering.

Arrangement of the Cell

A cell of type (I) consists of a tablet of a mixture of metal A and its oxide, a tablet of the electrolyte, and a tablet of a mixture of metal B and its oxide between Pt disks connected with Pt leads. The cell assembly is shown in Fig. 1. Since one lead goes to the top and the other lead to the bottom of the furnace, the external resistance between the leads in parallel to the cell is determined by the resistivity of the structural components of the cell assembly which are at room temperature with a negligible leakage current. The small distance between the electrodes minimizes local temperature differences within the cell and therefrom eventually resulting thermoelectric forces. The temperature of the cell can be measured with the help of a thermocouple next to the top electrode of the cell.

To assemble the cell, the bottom brass head with the vycor rod was lowered until the top of the vycor rod was outside the furnace. After assembling the cell on top of the vycor rod, the outer vycor tube was brought in position and the remaining parts of the cell assembly were installed so that the cell was under light pressure. Finally the whole cell assembly was raised so that the cell was in the middle of the resistance-heated furnace.

Use of an outer transparent vycor tube facilitated assembling of the cell but limited the maximum operating temperature to about 1150°C.

All measurements were made in purified nitrogen or argon. The gas was purified by passing over ascarite, anhydrous magnesium perchlorate, active copper at 200°C (13), and finally once more over ascarite and anhydrous magnesium perchlorate. The upper part of the copper tower was oxidized in order to remove hydrogen or hydrocarbons possibly present in the tank gas.

Conductivity Measurements

At elevated temperatures, concentrations of excess electrons and electron holes in the solid oxide electrolytes are presumably determined by the oxygen partial pressure of the surrounding atmosphere by virtue of the reactions

$$O_2(g) + 4 \text{ excess electrons} + 2 \text{ anion vacancies} = 2\,O^{2-} \quad [2]$$

$$O_2(g) + 4 \text{ valence electrons} + 2 \text{ anion vacancies} = 2\,O^{2-} + 4 \text{ electron holes} \quad [3]$$

In view of the low total conductivity, concentrations of excess electrons and electron holes are much smaller than the concentration of anion vacancies. Thus, concentrations of anion vacancies and valence electrons are virtually independent of the external oxygen partial pressure. Hence, on applying the ideal law of mass action to Eqs. [2] and [3], it follows that

$$c_- = K_1(p_{O_2})^{-1/4} \quad [4]$$

$$c_+ = K_2(p_{O_2})^{1/4} \quad [5]$$

where c_- and c_+, respectively, are the concentrations of excess electrons and electron holes, and K_1 and K_2 are constants.

In view of Eqs. [4] and [5], an appreciable contribution of excess electrons or electron holes is indicated by a rise of the total conductivity with decreasing or increasing oxygen partial pressure, respectively.

In order to test the dependence of the total conductivity on oxygen partial pressure, the electrical resistance of electrolyte tablets was measured between Pt electrodes with alternating current at 870°C. In order to minimize contact resistance, the tablets were provided either with thin Au layers applied by vacuum vaporization, or with thin Pt films obtained by cathodic sputtering.

The following atmospheres were used.

1. Oxygen of atmospheric pressure, $p_{O_2} = 1$ atm,
2. Air of atmospheric pressure, $p_{O_2} = 0.21$ atm,
3. Nitrogen of atmospheric pressure, $p_{O_2} \sim 10^{-5}$ to 10^{-6} atm,
4. Argon saturated with water vapor at room temperature with an addition of electrolytic hydrogen corresponding to a H_2O/H_2 ratio of the order of unity, $p_{O_2} \sim 10^{-17}$ atm,
5. Hydrogen of atmospheric pressure saturated with water vapor at 25°C, $p_{O_2} \sim 10^{-20}$ atm,
6. Hydrogen of atmospheric pressure saturated with water vapor at 0°C, $p_{O_2} \sim 4 \times 10^{-22}$ atm.

The electrical conductivity of electrolyte D (0.85 ZrO_2 + 0.15 CaO) at 870°C was found to be virtually constant (about 1.6×10^{-4} ohm^{-1}cm^{-1}) when the oxygen

partial pressure was varied within the aforementioned wide limits. In contrast, the conductivity of ThO_2-La_2O_3 solid solutions varied up to 50% whereby an objectionable magnitude of electronic conduction is indicated. Even greater variations have been observed with electrolyte C (ThO_2 + CaO). For this reason, the following measurements have been made with solid ZrO_2-CaO solutions.

Electronic conduction in ThO_2-La_2O_3 and ThO_2-CaO samples may have been caused by the presence of impurities. Further investigations are needed in order to clarify the nature of electronic conduction in such solid oxide solutions.

In order to determine small contributions of electronic conduction in ionic conductors, polarization measurements are profitable as has been shown recently (14). Measurements on the cell

$$\text{Fe, wüstite} \mid (ZrO_2 + CaO) \mid \text{Au} \qquad \text{(II)}$$

confirmed that electronic conduction yields only a minor contribution to the total conductivity. These measurements, however, were not carried sufficiently far in order to make possible a comprehensive quantitative evaluation.

Measurements on Cells Involving Iron Oxides

To verify the presupposition of predominant ionic conduction in ZrO_2-CaO solid solutions, there was investigated the cell

$$\text{Fe, } Fe_xO \mid (ZrO_2 + CaO) \mid Fe_yO, Fe_3O_4 \qquad \text{(III)}$$

where Fe_xO and Fe_yO denote wüstite coexisting with metallic iron and with magnetite, respectively.

Two-phase mixtures Fe, Fe_xO and Fe_yO, Fe_3O_4 with Fe/O ratios of 2 and 0.875, respectively, were made by pressing well mixed hydrogen-reduced iron powder (−200 mesh, Mallinckrodt A.R.) and magnetite powder (−200 mesh, prepared from C.P. Fe_2O_3) into tablets at a pressure of 10 tons/cm^2.

In each run, the emf of the cell was measured at rising and falling temperature. In general, steady potentials were attained more rapidly at higher temperatures than at lower temperatures. A single run lasted one or two days, or even longer. Observed emf values were plotted vs. temperature. Runs were considered to be satisfactory when values for ascending and descending temperatures agreed within 1 or 2 mv. Values for even temperatures read from these plots are listed in Table II.

In some runs, potentials were found to be ill-defined. In these runs, the electrolyte was not sufficiently dense as was indicated by penetration of the constituents of the electrodes toward the interior of the electrolyte tablet, possibly because of capillary suction by virtue of plastic flow, or surface diffusion. Other runs failed probably because of harmful impurities in the oxides used for the preparation of the electrolyte.

Table II. Electromotive force E of cell (III) Fe, Fe_xO | electrolyte | Fe_yO, Fe_3O_4

Temp, °C	Electrolyte 0.85 ZrO_2 + 0.15 CaO E (mv)		Electrolyte 0.6 ZrO_2 + 0.4 CaO E (mv)				Calc. from Eq. [6] E (mv)
800	72	73	71	71	71	70	72.5
900	103	103	103	103	102	101	102.1
1000	134	133	136	134	132	134	134.8
1100	166	165	—	166	—	166	168.5

Table III. Electromotive force E of cell (IV) Fe, wüstite | (0.85 ZrO_2 + 0.15 CaO) | Co, CoO and standard free energy change $\Delta F°$ of the reaction Co(s) + ½ O_2(g) = CoO(s) from emf measurements and calculations by Coughlin (11)

Temp, °C	No. of runs	E mv	$\Delta F°$ (kcal) cell (IV)	Coughlin
900	1	186	−36.30	−35.65
950	4	188 ± 2	−35.49	−34.75
1000	4	139 ± 2	−34.62	−33.80
1050	4	191 ± 2	−33.74	−32.90
1100	4	192 ± 2	−32.88	−31.95

The observed emf values may be compared with the results of gas equilibrium investigations. To this end, one may rewrite Eq. [1] as

$$E = \frac{RT}{2F} \ln \frac{(p_{CO_2}/p_{CO})_{II}}{(p_{CO_2}/p_{CO})_{I}} \qquad [6]$$

where the subscripts I and II, respectively, refer to the left-hand and the right-hand electrode of cell (I). Numerical values of these ratios according to Darken and Gurry (10) are listed in Table I. Emf values calculated from Eq. [6], which are listed in the last column of Table II, agree very satisfactorily with observed emf values.

Standard Molar Free Energy of Formation of Cobalt Oxide

Results for the cell

$$\text{Fe, } Fe_xO \mid (0.85\ ZrO_2 + 0.15\ CaO) \mid \text{Co, CoO} \qquad \text{(IV)}$$

and the standard molar free energy of formation $\Delta F°$ of cobalt oxide are shown in Table III. Reliable values were obtained only above 900°C. The reproducibility of the emf values is ±0.002 v or better corresponding to an uncertainty in $\Delta F°$ of ±0.1 kcal.

Upon substituting observed emf values and CO_2/CO ratios over iron and wüstite in Eq. [6], CO_2/CO ratios over cobalt and cobalt oxide and the standard free energy change of the reaction

$$CoO(s) + CO(g) = Co(s) + CO_2(g) \qquad [7]$$

have been calculated. Fig. 2 shows these values together with values deduced from gas equilibrium measurements by Emmett and Shultz (15), Watanabe (16), and Schenck and Wesselkock (17) as a

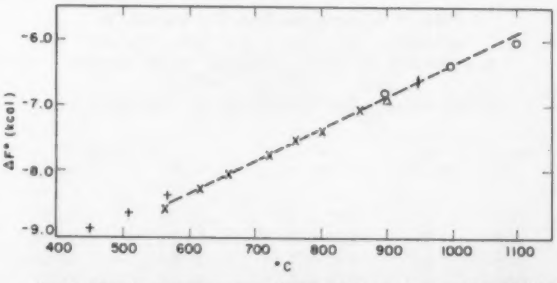

Fig. 2. Standard free energy change $\Delta F°$ of the reaction CoO(s) + CO(g) = Co(s) + CO_2(g) from gas equilibrium measurements [+ Emmett and Shultz (15), × Watanabe (16), Δ Schenck and Wesselkock (17)] and emf measurements (o). The uncertainty in the latter value is indicated by the length of the arrow.

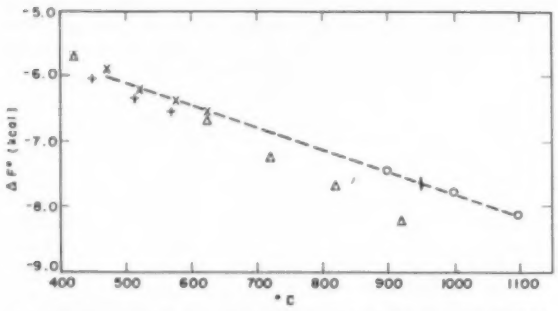

Fig. 3. Standard free energy change ΔF° of the reaction $CoO(s) + H_2(g) = Co(s) + H_2O(g)$ from gas equilibrium measurements [+ Emmett and Shultz (18), × Kleppa (19), Δ Shibata and Mori (20)] and emf measurements (o).

function of temperature. Both sets of data supplement each other and may be represented by a smooth curve.

Upon combining ΔF° values for reaction [7] and the water gas equilibrium calculated from data compiled by Coughlin (11), the standard free energy change for the reaction

$$CoO(s) + H_2(g) = Co(s) + H_2O(g) \qquad [8]$$

has been calculated. Fig 3 shows that these data agree with values calculated from determinations of the H_2O/H_2 ratio over cobalt and cobalt oxide according to Emmett and Shultz (18) and Kleppa (19) but differ from those reported by Shibata and Mori (20), possibly because of their neglect of thermal diffusion.

Standard Molar Free Energy of Formation of Nickel Oxide

Results of the cell

Fe, Fe_xO | 0.85 ZrO_2 + 0.15 CaO) | Ni, NiO (V)

are shown in Table IV. The reproducibility of the emf values is 0.002 v or better, corresponding to an uncertainty in ΔF° of ±0.1 kcal. Results were compared with results of gas equilibrium measurements in the same way as for cobalt, *see* Fig. 4 and 5. ΔF° values deduced from emf values for the reduction of NiO by means of CO lie between values calculated from CO_2/CO ratios according to Schenck and Wesselkock (17), Watanabe (21), and Fricke and Weitbrecht (22). Since the CO_2/CO ratios over nickel and nickel oxide are fairly large (63 to 454), errors

Table IV. Electromotive force E of the cell (V)
Fe, wüstite | (0.85 ZrO_2 + 0.15 CaO) | Ni, NiO
and standard free energy change ΔF° of the reaction
$Ni(s) + \frac{1}{2} O_2(g) = NiO(s)$
from emf measurements and calculations by Coughlin (11)

Temp, °C	No. of runs	E mv	ΔF° (kcal) cell (V)	Coughlin
750	2	261 ± 2	−35.20	−34.58
800	2	266 ± 1	−34.23	−33.49
850	3	271 ± 1	−33.29	−32.40
900	6	276 ± 1	−32.15	−31.31
950	6	281 ± 1	−31.19	−30.22
1000	6	286 ± 2	−30.15	−29.14
1050	5	291 ± 2	−29.12	−28.07
1100	5	296 ± 2	−28.11	−26.92
1140	2	300 ± 1	−27.22	−26.13

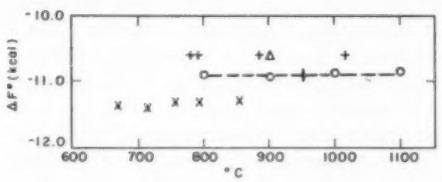

Fig. 4. Standard free energy change ΔF° of the reaction $NiO(s) + CO(g) = Ni(s) + CO_2(g)$ from gas equilibrium measurements [Δ Schenck and Wesselkock (17), × Watanabe (21), + Fricke and Weitbrecht (22)] and emf measurements (o).

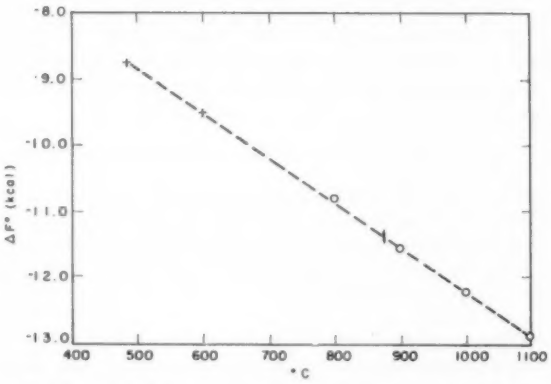

Fig. 5. Standard free energy change of the reaction $NiO(s) + H_2(g) = Ni(s) + H_2O(g)$ from gas equilibrium measurements [+ Pease and Cook (23)] and emf measurements (o).

are probably greater than for the analogous equilibria in the systems Fe-O and Co-O. ΔF° values for the reduction of NiO by means of H_2 according to Pease and Cook (23) are in accord with ΔF° values calculated from emf values at higher temperatures as is shown in Fig. 5.

For a comparison, Table IV lists standard molar free energies of the formation of nickel oxide recommended by Coughlin (11). These values are about 1 kcal more positive than values calculated from emf measurements. No explanation for this divergence can be given.

Standard Molar Free Energy of Formation of Cuprous Oxide

Emf values of the cells

Fe, Fe_xO | electrolyte | Cu, Cu_2O (VI)

Fe_yO, Fe_3O_4 | electrolyte | Cu, Cu_2O (VII)

with the electrolytes (0.85 ZrO_2 + 0.15 CaO) and (0.6 ZrO_2 + 0.4 CaO) are shown in Table V. Values

Table V. Electromotive force E of the cells
Fe, Fe_xO | electrolyte | Cu, Cu_2O (VI)
Fe_yO, Fe_3O_4 | electrolyte | Cu, Cu_2O (VII)

Temp, °C	E (mv) of cell (VI) 0.85 ZrO_2 + 0.15 CaO	E (mv) of cell (VI) 0.6 ZrO_2 + 0.4 CaO	E (mv) of cell (VII) 0.85 ZrO_2 + 0.15 CaO	E (mv) of cell (VII) 0.6 ZrO_2 + 0.4 CaO
800	532	532	456	461
850	536	537	448	448
900	539	540	436	436
950	541	542	424	423
1000	543	543	412	409
1035	544	544	402	398
1050	545	545	398	—

Table VI. Standard free energy change ΔF° of the reaction $2\,Cu(s) + \frac{1}{2}\,O_2(g) = Cu_2O(s)$ calculated from emf values of cells (VI) and (VII), emf measurements of Treadwell (24) (Tr) corrected for thermoelectric effects (25), and calculations by Coughlin (Co) (11).

Temp, °C	ΔF° (kcal) from cell (VI)	cell (VII)	Tr	Co
800	−21.96	−21.98	−21.17	−22.2
900	−19.97	−20.06	−19.70	−20.7
1000	−18.29	−18.17	−18.08	−19.1
1050	−17.42	−17.20	——	−18.4

for the standard molar free energy of formation of cuprous oxide are listed in Table VI. These values agree fairly well with results deduced from emf measurements made by Treadwell (24) with a correction for thermoelectric effects (25). Treadwell investigated the cell

$$Cu(s)\,|\,Cu_2O(s),\text{ borate melt}\,|\,\text{porcelain}\,|\,Ag(l),\,O_2(g) \qquad \text{(VIII)}$$

which involves the reaction $2Cu + \frac{1}{2}\,O_2 = Cu_2O$ on passing two faradays if oxygen ions alone carry the current in porcelain as an intermediate solid electrolyte.

The reproducibility of the emf values is ±0.002 v or better, corresponding to an uncertainty in ΔF° of ±0.1 kcal. For a comparison, Table VI also lists values of ΔF° calculated from various sources by Coughlin (11) with an estimated uncertainty of ±1.5 kcal. These values are about 1 kcal more negative than values from emf measurements.

No CO_2/CO and H_2O/H_2 equilibrium ratios over Cu and Cu_2O have been determined since these ratios are inconveniently high.

Roberts and Smyth (26) have determined oxygen partial pressures over liquid copper and solid Cu_2O between 1119° and 1184°C. Therefrom values between −14,100 and −14,250 cal for the standard molar free energy of formation of Cu_2O are calculated. These values are considerably more positive than the values listed in Table VI. In view of inherent difficulties discussed in the paper by Roberts and Smyth, it seems probable that the effect of side reactions has not been sufficiently eliminated in their measurements of oxygen partial pressures.

Standard Molar Free Energy of Formation of Silver Sulfide

Reinhold (4) has already determined the emf of the cell

$$Ag(s)\,|\,AgI(s)\,|\,Ag_2S(s), S(l), C \qquad \text{(IX)}$$

involving the virtual cell reaction

$$2Ag(s) + S(l) = Ag_2S(s) \qquad [9]$$

Additional measurements were made in order to obtain a higher accuracy. The setup of the cell is shown in Fig. 6. To assemble the cell, silver iodide was melted in the Pyrex tube, and the graphite electrode B, the glass tube A, and the thermocouple shield were immersed. Then the cell was transferred to another furnace whose temperature was below the melting point of AgI but above its transformation point at 146°C. After the AgI had solidified,

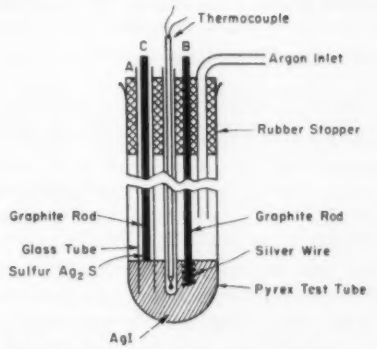

Fig. 6. Cell Ag(s) | AgI(s) | Ag_2S(s), S(l), C

sulfur was introduced into glass tube A, and the graphite electrode C was brought in contact with the AgI. To start a run, silver sulfide was formed electrolytically at graphite rod C by passing a current of 5 to 20 ma for about half an hour with graphite rod B as anode. In some runs, more silver sulfide was formed after the first emf measurements had been made. In other runs, graphite rod C was wrapped with silver wire which transformed to silver sulfide. The emf values were found to be independent of the procedure of preparation of silver sulfide and its amount.

Observed emf values are shown in Table VII. They agree with Reinhold's values within 0.01 v, which is the limit of accuracy of the latter values. In addition, Table VII lists values for the free energy of formation of silver sulfide computed from emf values with the aid of the formula

$$\Delta F^\circ = -2EF \qquad [10]$$

The reproducibility of the emf values is ±0.001 v, corresponding to an uncertainty in ΔF° of ±0.05 kcal.

The equilibrium of the reaction

$$Ag_2S(s) + H_2(g) = 2Ag(s) + H_2S(g) \qquad [11]$$

has been investigated by various authors, most recently by Rosenqvist (27) between 490° and 900°C. ΔF° values for reaction [11] extrapolated to 200°-400°C from Rosenqvist's data agree within ±0.2 kcal with values calculated from standard molar free energies of formation of Ag_2S according to Table VII and values for H_2S recommended by Rossini, *et al.* (28) and Kelley (29).

Table VII. Electromotive force E of cell (IX) Ag(s) | AgI(s) | Ag_2S(s), S(l), C and standard free energy change ΔF° of the reaction $2\,Ag(s) + S(l) = Ag_2S(s)$

Temp, °C	No. of runs	E mv	ΔF° kcal
150	3	220 ± 1	−10.15
178	3	224 ± 1	−10.35
200	3	228 ± 1	−10.52
250	3	236 ± 1	−10.89
300	5	244 ± 1	−11.24
350	5	252 ± 1	−11.62
400	5	260 ± 1	−11.99
425	3	264 ± 1	−12.18

Standard Molar Free Energy of Formation of Silver Selenide

Similarly, the emf of the cell

$$Ag(s) \mid AgI(s) \mid Ag_2Se(s), Se(s,l), C \qquad (X)$$

has been determined. Results are shown in Table VIII.

The emf of cell (X) was found to be well reproducible below 380°C. In some runs, higher, unsteady potentials were observed above 380°C, presumably because Ag_2Se dissolved in liquid selenium (30) and its amount was insufficient for saturation. Only if excess silver selenide is present, the chemical potentials of silver and selenium are well defined. Even under these conditions, a correction for the calculation of the standard free energy of silver selenide is needed because selenium as a reactant is not present in its standard state. This correction is supposedly not significant below 400°C because the solubility of Ag_2Se in liquid selenium is small (31)

Solid-state coulometric titrations analogous to those made with Ag_2S (32) indicate variations of the Ag/Se ratio as low as 0.004 to 0.005 between 200°-300°C. Therefore, deviations from the ideal composition of silver selenide in cell (X) are insignificant.

Cell (X) has previously been investigated by Reinhold (4). These values show considerable scatter and differ up to 0.1 v from values shown in Table VIII for unknown reasons.

From the temperature dependence of the standard free energy of formation of Ag_2Se it follows that

$$2Ag(s) + Se(l) = Ag_2Se(s)$$
$$\Delta F^\circ = -13.46 - 0.0074 \times (T - 500) \text{ kcal};$$
$$\Delta H^\circ = -9.76 \text{ kcal}; \Delta S^\circ = 7.4 \text{ e.u. at } T > 500°K \quad [12]$$

Upon using enthalpy and entropy increments of Ag, Se, and Ag_2Se between 298° and 500°K as compiled by Kelley (29), the values of ΔH° and ΔS° at 298°K are obtained. Therefrom $\Delta F^\circ = \Delta H^\circ - T\Delta S^\circ$ at 298°K may be calculated. Thus,

$$2Ag(s) + Se(s) = Ag_2Se(s)$$
$$\Delta F^\circ = -11.94 \text{ kcal}; \Delta H^\circ = -11.38 \text{ kcal};$$
$$\Delta S^\circ = 5.24 \text{ e.u. at } 298°K \quad [13]$$

The value $\Delta H^\circ = -11.38$ kcal seems to be more consistent than the value of −2.9 kcal, which was obtained by Fabre (33) on combining the values for several reactions which were investigated calorimetrically.

The standard molar entropy of Ag_2Se at 298°K is obtained as

$$S^\circ_{Ag_2Se} = \Delta S^\circ + 2S^\circ_{Ag} + S^\circ_{Se}$$
$$= 5.24 + 2 \times 10.206 + 10.0 = 35.65 \text{ e.u. at } 298°K \quad [14]$$

with standard entropy values for Ag and Se recommended by Rossini, *et al.* (28).

Table VIII. Electromotive force E of the cell (X) $Ag(s) \mid AgI(s) \mid Ag_2Se(s), Se(s,l), C$ and standard free energy change ΔF° of the reaction $2Ag(s) + Se(s,l) = Ag_2Se(s)$

Temp, °C	No. of runs	E mv	ΔF° kcal
160	2	281.0 ± 0.6	−12.96
170	3	282.5 ± 0.5	−13.03
200	3	287.4 ± 0.6	−13.26
250	3	295.4 ± 0.5	−13.63
300	3	303.5 ± 0.6	−14.00
350	3	311.6 ± 0.7	−14.37
370	3	314.8 ± 0.7	−14.52

Standard Molar Free Energy of Formation of Lead Sulfide

Solid lead chloride, pure or doped with KCl, is known to be an anionic conductor (34-36). Thus, the standard free energy of formation of lead sulfide should be obtainable from a cell analogous to cell (IX),

$$Pb(s) \mid PbCl_2(s) \mid PbS(s), S(l), C \qquad (XI)$$

The emf of cell (XI) was found to be not well reproducible, presumably for the following reason. In view of the shrinkage during the solidification of $PbCl_2$ and lack of plasticity, no tight seal of lead chloride between the two electrodes was obtained and, therefore, sulfur vapor could diffuse to the lead electrode so that a mixed potential rather than an equilibrium potential prevailed.

Therefore, a cell involving a Ag-Ag_2S electrode instead of a sulfur electrode was investigated,

$$Pb(s,l) \mid PbCl_2(+KCl) \mid PbS(s), Ag_2S(s), Ag(s) \qquad (XII)$$

with the virtual cell reaction

$$Pb(s,l) + Ag_2S(s) = PbS(s) + 2Ag(s) \quad [15]$$

Preliminary investigations have shown that the solubility of Ag_2S in PbS is less than 1 mole % below 400°C. Similarly, a low solubility of PbS in Ag_2S is assumed. Ag_2S and PbS are, therefore, considered to be present virtually in their standard states.

The electrolyte was solid lead chloride containing 0.5 w/o KCl in order to increase the conductivity, presumably due to a higher anion vacancy concentration (37). To prepare the electrolyte, $PbCl_2$ and KCl were melted under a stream of argon containing a small amount of chlorine. The solidified melt was crushed to powder.

In order to extend measurements above the melting point of lead at 327°C, a crucible of lead chloride filled with liquid lead was used. Fig. 7 shows the assembled cell which was placed in the furnace shown in Fig. 1.

Crucibles of lead chloride were pressed in the tool shown in Fig. 8. A nearly uniform density was obtained by applying pressure from top and bottom punches and by providing nearly equal compression ratios of the powder at the bottom and in the walls

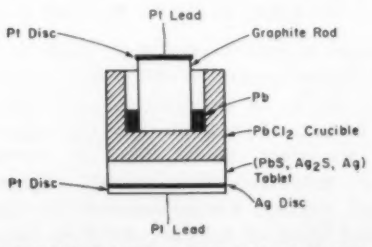

Fig. 7. Cell $Pb(s,l) \mid PbCl_2(+KCl) \mid PbS(s), Ag_2S(s), Ag(s)$

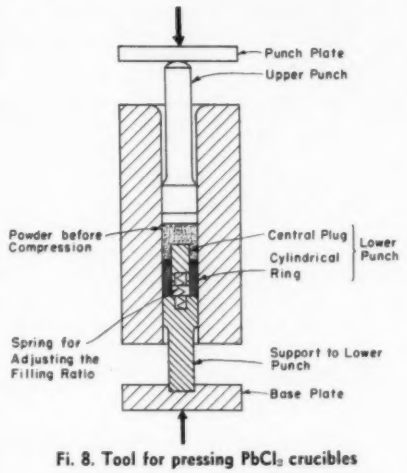

Fi. 8. Tool for pressing $PbCl_2$ crucibles

of the crucible. The pressed crucibles were ejected through the upper end of the die, which was slightly tapered. The crucibles were used either as such, or after sintering under argon at about 400°C. Different procedures did not result in systematic differences in the measured emf.

On replacing the lower punch by a short steel rod, cylindrical tablets of a mixture of Ag, Ag_2S, and PbS for the right-hand electrode in cell (XII) could be made.

Results of emf measurements are listed in Table IX.

Upon combining $\Delta F°$ values for reactions [9] and [15], values for the standard free energy of formation of PbS are obtained. These values are also shown in Table IX.

The equilibrium

$$PbS(s) + H_2(g) = Pb(l) + H_2S(g) \qquad [16]$$

has been investigated by Jellinek and Zakowski (38), Jellinek and Deubel (39), and Sudo (40). $\Delta F°$ values for reaction [16] calculated from standard free energies of formation of PbS listed in Table IX and values for H_2S recommended by Rossini, *et al.* (28) and Kelley (29) are consistent with Sudo's measurements (40) but diverge from earlier measurements by Jellinek and his associates (38, 39).

The System Silver-Tellurium

The phase diagram of the system silver-tellurium has been investigated by Pélabon (41), Pellini and Quercigh (42), Chikashige and Saito (43), Koern (44), and Kracek and Ksanda (45). In addition to the compound Ag_2Te, which has a congruent melting point at about 958°C, there is at least one other intermediate phase involving a smaller Ag/Te ratio with an incongruent melting point, for which the formulas

$$AgTe\,(42),\ Ag_7Te_4 = Ag_{1.75}Te\,(43),\ Ag_{12}Te_7 = Ag_{1.71}Te\,(44),\ \text{and}\ Ag_{1.50}Te\,(45)$$

have been suggested.

Table IX. Electromotive force E of the cell (XII) $Pb(s,l) \mid PbCl_2\ (+KCl) \mid PbS(s), Ag_2S(s), Ag(s)$ and standard free energy change $\Delta F°$ of the reaction $Pb(s,l) + S(l) = PbS(s)$

Temp, °C	No. of runs	E mv	$\Delta F°$ kcal
250	7	254 ± 3	−22.60
300	7	240 ± 3	−22.33
327	7	232 ± 3	−22.14
350	6	226 ± 3	−22.05
400	6	211 ± 2	−21.73
427	2	203 ± 1	−21.54

To clarify, the activity a_{Ag} of silver in Ag-Te "alloys" has been determined as a function of the Ag/Te ratio by measuring the emf of the cell

$$Ag(s) \mid AgI(s) \mid (Ag, Te) \qquad (XIII)$$

Since silver iodide is an ionic conductor, the emf E of the cell (XIII) is

$$E = -(RT/F) \ln a_{Ag} = -F^M_{Ag} \qquad [17]$$

where F^M_{Ag} is the partial molar free energy of mixing of silver for pure solid silver as reference state.

Upon passing current across cell (XIII) from right to left, a definite amount of silver can be transferred from the alloy to the left-hand electrode consisting of pure silver. Thus, cell (XIII) permits a solid-state titration analogous to that used for silver sulfide (32). The change in the Ag/Te ratio, Δr, is in view of Faraday's law

$$\Delta r = it/n_{Te}F \qquad [18]$$

where i is the current applied during time t, n_{Te} is the number of moles of tellurium, and F is the Faraday constant.

At the beginning of a titration, the Ag-Te alloy was equilibrated with metallic silver by short-circuiting cell (XIII). Subsequently, silver was removed. In contradistinction to measurements of the analogous cell for the system Ag-S, a steady potential was attained not immediately but only after about half an hour.

Results for 250° and 300°C are shown in Fig. 9 and 10. Points indicated by solid squares were obtained from measurements of cells with predetermined constant composition of the Ag-Te alloy. There are three regions involving a variable potential E corresponding to three different phases designated as α, γ, and ϵ. The one-phase regions are

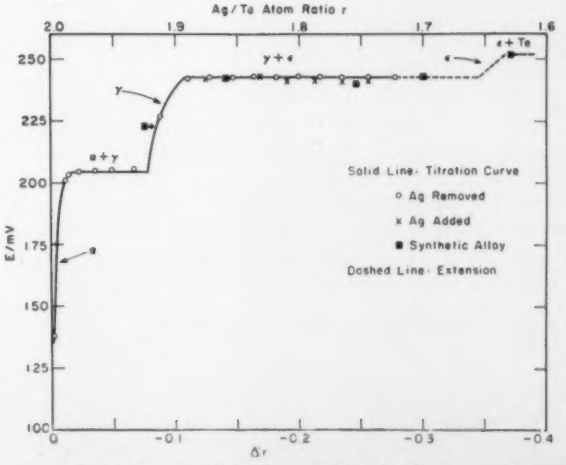

Fig. 9. Emf E of cell Ag | AgI | (Ag, Te) vs. Ag/Te ratio r at 250°C

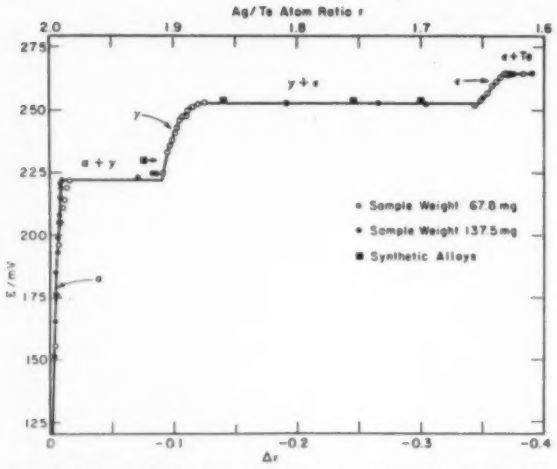

Fig. 10. Emf E of cell Ag | AgI | (Ag, Te) vs. Ag/Te ratio r at 300°C

separated by two-phase regions indicated by plateaus in the E vs. Δr plots.

Since the homogeneity range of the alpha phase is rather narrow, it may be assumed without considerable error that the phase equilibrated with metallic silver has nearly the formula Ag_2Te whereupon the Ag/Te ratio shown on top of Fig. 9 and 10 may be calculated as

$$r = 2 - \Delta r \qquad [19]$$

At 300°C, the Ag/Te ratio ranges from 1.99 to 2.00 for the α phase, from 1.88 to 1.91 for the γ phase, and from 1.63 to 1.66 for the ϵ phase.

From the values shown in Fig. 9 and 10, the free energy of formation of a one-phase or two-phase alloy involving N_{Ag} g-atom Ag and $(1-N_{Ag})$ g-atom Te may be calculated as (46)

$$F^N = (1-N_{Ag})\int_0^{N_{Ag}} \frac{F^N{}_{Ag}}{(1-N_{Ag})^2}\, dN_{Ag} \qquad [20]$$

Upon dividing F^N by $N_{Te} = (1 - N_{Ag})$, the standard molar free energies of formation $\Delta F°$ of the silver tellurides having the formulas Ag_2Te, $Ag_{1.90}Te$, and $Ag_{1.64}Te$ have been calculated. These values are listed in Table X.

The emf of the cell

$$Ag \mid AgNO_3(aq) \mid (Ag,Te) \qquad (XIV)$$

has been determined at room temperature by Puschin (47). A plot of emf vs. the Ag/Te ratio does not indicate another compound in addition to Ag_2Te. It is possible, however, that the scatter in Puschin's plot of E vs. composition obscures small steps corresponding to different compounds. Moreover, complete electrochemical equilibrium may not have been reached at room temperature as has been found, e.g., for the system Cu-Zn by Sauerwald (48).

Manuscript received August 9, 1956. The paper is based on a thesis submitted by K. Kiukkola in partial fulfillment of requirements for the degree of D.Sc. in metallurgy, Massachusetts Institute of Technology, Cambridge, Mass. Work was done under Contract AT(30-1)-1002 with the U.S.A.E.C.

Any discussion of this paper will appear in a Discussion Section to be published in the December 1957 JOURNAL.

Table X. Thermodynamic values for the system silver-tellurium

	250°C	300°C
$\Delta F°(2Ag + Te = Ag_2Te)$	−11.4	−12.0 kcal
$\Delta F°(1.90Ag + Te = Ag_{1.90}Te)$	−11.0	−11.5 kcal
$\Delta F°(1.64Ag + Te = Ag_{1.64}Te)$	−9.5	−10.0 kcal

REFERENCES

1. F. Haber and S. Tolloczko, *Z. anorg. Chem.*, **41**, 407 (1904).
2. M. Katayama, *Z. physik. Chem.*, **61**, 566 (1908).
3. H. Reinhold, *Z. anorg. u. allgem. Chem.*, **171**, 181 (1928).
4. H. Reinhold, *Z. Elektrochem.*, **40**, 361 (1934).
5. W. D. Treadwell, H. Ammann, and Th. Zürrer, *Helv. Chim. Acta*, **19**, 1255 (1936).
6. U. Croatto and C. Bruno, *Ricerca Sci.*, **17**, 1998 (1947).
7. B. A. Rose, G. J. Davis, and H. J. T. Ellingham, *Disc. Faraday Soc.*, **4**, 154 (1948).
8. A. Sator, *Compt. rend.*, **234**, 2283 (1952).
9. F. Hund, *Z. physik. Chem.*, **199**, 142 (1952).
10. L. S. Darken and R. W. Gurry, *J. Am. Chem. Soc.*, **67**, 1398 (1945).
11. J. P. Coughlin, *U. S. Bur. Mines Bull. 542* (1954).
12. F. Hund and W. Dürrwächter, *Z. anorg. u. allgem. Chem.*, **265**, 67 (1951).
13. F. Meyer and G. Ronge, *Angew. Chem.*, **52**, 637 (1939).
14. C. Wagner, *Z. Elektrochem.*, **60**, 4 (1956); *Proc. C.I.T.C.E.*, in press. J. B. Wagner and C. Wagner, *J. Chem. Phys.*, June 1957.
15. P. H. Emmett and J. F. Shultz, *J. Am. Chem. Soc.*, **52**, 1782 (1930).
16. M. Watanabe, *Sci. Repts. Tohoku Imp. Univ. I*, **22**, 892 (1933).
17. R. Schenck and H. Wesselkock, *Z. anorg. u. allgem. Chem.*, **184**, 39 (1929).
18. P. H. Emmett and J. F. Shultz, *J. Am. Chem. Soc.*, **51**, 3249 (1929).
19. O. J. Kleppa, *Svensk Kem. Tidskr.*, **55**, 18 (1943).
20. Z. Shibata and I. Mori, *Z. anorg. u. allgem. Chem.*, **212**, 305 (1933).
21. M. Watanabe, *Sci. Repts. Imp. Tohoku Univ. I.*, **22**, 436 (1933).
22. R. Fricke and G. Weitbrecht, *Z. Elektrochem.*, **48**, 87 (1942).
23. R. N. Pease and R. S. Cook, *J. Am. Chem. Soc.*, **48**, 1199 (1926).
24. W. D. Treadwell, *Z. Elektrochem.*, **22**, 414 (1916).
25. J. Gundermann, K. Hauffe, and C. Wagner, *Z. physik. Chem. B.*, **37**, 148 (1937).
26. F. H. Smyth and H. S. Roberts, *J. Am. Chem. Soc.*, **43**, 1061 (1921).
27. T. Rosenqvist, *Trans. Am. Inst. Mining Met. Engrs.*, **185**, 451 (1949).
28. F. D. Rossini, D. D. Wagman, W. H. Evans, S. Levine, and I. Jaffe, *Nat. Bur. Standards Circ. 500*, U. S. Government Printing Office, Washington (1952).
29. K. K. Kelley, *Bureau of Mines Bull. 476*, U. S. Government Printing Office, Washington (1949).
30. C. Tubandt, H. Reinhold, and A. Neumann, *Z. Elektrochem.*, **39**, 227 (1933).
31. M. Hansen, "Der Aufbau der Zweistofflegierungen," p. 59, Springer, Berlin (1936).
32. C. Wagner, *J. Chem. Phys.*, **21**, 1819 (1953).
33. C. Fabre, *Ann. chim. phys.*, **14**, 110 (1888).
34. C. Tubandt and S. Eggert, *Z. anorg. u. allgem. Chem.*, **110**, 196 (1920); C. Tubandt, *ibid.*, **115**, 105 (1921).

35. C. Tubandt and H. Reinhold, *Z. Elektrochem.*, **29**, 313 (1923).
36. J. B. Wagner and C. Wagner, *This Journal*, To be published.
37. E. Koch and C. Wagner, *Z. physik. Chem. B*, **38**, 295 (1937).
38. K. Jellinek and K. Zakowski, *Z. anorg. u. allgem. Chem.*, **142**, 1 (1925).
39. K. Jellinek and A. Deubel, *Z. Elektrochem.*, **35**, 451 (1929).
40. K. Sudo, *Sci. Repts. Res. Inst. Tohoku Univ. A*, **2**, 325 (1950).
41. H. Pélabon, *Compt. rend.*, **143**, 295 (1906).
42. G. Pellini and E. Quercigh, *Atti R. Accad. dei Lincei Roma*, (5) **19**, *II*, 415 (1910).
43. M. Chikashige and I. Saito, *Mem. Coll. Sci. Kyoto Imp. Univ.*, **1**, 361 (1916).
44. V. Koern, *Naturwissenschaften*, **27**, 432 (1939).
45. F. C. Kracek and C. J. Ksanda, *Tran. Am. Geophys. Union*, **21**, 363 (1940).
46. C. Wagner, "Thermodynamics of Alloys," p. 14, Addison-Wesley Press, Cambridge, Mass. (1952).
47. N. Puschin, *Z. anorg. u. allgem. Chem.*, **56**, 1 (1908).
48. F. Sauerwald, *ibid.*, **111**, 243 (1920).

Technical Notes

Measurement of Ion and Water Transport across Membranes

J. G. McKelvey, Jr., K. S. Spiegler, and M. R. J. Wyllie

Gulf Research & Development Company, Pittsburgh, Pennsylvania

Electrical migration of ions and solvent (electroösmosis) plays an important part in the study of membrane transport processes. The different transport processes, such as diffusion, conductance, and hydraulic permeation, are related to each other by a system of equations based on the thermodynamics of the steady state (1,2). In order to comply with the definitions used in this system and thus obtain maximum accuracy, the transport should be measured when the solutions separated by the membrane are of equal concentration and without changing this condition during the experiment. This restriction limits the applicability of the conventional methods for the measurement of electrical ion and water transport.

Transport numbers of ions across membranes can be computed from membrane potentials ("emf method") or may be determined directly by electrolysis ("dynamic" method). The emf method is dependent on a concentration gradient, and, therefore, only an average transport number with respect to solution concentration can be calculated. Also, the potential depends not merely on the ion transport number, but on a combination of ion and solvent transport (3,4).

In the dynamic method, electric current is passed through the system:

Electrode 1 - Solution 1 - Membrane - Solution 2 - Electrode 2

Transport numbers are then calculated from concentration changes caused by the electrolysis. When Pt electrodes are used, the electrode reactions produce hydrogen and/or hydroxyl ions, both of which have high membrane mobilities and may interfere. However, the dynamic method allows separate determination of ion migration and electroösmotic water transport.

In order to overcome the difficulties inherent in the dynamic method, Murakoshi (5) used a K amalgam anode and Hg cathode in his study of systems of KCl solutions and cation-exchange membranes. Ag-AgCl electrodes have frequently been employed (2,6-8). Their effective use is restricted to chloride systems and, in the case of cation-exchange membranes, they do not eliminate the creation of a concentration difference across the membrane.

For these reasons a new method was devised here using radioactive tracers, which allows ion and water transport to be measured at a constant concentration, without interference from electrode reactions, and with a high degree of precision. In this method the solution concentration is kept constant by adding small amounts of ion-exchange resins, which act as buffers, to each electrode compartment. While the solution concentration remains constant, the specific radioactivity of at least one solution changes. The ion transport is then determined from this change in the specific activity of the solution after electrolysis.

This method overcomes limitations imposed on conventional transport measurements which need special electrodes (e.g., Ag-AgCl electrodes for measurements in chloride solutions) and which almost always cause concentration changes. For instance, even Ag-AgCl electrodes cause enrichment of NaCl in the cathode compartment in transport measurements across cation-exchange membranes. The present method should be applicable to solutions of other salts also, e.g., sulfates, perchlorates, phosphates, etc., for which no suitable electrodes are available.

The cell (Fig. 1) consists of two "Lucite" compartments, each equipped with a calibrated buret, thermometer, Pt electrode, and a plug for removing samples. Each half-cell holds about 260 ml of solution and measures about 7.5 cm on the outside edges. The membrane is mounted between the two half-

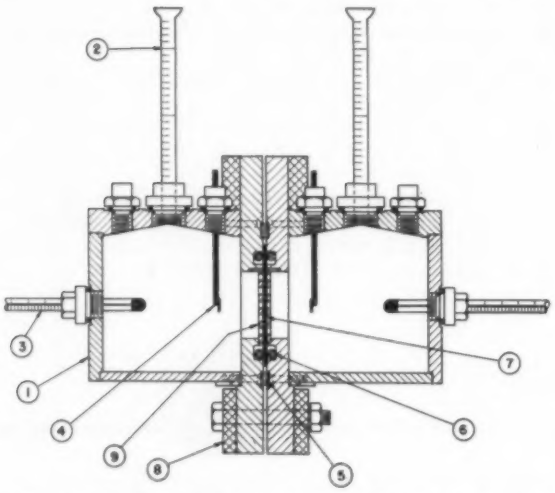

Fig. 1. Sectional view of transport cell: 1, cell body; 2, calibrated buret; 3, thermometer; 4, Pt electrode; 5, rubber dam gasket; 6, "O" ring gasket; 7, membrane; 8, Al support plate; 9, perforated "Lucite" disk. Cell material : "Lucite"; fittings: "Teflon" except thermometer fitting which is "Nylon"; gaskets: "O" rings (except No. 5). Plugs on the extreme left and right close holes which have been provided for future insertion of other probes.

cells and held securely in place by two "O" rings. Two perforated "Lucite" disks are mounted, one on each side of the membrane, to prevent bulging caused by unequal liquid levels in the two burettes. Stirring is accomplished by a small (⅞ x ¼ in.) "Kel-F" coated magnetic stirring bar in each compartment. The stirrer is driven by a commercial magnetic stirring device slightly modified to fit the limited space. Small tubes filled with "Drierite" are mounted on top of each buret to determine minor losses due to evaporation and spray. A silver coulometer was used to measure the amount of charge passed. [A photographic reproduction of the cell in actual operation may be found in (10).]

In operation, each half-cell is filled with a salt solution, and current is passed between the two Pt electrodes. Drastic concentration changes and contamination by electrode reactions during the passage of current are overcome by adding a few grams of a weakly acid carboxylic cation-exchange resin[1] to each half-cell. In transport measurements across a cation-exchange membrane, the resin in the cathode compartment is in the hydrogen form; that in the anode compartment, in the appropriate metal form. The presence of these resins buffers the concentrations of sodium ions, which migrate through the membrane to a much greater extent than the chloride ions. The transport experiment can be represented schematically for NaCl and a cation-exchange membrane in the following manner:

		Membrane		
Pt anode	Na*Cl solution		NaCl solution	Pt anode
+	+ Na*R		+ HR	−
Anode compartment			Cathode compartment	

where R represents the ion-exchange resin radical. The asterisk signifies that the Na ion in the anode compartment is traced with 2.6 y Na^{22}. The specific activity of Na in the anode solution and on the granular resin is the same. As current is passed between the two electrodes, the following reactions take place in the cathode compartment:

$$H_2O + e^- \rightarrow OH^- + \tfrac{1}{2} H_2\ (g) \qquad [1]$$

$$Na^+ + OH^- + HR \rightarrow NaR + H_2O \qquad [2]$$

where e^- represent the electron. The net cathode reaction is, therefore:

$$Na^+ + e^- + HR \rightarrow NaR + \tfrac{1}{2} H_2\ (g) \qquad [3]$$

Thus the transported cation is removed without introducing extraneous ions or water. Anode compartment reactions are based on the high affinity of the resin for hydrogen ions:

$$Cl^- - e^- \rightarrow \tfrac{1}{2} Cl_2\ (g) \qquad [4]$$

or

$$\tfrac{1}{2} H_2O - e^- \rightarrow \tfrac{1}{4} O_2\ (g) + H^+ \qquad [5]$$

In the latter case, hydrogen ions are removed from the solution by the granular resin:

$$H^+ + NaR \rightarrow HR + Na^+ \qquad [6]$$

When reaction [5] predominates over [4], as is the case in dilute chloride solutions, the concentration on both sides of the membrane remains about constant. At any rate, no new types of ions are introduced into the solution phase. In more concentrated solutions, where reaction [4] becomes appreciable, the percentage change of chloride concentration for a given amount of current transferred can always be kept low, because of the high concentration of the solutions.

In the region of imperfect membrane selectivity, the electrode reactions do not even compensate approximately for the ion transport across the membrane. In fact, if less than half of the current is carried by cations, concentration changes in the electrode compartments are greater than in a cell with Ag-AgCl electrodes. In this case it may be possible to substitute a weakly basic granular anion exchange resin in both compartments. An analogous series of reactions may be expected to those described above for the weakly acid cation exchange resin.[2] Use of the weakly basic resin should prove particularly useful in the study of anion exchange membranes.

In a typical experiment it was verified by analysis of the resin grains and the solutions that the reactions do indeed take place as cited above. The pH of the solutions was determined after each experiment using "Alkacid" test paper, and in all cases was found to be neutral. In order to verify that solutions remained neutral at all times during the experiment, methyl red was added to the anode compartment and phenolphthalein to the cathode compartment. Under these conditions, current densities of 2.5 ma/cm^2 or lower did not produce any color change. When smaller resin grains are used and stirring is more vigorous, higher current densities are permissible.

[1] Amberlite IRC-50, Rohm & Haas, Philadelphia, Pa., >#12 U.S. mesh.

[2] The authors are indebted to Dr. N. W. Rosenberg, of Ionics, Inc., Cambridge, Mass., for this suggestion.

Table I. Ion and water transport across "Permaplex C-1" membrane (product of the Permutit Co., London)
Water content: 37.5%. Capacity: 1.75 meq. per g wet membrane or 0.146 meq. cm^{-3}. Thickness: 0.077 cm.

Experiment			1	2	3	4	5
Ion transport data							
Normality of NaCl solutions	Cathode compartment	before	0.1013	0.1023	0.1014	0.3044	0.3002
		after	0.1019	0.1017	0.1004	0.3054	0.3021
	Anode compartment	before	0.1013	0.1085	0.1014	0.3104	0.3017
		after	0.1002	0.1024	0.1009	0.3043	0.2945
Charge passed (millifaradays)			9.22	13.38	7.38	11.28	11.28
Transport number, t_{Na^+}							
From radiotracer transfer			—	0.97	—	1.02	1.03
From chloride-ion concentration change in cathode compartment			—	0.976	—	0.985	1.009
Avg			—	0.973±.03	—	1.00±.03	1.02±.03
Water transport data							
Anode buret loss (ml)			1.11	—	0.91	—	1.33
Cathode buret gain (ml)			1.04	1.57	1.00	—	1.40
Average water transport (ml)			1.08	1.57	0.96	—	1.36
Water transport (moles faraday^{-1})			6.4±0.3	6.5±0.3	7.2±0.4	—	6.7±0.3

The transport number of the anion is calculated from the change in chloride concentration of the cathode compartment. With appropriate minor corrections for water transport and swelling and exclusion of sorbed salt by the resin when changing from the hydrogen to sodium form, the anion transport number can be determined within at least ±0.03.

The transport number of the cation is determined independently by tagging the solution and resin in the anode compartment, as well as the membrane, with a radioactive isotope of the cation under consideration and observing the change in specific activity in both compartments with passage of current. Thus, the transport number of the cation can be determined within ±0.03 transport units. The specific activity of Na in the solution and resin in the anode compartment and on the membrane is the same at the start and throughout the whole experiment. It is important to remove the solution from the cathode compartment as soon as possible after the stoppage of the current and the reading of the liquid level in the burets. If this solution is kept in contact with the membrane for more than about 10 min, an appreciable error may result from the increase of the specific activity of the solutions by exchange of ions with the membrane.

On the other hand, exchange with the granular resin in the compartments is much faster than with the membrane and therefore the specific activity on the granular resin is not appreciably smaller than in the solution. This was verified by the authors in one experiment. However, for precision measurements they recommend that the specific activity in the granular resin, on the membrane and in the solution, be determined at the end of the experiment, thus verifying the equality of the specific activities of anolyte and membrane, on the one hand, and catholyte and granular resin in the cathode compartment on the other hand. Corrections can then be made for minor deviations from the expected specific activities.

The activity of the solutions was determined by evaporating a sample to dryness and counting, using a thin end-window G.M. tube connected to a Model 1070 "Multiscaler".[3] Sufficient activity was incorporated in the anode compartment so that, at the end of the experiment, the activity in the cathode compartment was at least 10% of that in the anode compartment. The counting rate varied between 200 to 3000 counts/min in different samples (background: about 28 counts/min). At least four different samples of each solution were prepared and about 10,000 counts were accumulated for each sample. Counting rates were corrected for background and nonlinearity. Under these conditions, the activities of the solutions could be determined within ±1%.

Since the sum of the electrical transport numbers is unity, the above two methods, used in conjunction, provide useful checks on the individual procedures as well as an increase in over-all accuracy. Table I lists ion and water transport data taken from several representative experiments.

It is seen that, within the estimated error of 3%, the transport number of sodium, t_{Na^+}, in "Permaplex C—1" was found to be unity in solutions about 0.1 and 0.3*N* with respect to NaCl. There is little in the literature with which to compare this result. Kressman and Tye (9) reported $t_{Na^+} = 0.98$ for 0.1*N* NaCl. The authors' result is not inconsistent with theirs. It is important that calculations of the transport number (*a*) from the radiotracer transfer and (*b*) from the chloride ion concentration change in the cathode compartment lead to the same result, within experimental error, although these determinations are essentially independent of each other.

Water transport is determined directly from the buret readings after correction for temperature changes, electrolytic decomposition (reaction [5]), evaporation, and spray. All gas bubbles which are evolved at the electrodes must be removed carefully before the final reading of the buret level. This was accomplished in this cell by designing the inside surface of the roof of each compartment in the shape of a dome and by carefully polishing it so that the gas bubbles escaped speedily through the

[3] Atomic Instrument Co., Cambridge, Mass.

burets. It was found that a trace of a commercial nonionic detergent was very helpful in removing gas bubbles continuously. The type of detergent to be used depends on the salt under investigation, solution concentration, and current density. In the case of NaCl solutions, the authors added a 1:9 mixture of "Pluronic" L-61 and L-72[4] in the cathode compartment, and "Triton" X-45[5] in the anode compartment. When used in the cathode compartment, however, Triton X-45 produced excess foam, while the Pluronics appeared ineffective in the presence of chlorine when used in the anode compartment. The effective detergent concentration for 1*N* solutions is about 0.075 ml of the commercial detergent per liter. In experiments with $CaCl_2$ solutions, Fisher Aerosol[6] was used in both compartments.

Water transport is calculated as the average of the volume decrease in the anode compartment and the volume increase in the cathode compartment. It is, of course, necessary to expel all gas bubbles before reading the burets. It is estimated that the values so obtained are accurate within 5%.

The magnetic stirrers used generate considerable heat, even when operated from rheostats located some distance from the cell. Large changes in temperature, however, were overcome by blowing compressed air through the motor housings.

[4] Wyandotte Chemical Corp., Wyandotte, Mich.

[5] Rohm & Haas Co., Philadelphia, Pa.

[6] Fisher Scientific Co., Pittsburgh, Pa.

The same cell may be used for the measurement of membrane potentials and diffusion across membranes. In the latter cases it is advisable to use more vigorous stirrers or circulation systems for the solutions.

Manuscript received July 24, 1956. The method used in these studies was presented at the A.A.A.S. Gordon Conference on Ion Exchange in 1954.

Any discussion of this paper will appear in a Discussion Section to be published in the December 1957 JOURNAL.

REFERENCES

1. A. J. Staverman, *Trans. Faraday Soc.*, **48**, 176 (1952).
2. J. W. Lorimer, E. I. Boterenbrod, and J. J. Hermans, *Disc. Faraday Soc.*, **21**, 141 (1956).
3. G. Scatchard, *J. Am. Chem. Soc.*, **75**, 2883 (1953).
4. M. R. J. Wyllie, *J. Phys. Chem.*, **58**, 67 (1954).
5. M. Murakoshi, Paper presented at Ion Exchange Symposium (Japan) June 19, 1954; *see* also Y. Kosaka, *J. Electrochem. Soc. Japan*, **23**, 659 (1955).
6. W. Juda, J. A. Marinsky, and N. W. Rosenberg, *Ann. Rev. Phys. Chem.*, **4**, 373 (1953).
7. N. W. Rosenberg, J. H. B. George, and W. D. Potter, *This Journal*, **104**, 111 (1957).
8. A. G. Winger, R. Ferguson, and R. Kunin, *J. Phys. Chem.*, **60**, 556 (1956).
9. T. R. E. Kressman and F. L. Tye, *Disc. Faraday Soc.*, **21**, 185 (1956).
10. F. C. Nachod and J. Schubert, Editors, "Ion Exchange Technology," p. 137, Academic Press, New York (1956).

Anodic Behavior of Iron in Acid Solutions

Milton Stern and Richard M. Roth[1]

Metals Research Laboratories, Electro Metallurgical Company,

A Division of Union Carbide Corporation, Niagara Falls, New York

The electrochemical behavior of iron has been the subject of extensive research within the last few years. Stern (1) has described the relationships which exist betweeen the corrosion potential, the corrosion rate, and the hydrogen activation overvoltage of pure Fe in acid NaCl solutions. Anodic polarization measurements were not reproducible and showed marked hysteresis. Thus, a quantitative description of the local anodic polarization curve for the material could not be presented. However, since the corrosion rate and the hydrogen activation overvoltage parameters, i_o and β, were constant over the pH range 1-4 and the corrosion potential varied by 0.056 v for each unit pH change, it was concluded that the local anodic polarization curve for Fe at currents corresponding to the corrosion current is extremely steep.

On the other hand, another explanation is possible if one considers that the anodic formation of ferrous ions from iron is pH dependent. In particular, for this mechanism to explain the data properly, anodic polarization must show an RT/F dependence on pH. The former explanation was selected because no obvious process could be devised which gave the anodic reaction the proper pH dependence.

Bonhoeffer (2) described the work of Heusler and Kaesche, two of his associates at the Max-Planck-Institut. These investigators also found a hysteresis effect during anodic polarization but reported that in $HClO_4$ solutions the local anodic polarization behavior of Fe does indeed show the pH dependence required to support the second explanation described above. However, anodic measurements in $HClO_4$ cannot be considered typical of behavior in acid NaCl solutions, particularly for a situation where ferrous ion complexing may be important.

These results, however, required that anodic behavior in acid NaCl be examined critically to determine which of the possible proposals is correct.

The question can be summarized simply. Does the Tafel slope for dissolution of Fe ($Fe \rightarrow Fe^{++} + 2e$) have a normal value of about 0.1 v, or is the slope an order of magnitude greater?

Procedure

Two new experimental approaches are possible, either of which can supply the answer to this question. Both have been described by Stern and Geary

[1] Present address: Lehigh University, Bethlehem, Pa.

(3). The techniques have been applied to the Fe problem, and thus are discussed here briefly. The methods make use of accurate low-current polarization measurements close to the corrosion potential and thus have the advantage of eliminating changes in surface composition and structure which may occur at higher currents.

Equipment and experimental techniques have been described elsewhere (1).

Method I.—If the corrosion potential and current are determined by the intersection of anodic and cathodic Tafel-type polarization curves, it can be shown that

$$\left(\frac{d\mathcal{E}}{di_{app}}\right)_{\substack{\mathcal{E}\to 0\\ i_{app}\to 0}} = \frac{\beta_c \beta_A}{(2.3)\,(i_{corr})\,(\beta_c + \beta_A)} \qquad (I)$$

where β_c is the cathodic Tafel slope, β_A is the anodic Tafel slope, and $\mathcal{E}$ is the difference between the polarized potential and the corrosion potential. Thus, a linear plot of potential as a function of applied current yields a straight line for sufficiently small values of applied anodic or cathodic current. The slope of this straight line section is $d\mathcal{E}/di$. Simultaneous measurement of the corrosion rate and hydrogen overvoltage yields values of i_{corr} and β_c. Thus, sufficient information is available to calculate the slope of the anodic polarization curve using Eq. (I).

Such measurements have been conducted in 4% NaCl acidified with HCl to a pH value of 1.5. The analysis of the Fe used was different from that reported previously (1), the S content being 0.01%. The material thus exhibited different values for the hydrogen activation overvoltage parameters. The exchange current, i_o, was found to be 0.041 μ amp/cm^2, while β_c was determined as 0.083 v. The corrosion rate in this case is equivalent to 26.2 μ amp/cm^2. Fig. 1 is a plot of the cathodic polarization data in the low-current region where the potential is a linear function of applied cathodic current. The value of $d\mathcal{E}/di$ is $6.7(10^{-4})$ v/μamp/cm^2. Using the above data in Eq. (I) produces a calculated value of β_A of 0.078 v.

It is interesting to note that the factor $\left(\frac{d\mathcal{E}}{di}\right)_{\mathcal{E}\to 0}$ is exactly the term which Bonhoeffer (4) prefers to call "polarization resistance." In Eq. (I), which expresses this term, the corrosion current is in the denominator. This explains the increase in polarization resistance which is found with decreasing corrosion rates. Actually, $\left(\frac{d\mathcal{E}}{di}\right)_{\mathcal{E}\to 0}$ is neither a resistance in the usual sense of the term nor a fundamental electrochemical parameter which controls corrosion rate. The linear dependence of potential on current only exists because the difference between two logarithmic functions of current approximates a linear function when the logarithmic functions are of the same order of magnitude (3).

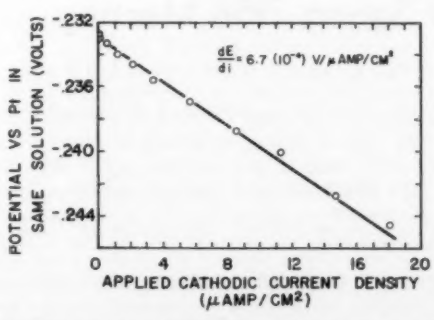

Fig. 1. Linear relation between potential and applied cathodic current.

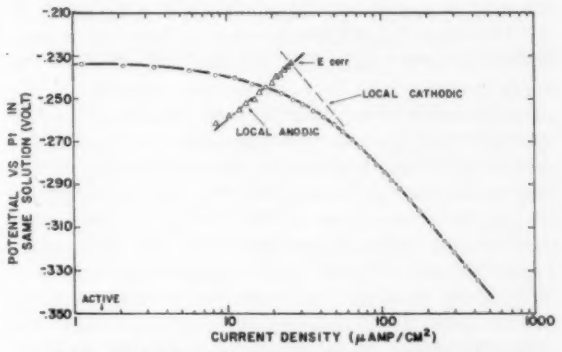

Fig. 2. Potential as a function of applied cathodic current

Method II.—For a system in which the corrosion potential and corrosion rate are determined by the intersection of two Tafel lines, where the intersection is sufficiently removed from the equilibrium potentials of the oxidation and reduction reactions involved, it has been shown (3) that the experimental cathodic polarization curve is described by the following equation:

$$\mathcal{E} = -\beta_c \log \frac{i_{app} + i_A}{i_{corr}} \qquad (II)$$

where i_{app} is the applied cathodic current and i_A is the total anodic current. Hydrogen activation polarization measurements in the Tafel region supply a value for β_c.

Thus, using Eq. (II), the local anodic current may be calculated as a function of potential during cathodic polarization.

Fig. 2 is a plot of potential as a function of applied cathodic current. Calculated values of i_A are included and trace the shape of the local anodic polarization curve. It is quite apparent here again that the local anodic polarization curve is not steep, the measured value being 0.068 v. Thus, it has been established that anodic behavior in HCl is similar to that reported by Bonhoeffer in $HClO_4$.

Discussion

It is necessary to explain the particular pH dependence of anodic polarization which produces the potential and corrosion rate dependence already reported by several investigators. In the pH range 1-4, it is difficult to accept the fact that the equilibrium potential of the Fe solution reaction is pH sensitive. Thus, one possible alternative explanation resides in a reduction of the exchange current density for the reaction $Fe \rightleftarrows Fe^{++} + 2e$ as the hydrogen

ion activity increases. This is not the only possibility, however. It has already been shown that during corrosion of Fe in acids, the major portion of the surface appears to function as the cathode. If one considers that the cathodic area increases as the hydrogen ion activity increases, possibly caused by greater hydrogen adsorption, then a decrease in the real area of the anode results. The anodic and cathodic polarization curves in Fig. 2 are based on a current-density calculation which uses the entire geometric sample surface area. Essentially, this is a plot of the polarization curves on a current basis rather than a current-density basis so that the curves intersect at the corrosion potential and the corrosion current. Thus, even though the equilibrium potential, β_A, and i_o for the solution of Fe are completely independent of pH, a decrease in the anode area will shift a plot of potential vs. anodic current to the left and produce a decrease in the exchange current even though the exchange current density is constant. Therefore, the pH dependence of the corrosion rate and corrosion potential of Fe may also be explained as a decrease in anodic area with an increase in hydrogen ion activity.

It is interesting to note that Hillson (5) reported that a Cu/Cu^{++} electrode showed a decrease in active area as a function of concentration of surface active agent. This produced a decrease in the exchange current. However, the exchange current density remained constant.

There is no obvious experiment which can distinguish between a shift in the real exchange current density and a change in the anode area of Fe. However, without any apparent reason for considering the reaction $Fe \rightleftarrows Fe^{++} + 2e$ to be pH dependent, it appears that the better of the two explanations is that based on a decreasing anode area as the pH is decreased.

Manuscript received July 24, 1956.

Any discussion of this paper will appear in a Discussion Section to be published in the December 1957 JOURNAL.

REFERENCES

1. M. Stern, *This Journal*, **102**, 609 (1955).
2. K. F. Bonhoeffer, Paper presented at ECS Meeting, San Francisco, April 30, 1956.
3. M. Stern and A. L. Geary, *This Journal*, **104**, 56 (1957).
4. K. Bonhoeffer and W. Jena, *Z. Elektrochem.*, **59**, 151 (1951).
5. P. J. Hillson, *Trans. Faraday Soc.*, **50**, 385 (1954).

Manuscripts and Abstracts for Spring 1958 Meeting

Papers are now being solicited for the Spring 1958 Meeting of the Society, to be held at the Statler Hotel in New York City, April 27, 28, 29, 30, and May 1, 1958. Technical Sessions probably will be scheduled on Electric Insulation, Electronics, Electrothermics and Metallurgy, Industrial Electrolytics, and Theoretical Electrochemistry.

To be considered for this meeting, triplicate copies of abstracts *(not to exceed 75 words in length)* must be received at Society Headquarters, 1860 Broadway, New York 23, N. Y., *not later than January 2, 1958. Please indicate on abstract for which Division's symposium the paper is to be scheduled.* Complete manuscripts should be sent to the Managing Editor of the JOURNAL at 1860 Broadway, New York 23, N. Y.

* * *

The Fall 1958 Meeting will be held in Ottawa, Canada, September 28, 29, 30, October 1, and 2, 1958, at the Chateau Laurier.

Discussion Section

Anodic Transients of Copper in Hydrochloric Acid

Ralph S. Cooper (pp. 307-315, Vol. 103)

James H. Bartlett[1]: (*A*) If the anode be horizontal and shielded, and if the current has decreased to zero, what is the nature of the break transient and what factors govern its duration?

(*B*) During a break transient, is the main process dissolution of the anode layer or is it diminution of the amount of $CuCl^-_2$ in the pores, with the attendant consequences?

Ralph S. Cooper: (*A*) For horizontal shielded anodes the current decreases monotonically, approaching zero as the layer resistance increases with time but never actually becoming zero. Upon breaking the circuit, the anode voltage will change by the amount of the *IR* drop across the layer, and will immediately assume the open circuit electrode potential. No extensive experiments of this type have been performed, but it may be expected that the break transients observed will be similar to those for unshielded anodes with three differences. First, for $V_a \leq -0.05$, an appreciable layer resistance is to be expected. Secondly, the duration of the −0.05 v voltage decay plateau may possibly be longer because of the lower rate of solubility of the layer. Finally, the electrode potential will not drop below −0.27 v as the anolyte will remain saturated with CuCl.

(*B*) There are, in general, two processes associated with the break transient. The first is the opening of the pores in the CuCl layer, which results in decay of the layer resistance. The completion of the resistance decay is coincident with the end of the −0.05 v voltage decay plateau. Only 1% of the CuCl layer need dissolve in order for its resistance to become small compared to the solution resistance. The second process is the removal of the bulk of the CuCl layer. This occurs only for unshielded electrodes where convection can act to remove the $CuCl^-_2$ ion complex at an appreciable rate. This process requires of the order of 10 sec for completion, during which the anode potential remains at −0.27 v. Upon completion the solution becomes unsaturated with respect to CuCl and the potential falls below −0.27 v, ending the second voltage decay plateau.

The Nature of the Film Formed on Copper during Electropolishing

E. C. Williams and Marjorie A. Barrett (pp. 363-366, Vol. 103)

I. Epelboin and M. Froment[2]: The study, by electron diffraction, of metals polished electrolytically gives contradictory results. Thus, Bouillon, Bouillon-Nyssen, and Delplancke[3] have reported that it is possible to obtain, by electrolytic polishing, copper surfaces free of all foreign layers. This conclusion is in disagreement with the results of Williams and Barrett, although in both cases the copper was polished in phosphoric acid.

We think that it is difficult to draw conclusions from an examination carried out after the specimen has been removed from the solution. This is why we study the polishing during the course of the electrolysis, by superimposing a low-amplitude alternating current on the continuous current. The study of variations of the components of impedance as a function of frequency enables one to obtain information about the structure of the anode layer, and it has been established[4] that the phenomena are more complex in phosphoric acid than in solutions based on ClO_4^- ions.

Assuming that it is possible to polish small copper surfaces in magnesium perchlorate-ethyl alcohol mixtures, it would be interesting to examine such surfaces by electron diffraction.

E. C. Williams and Marjorie A. Barrett: Our observations are not necessarily in disagreement with those of Bouillon, Bouillon-Nyssen, and Delplancke. They confirm the previous results of Hoar and Farthing concerning the existence of a film during polishing and we have furthermore emphasized that the film is formed, and remains on the surface, under the current-density conditions for polishing but that it dissolves in the acid when the circuit is opened. It is therefore possible to obtain a surface substantially free of a nonmetallic layer by withdrawing the specimen from the electrolyte some time after the cessation of current. Whether or not it is then completely free of all adsorbed radicals is doubtful, but we think that Messieurs Epelboin and Froment probably do not have in mind contamination of a molecular order of magnitude.

We agree that it is difficult to draw conclusions from an examination carried out after the specimen has been removed from solution. On the other hand our conclusions, which we arrived at after taking due precautions, do not in any way offend electrochemical principles and they appear to complete a fairly satisfactory picture of the polishing process based on Elmore's theory. The superimposed alternating current technique is no doubt promising as a means of providing information on the structure of the anode layer, but in our opinion it is a very indirect method and difficult to interpret.

Pitting Corrosion of 18Cr-8Ni Stainless Steel

M. A. Streicher (pp. 375-390, Vol. 103)

N. D. Greene, Jr.[5]: In his paper the author states that pitting may be divided into two distinct steps:

This Discussion Section includes discussion of papers appearing in the JOURNAL of The Electrochemical Society, 103, No. 6-12 (June-December 1956). Discussion not available for this issue will appear in the Discussion Section of the December 1957 JOURNAL.

[1] Dept. of Physics, University of Illinois, Urbana, Ill.

[2] Lab. de Physique Enseignement de la Faculté des Sciences de Paris, 1 rue Victor Cousin, Paris, France.

[3] F. Bouillon, Y. Bouillon-Nyssen, and A. Delplancke, *Bull. soc. chim. Belges*, 65, 245 (1956).

[4] I. Epelboin, *J. chim. phys.*, 49, C214 (1952); *Métaux (Corrosion-Inds.)*, [376], 31, 475 (1956).

[5] Corrosion Research Lab., Ohio State University, Columbus 10, Ohio.

pit initiation and pit growth. Pit initiation is a most curious technical term. To my knowledge, it has never been defined. True, a pit does start at some point; however, this fact surely does not constitute a definition of an initiation step.

If pitting involves two distinct steps it must be possible to characterize and separate each of these steps. Likewise, it should be possible to state the point at which the initiation step ceases and the growth step begins or assumes major importance. I would appreciate having the author's definition of the pit initiation step and his comments on the above points.

How does the author separate the initiation and growth steps in the test he describes? If pitting is a two-step process, as proposed, wouldn't the number of pits which appear during the test represent the cumulative action of initiation and growth under conditions of impressed current?

A test similar to the author's test in 0.1*N* sodium chloride was performed in this laboratory. Microscopic examination of the specimen showed numerous extremely small pits in addition to those visible to the naked eye. Many of these fine pits were clustered around the larger macroscopic pits. Probing indicated that they were definitely pit depressions and not the result of "roof collapse" of the larger pit cavities. Fig. 11 in the author's paper illustrates this phenomenon. Close examination of this photograph indicates the presence of approximately six tiny pits. Were these numerous microscopic pits included in the total pit counts?

M. A. Streicher: The division of pitting into pit initiation (surface break-down) and pit growth is a convenient method for separating various factors involved in each of these two steps, and follows naturally from the fact that one large, deep pit may be of much greater importance than many shallow pits. The factors in the metal or the environment which lead to surface break-down are not necessarily the same as those which promote excessive growth. These concepts of pit initiation and pit growth (propagation) have been found useful by other investigators.[6]

The break-down of the surface may be detected in several ways, by changes in electrode potential (*see* Ref. 25 of the discussed paper) or by the appearance of a pit. In my investigation, electrolytic methods were used to break down the passive surface. The number of pits formed in this way was used as a measure of the pitting resistance of the steel. The actual size of the pit was largely a function of the number of pits formed and the amount of current passing through the cell. Therefore, this method was not suitable for the study of pit growth and was not used for this purpose. Pits were grown only to reveal the number of points of break-down in the surface.

In order to observe pits in their relationship to the metallurgical structure the growth process must be stopped while they are still very small. Also, for metallographic studies a very large number of pits must be formed in order to obtain pits within the minute area under observation in the microscope. The current densities required to form these large numbers of pits are much greater than those used in the standard test described in the paper; i.e., a gradual increase of anodic current from zero to 3 ma/cm^2 in about 15 min.

For metallographic observation of pit formation a large current was applied for a short period, which resulted in many pits, a few of which grew to the cavity stage before the current was stopped. This phenomenon was also shown by time-lapse motion pictures taken during the extended application of an anodic current. Pits grew irregularly. After some growth a few pits stopped growing, while others continued, and then suddenly grew again.

Microscopic examination of specimens which had been subjected to the standard pitting test, as described in the paper, did not reveal any pits which were not readily visible to the unaided eye.

[6] P. M. Aziz, *Corrosion*, **9**, 85 (1953); R. May, *J. Inst. Metals*, **82**, 65 (1953).

Natural and Thermally Formed Oxide Films on Aluminum

M. S. Hunter and P. Fowle (pp. 482-485, Vol. 103)

D. A. Vermilyea[7]: This paper is extremely interesting and does much to clarify the phenomena occurring during the gaseous oxidation of Al. One of the most interesting results of the study is the fact that the barrier layer thickness is a linear function of the temperature of oxidation. According to the theory of Mott and Cabrera[8] a plot of the reciprocal of the thickness against temperature should be linear. The experiments of Rhodin[9] on Cu agree well with the Mott-Cabrera theory, but the present results on Al do not. To my knowledge there is at present no theory which predicts the observed dependence of barrier thickness on temperature, and a further study of this system might prove very enlightening.

M. S. Hunter and P. Fowle: The linear relationship between barrier thickness and temperature is an observed fact which has not yet been explained by theory. Work is continuing in an attempt to evolve such an explanation. A possible key to this behavior may be the fact that the thickness of anodically formed barrier oxide films is a linear function of voltage, which suggests that the thermal forces which create natural barriers may be analogous to voltage which creates anodic barriers.

Preparation of High Purity Rhenium

D. M. Rosenbaum, R. J. Runck, and I. E. Campbell (pp. 518-521, Vol. 103)

Alan Seybolt[10]: Would it be possible to reduce the $ReCl_6$ to metal directly by hydrogen, instead of going through the ReO_3 step?

D. M. Rosenbaum, R. J. Runck, and I. E. Campbell: We have prepared rhenium metal by hydrogen reduction of the chloride, but the "hydrolyzed method" gave a purer product, that was in a form

[7] Research Lab., General Electric Co., Schenectady, N. Y.

[8] N. Cabrera and N. F. Mott, *Repts. Progr. Phys.*, **12**, 163 (1948-49).

[9] T. N. Rhodin, *J. Am. Chem. Soc.*, **72**, 5102 (1950); *ibid.*, **73**, 3143 (1951).

[10] Research Lab., General Electric Co., Schenectady, N. Y.

more suitable for the intended processing by powder-metallurgy techniques.

A Mechanism for the Anodic Dissolution of Magnesium

J. H. Greenblatt (pp. 539-543, Vol. 103)

I. Epelboin and M. Froment[11]: (*A*) The work of J. H. Greenblatt is very interesting, because for certain problems it is important to know the proportion between the quantity of magnesium retained in the anodic corrosion products and those rendered soluble in the 3% NaCl solution. On the other hand, it appears to us that for the understanding of the mechanism of the irregular dissolution of different metals, it is preferable to avoid the formation of an insoluble layer, and it is for this reason that we use electrolytic polishing. The latter applies actually to all the metals and it permits[12-15] us to distinguish, by the application of Faraday's law, two modes of anodic dissolution. The first is characterized by the dissolution of the metal in the form of such stable ions as: Ag^+, Au^{3+}, Hg^+, Ni^{2+}, Co^{2+}, Cu^{2+}, Zn^{2+}, Cd^{2+}, Ge^{4+}, Si^{4+}, Fe^{2+}, Mn^{2+}, Ga^{3+}, Mo^{6+}, W^{6+}, Zn^{2+}, Mg^{2+}, U^{6+}, V^{4+}, Al^{3+}, Be^{2+}. The other mode of dissolution becomes evident with ions as: Au^+, Cu^+, Ge^{2+}, Si^{2+}, Ga^+, W^{4+}, Zn^+, Mg^+, U^+, V^{3+}, Al^+, Be^+, La^+, Ce^+, Ti^+, Li^+, and it takes place in the presence of a compact adsorption of certain anions on the surface of the metal, notably with ClO^-_4 ions. The majority of the metals which we have mentioned are polished in the presence of these anions and we have proved, by gravimetric determination of Cl^-, that unstable ions such as Mg^+, Zn^+, V^{3+}, Al^+, Be^+, La^+, Ti^+, reduce the ClO^-_4 anions. The perfect agreement between the coulometric data and the gravimetric determination of Cl^-, which persists in a large range of current density, as well as other experimental work (*see* footnotes 14 and 15), seems to remove certain hypotheses such as: chemical attack of the anode, formation of complexes, presence of simultaneous reactions at the electrode, etc.

(*B*) We do not understand how the comparison between the amount of Mg equivalent to the liberated hydrogen and the distribution of Mg after its dissolution is capable of informing us of the eventuality of reactions I and IV shown on page 542 of the paper. It is a pity that for the discussion of these reactions Mr. Greenblatt has not sufficiently utilized his own data indicated, for example, in Table I, p. 541. In effect, if one supposes that the ions Mg^+ eventually reduce water, the agreement between the coulometric data (column 5) and the total quantity of liberated hydrogen (column 4) is excellent. One deduces by the two methods, with the exception of the measurements made at very low current densities (0.0196 amp/cm^2), that the initial average valence is equal to 1.3. This figure permits the deduction, according to Eq. I and IV, that the dissolution of one gram atom of Mg involves 70% ions of the Mg^+ state and 30% of the Mg^{2+} state. By creating a more compact adsorption of certain anions on the surface of the metal, one can increase the percentage of Mg^+ ions. For example, with the polishing baths with a base of magnesium perchlorate we have found that 80% of the Mg ions are in the monovalent state. This result, published three years ago,[16] confirms that the mechanism of the irregular anodic dissolution of Mg, like that of other metals, must be connected with the constitution of the electrochemical double layer.[16]

J. H. Greenblatt: The comments of I. Epelboin and M. Froment have been noted and the author finds no disgreement with them. The author became aware of the work of Epelboin and co-workers late in 1955 after the paper under discussion had been submitted for publication and has followed their work with interest since that time.

The author has attempted to explain the solution of Mg under what might be called "normal" conditions of use for Mg anodes when insoluble products do form. To do this, of course, it is necessary to establish the amounts of dissolved material found in the various reaction products. The distribution of products and their ratios is a consequence of the relative occurrence of reactions (I) and (IV), since insoluble Mg can only result if reaction (I) is occurring and there is no self-corrosion. When self-corrosion did occur, the excess weight loss always appeared as insoluble product, and this reaction path could be thus accounted for. If no self-corrosion occurred, efficiencies of roughly 50% were obtained and the insoluble and soluble Mg were in roughly 1:1 ratio. This product distribution could only occur through the predominance of 1. What is said in effect is that Mg^+ reacts close to the surface with H_2O and the amount of reaction can be deduced from the amount of MgO produced. This is an exactly analogous procedure to that of Epelboin and Froment who determine the amount of Mg^+ present by determining the amount of reaction product between Mg^+ and ClO^-_4, i.e., Cl^-.

The author did not utilize the data of Table I, p. 541, in the manner suggested by Epelboin and Froment because he felt that it was sufficiently accurate to draw only the broader and more general conclusions about the kinetic mechanism proposed. The quantities of hydrogen collected were thought to suffer from the maximum experimental error because of the method of conducting the experiments. Small variations in this quantity would lead to reasonably large variations in apparent valence which the author felt might not reflect the true situation.

More accurate analyses of the distribution of reaction products have been obtained since the above mentioned work, and they can be used to distinguish between reactions (I) and (IV) as follows:

$$Mg \rightarrow Mg^+ + e \qquad (I)$$

$$2Mg^+ + H_2O \rightarrow Mg^{++} + MgO + H_2 \qquad (II)$$

$$Mg \rightarrow Mg^{++} + 2e \qquad (IV)$$

[11] Lab. de Physique Enseignement de la Faculté des Sciences de Paris, 1 rue Victor Cousin, Paris, France.

[12] I. Epelboin and M. Froment, *Compt. rend.*, 238, 2416 (1954).

[13] Ph. Brouillet, I. Epelboin, and M. Froment, *Compt. rend.*, 239, 1795 (1954).

[14] Ph. Brouillet, Thesis, Paris (1955); *Métaux (Corrosion-Inds.)*, 30, 141 (1955).

[15] I. Epelboin, 54e Réunion de la Bunsen-Gesellschaft, Goslar, May 1955; *Z. Elektrochem.*, 59, 689 (1955).

[16] I. Epelboin and M. Froment, 73e Colloque International de la Centre National de la Recherche Scientifique, Paris, October 1956.

Table I. Electrolysis data for pure Mg anodes at room temperature 22°C

Current density (amp/cm²)	Wt loss (mg)	Calculated wt loss $Q/F \cdot 12$ (mg)	Soluble Mg (mg)	Insoluble Mg (mg)	α
0.027	259	136	136	117	0.86
0.027	260	136	136	124	0.91
0.036	262	134	133	133	1.00
0.036	265	134	139	130	0.97
0.044	254	131	133	120	0.92
0.044	248	131	131	121	0.93
0.052	250	136	139	116	0.85
0.052	246	136	139	123	0.91
0.056	248	136	138	122	0.90
0.056	234	136	141	110	0.81
0.056	257	136	136	133	0.98
0.064	230	131	139	115	0.88
0.064	231	131	136	114	0.87
0.064	227	131	135	102	0.77

Suppose α is the fraction of (I) occurring and $(1-\alpha)$ the fraction (IV). Then for the passage of Q coulombs, $\alpha(Q/F) \cdot 24$ g of Mg will dissolve according to (I), of which, if (II) holds true, $Q\alpha \cdot 24/2F$ will be soluble and $\alpha Q \cdot 24/2F$ will be insoluble. The amount dissolving by (IV) is $(1-\alpha)\ Q/F \cdot 12$, all of which is soluble.

Total soluble Mg^{++} is then $Q/F \cdot 12$. The insoluble magnesium is $\alpha Q/F \cdot 12$. According to this, the soluble reaction product should always be constant at $Q/F \cdot 12$ while the insoluble material and total weight loss should decrease if (IV) occurs. The data above obtained over a range of current densities indicate that this is essentially true.

Values of α or the fraction of (I) occurring are seen to average about 0.9. At higher current densities it can be seen that the totals of columns 4 and 5 are greater than the total weight loss. This strengthens the author's contention that such data should be used in a general way and that the conclusion to be drawn from the above table is that, under the conditions of electrolysis as carried out in the author's work, reaction (I) predominates almost exclusively and that (IV) is relatively unimportant.

Depth of Surface Damage Due to Abrasion on Germanium

T. M. Buck and F. S. McKim (pp. 593-597, Vol. 103)

B. A. Irving[17]: The figures for depths of surface damage on abraded Ge reported by Buck and McKim represent average depths over the area of their measurement (about 2 cm²). In the course of work in this laboratory on the etching of Ge it has been shown that damage caused by a scratch can reach considerably greater depths.

A (100) surface on a single-crystal Ge specimen was ground on 320 mesh Carborundum paper and then on progressively finer abrasive down to one micron diamond dust, to give a metallographically polished surface. A distincitve array of scratches was observed during the initial stages of grinding with the 320 mesh Carborundum paper. It is estimated that at least 20 μ of material were removed during grinding and polishing. The specimen was

[17] Research Lab., Associated Electrical Industries Ltd., Aldermaston Court, Aldermaston, Berkshire, England.

Fig. 1. Etched Ge surface, showing facetted etch-marks. 5X before reduction for publication.

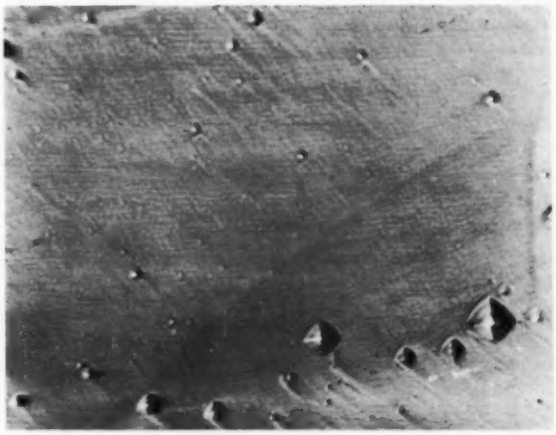

Fig. 2. Single facet enlarged to show etch pits. 2,000X before reduction for publication.

then etched in hypochlorous acid until a further layer, 40 μ thick, had been removed. The distinctive scratches, noticed during grinding, were reproduced with others as an array of facetted etch-marks (Fig. 1). Small etch pits occurred distributed over the surface but concentrated along the etch-marks (Fig. 2). The density and distribution of the pits (other than those on the etch-marks) were similar to that obtained for the same specimen etched in CP-4 which is known to produce pits at dislocations.[18] It is suggested that dislocations are responsible for the persistence of the scratches as etch-marks.

Abrasion can, therefore, cause local damage at depths greater than 40 μ taking the form of rows of dislocations.

T. M. Buck and F. S. McKim: Our data showed principally that, by etching to depths approximately equal to the particle size of the abrasive used in lapping or polishing, the average recombination velocity over the surface area used was reduced to low levels ($\sim$ 100 cm/sec) where no further significant change could be detected in the PME method.

[18] F. L. Vogel, W. G. Pfann, H. E. Corey, and E. E. Thomas, *Phys. Rev.*, **90**, 489 (1953).

We have, in our paper, recognized the possibility of deeper local damage, in view of Uhlir's[19] studies of reverse characteristics of electrolyte-Ge barriers. Mr. Irving's data furnish useful information regarding the nature of such local damage. The scratches he observes are probably deeper than any we have encountered since he used 320 mesh abrasive (maximum particle diameter 50-60 μ) as the initial lapping treatment. However, we have observed that the recombination velocity does not drop as sharply, with etching, for a fine-polished surface on which numerous scratches are visible owing to insufficient polishing or foreign particles in the polishing compound.

Kinetics of Formation of Porous or Partially Detached Scales

C. Ernest Birchenall (pp. 619-624, Vol. 103)

U. R. Evans[20]: The effect of vacancies developing at the base of a growing oxide film on the growth law is of great interest today, and Professor Birchenall's detailed treatment should be welcomed.

In a slightly different way, it has been possible[21] to arrive at an equation which seems to fit such facts as are known to us. Any vacancy arising from the passage of an atom (as cation) into the film may either (a) move into the oxide or metallic phase—possibly, in the latter case, becoming extinguished on arrival at a dislocation or (b) settle at the oxide-film interface, not necessarily at the original point of formation.

The second of these occurrences must help to cut down the area over which movement of ions across the film can occur. Presumably the chance of it happening will be proportional to the number of sites still available. The assumption led me a few years ago to an expression for the weight change (W) at time (t)

$$W = k_1 \log (t^{1/2} + k_2) + k_3$$

when k_1, k_2, and k_3 are constants. Somewhat later Mills,[22] studying the oxidation of Cu, experimentally found this equation to be obeyed under circumstances where neither the parabolic nor the ordinary logarithmic equation was obeyed.

Of course, in other cases the conditions on which this equation is based may not be fulfilled, and then those developed by Professor Birchenall, starting from different premises, may have useful application.

L. Seigle[23]: We have found Dr. Birchenall's paper interesting because of the similarity of the phenomenon he is considering to that of void formation in metals during diffusion. Studies of the latter process[24] indicate that the formation of voids is sometimes catalyzed by oxides in the solid metal, suggesting that the oxide-metal interface can be a favored site for vacancy condensation. If void formation by this mechanism is looked upon as a nucleation and growth process, the nucleation frequency is seen to be dependent upon the relative interfacial energy of the oxide-metal interface, and the degree of vacancy supersaturation attained at this interface.

The same ideas might be applied to the nucleation of voids at the oxide-metal interface during scale formation. For example, if it is assumed that vacancies pass across an initially coherent interface into the base metal, the vacancy concentration at the interface will tend to build up until a quasi-steady state is reached in which the rate of arrival of vacancies through the oxide is equal to the rate of removal through the metal. The excess vacancy concentration in the metal at the interface, N_i, can then be obtained by solving the equation (*see* footnote 24):

$$I_v = D_v \frac{\partial^2 N_v}{\partial x^2} - \frac{N_v}{\tau} = 0$$

with the boundary conditions $N_v = 0$ for $x = \infty$ and $-D_v(dN_v/dx) = (D_o \Delta X_o/l)$ for $x = 0$.

The solution is

$$N_v = \frac{D_o X_o}{l} \sqrt{\frac{\tau}{D_v}} \exp\left(-\frac{x}{\sqrt{D_v \tau}}\right)$$

$$\text{and } N_i = N_v\,(x = o) = \frac{D_o \Delta X_o}{l} \sqrt{\frac{\tau}{D_v}}$$

In the above equations N_v, D_v, and τ are the excess concentration, diffusion coefficient, and lifetime of vacancies in the metal, respectively, ΔX_o and D_o are the concentration differential and diffusion coefficient of cations in the oxide, and l is the thickness of the scale. The quantity τ/D_v can be written in terms of density of dislocations, N_d, jogs on dislocations, j, equilibrium vacancy concentration, N_v, and self-diffusion coefficient, D_m, in the metal, and expressions obtained for the relative excess concentration of vacancies at the oxide-metal interface:

$$\frac{N_i}{N_v} = \frac{D_o \Delta X_o}{D_m\, l\, N_d^{1/2}} \text{ (low temperatures)}$$

$$\frac{N_i}{N_v} = \frac{D_o \Delta X_o}{D_m\, l (N_d\, ja)^{1/2}} \text{ (high temperatures)}$$

In the above a is the atom spacing in the metal and ΔX_o must be expressed as atom fraction. Making appropriate assumptions about N_d and j, a value of N_i/N_v can be calculated which might indicate the probability of nucleation at the interface. No attempt has been made to apply these equations, but they are offered as a possible approach.

It is also possible that the oxide-metal interface acts as a source and sink for vacancies in the way that grain boundaries in metals seem to.[25] If this is true, the vacancy flow would not cross the interface, but be eliminated at it by a mechanism whose details are not yet understood.

C. E. Birchenall: The author appreciates the additional remarks furnished by Doctors Evans and Seigle. Since I am in general agreement with

[19] A. Uhlir, *Bell System Tech. J.*, **35**, 333 (1956).

[20] 19 Manor Court, Grange Rd., Cambridge, England.

[21] U. R. Evans, *Reviews of Pure and Applied Chemistry (Melbourne)*, **5**, 1 (1955).

[22] T. Mills and U. R. Evans, *J. Chem. Soc.*, 1956, 2182.

[23] Metallurgy Labs., Sylvania Electric Products Inc., Bayside, N. Y.

[24] R. Resnick and L. Seigle, *J. Metals*, **9**, 87 (1957).

[25] R. Balluffi and L. Seigle, *Acta Met.*, **3**, 170 (1955).

these observations, I should like to take the opportunity to make several comments which may be somewhat repetitious but seem to me to be important, if only as points requiring further experimental or theoretical study.

I, as well as others, have looked for porosity developing within a metal while an oxide grows upon it. Such porosity has not been found when the substrate is a pure metal, only when it is an alloy. In the latter case the porosity is probably Kirkendall porosity arising from metallic interdiffusion as the oxidation preferentially removes one component.

Porosity does occur frequently within the oxide layer. Its extent and distribution seems to be very sensitive to specimen geometry, indicating that inclusions or impurities are not all-important, although they be major factors in determining where pores start in any given geometry.

In an ionic crystal it appears that annihilation of vacancies of one charge requires a deformation of the lattice of ions of the other charge. For this reason it becomes important to learn more of the behavior of the immobile ions in order to construct a more complete picture of the oxidation process.

It is evident that the critical region is at the metal-oxide interface. The region is liable to modification by the accumulation of inclusions and slowly diffusing impurities. It is also difficult to prepare for metallographic examination. In the long run, new techniques must be refined to give explicit answers about the exact state of the interfacial region.

Rectifying Semiconductor Contacts

H. K. Henisch (pp. 637-643, Vol. 103)

R. E. Burgess[26]: In discussing the number of impurities in the barrier layer, the appropriate quantity would seem to be the number in a cube of edge equal to the barrier thickness and not the total number present.

[26] Dept. of Physics, University of British Columbia, Vancouver, B. C., Canada.

H. K. Henisch: In order to make a quantitative assessment, it is convenient to assume that the impurities are distributed in the form of a regular superlattice. The parameter which concerns us then is the distance between neighboring impurities in relation to the thickness which the barrier would have if the space charge were continuous. In practice, the impurity distribution would, of course, be random or at any rate nonperiodic in some other way. An approximate treatment of this case has been given by Wiles.[27]

New Method of Studying Corrosion Inhibition of Iron with Sodium Silicate

E. F. Duffek and D. S. McKinney (pp. 645-648, Vol. 103)

L. Lehrman and H. L. Shuldener[28]: The authors assume that the protective action is due to an invisible film on the metal. If this is true, then it is conceivable that this film is a combination of the initial corrosion products with silica.

It would be interesting to know if any silica was removed from the test solutions. Our work clearly indicated that, when sodium silicate acts as a corrosion inhibitor, corrosion products at the surface of the metal combine with silica to form a protective deposit.

The experimental technique used is very interesting. It might also be used for determining the effect of silica occurring naturally in water vs. that added as sodium silicate. Sodium silicate could be added to a low silica water and caustic soda added to a high silica water, both of the same pH and final silica content, and the passifying effects of both solutions observed.

We agree with the emphasis put on visual examination as against weight loss in experimental work of this type.

[27] G. G. Wiles, *Phil. Mag.*, 46, 363 (1955).

[28] Water Service Labs., Inc., 423 West 126th St., New York 27, N. Y.

December 1957 Discussion Section

A Discussion Section, covering papers published in the January—June 1957 JOURNALS, is scheduled for publication in the December 1957 issue. Any discussion which did not reach the Editor in time for inclusion in the June 1957 Discussion Section will be included in the December 1957 issue.

Those who plan to contribute remarks for this Discussion Section should submit their comments or questions in triplicate to the Managing Editor of the JOURNAL, 216 W. 102 St., New York 25, N. Y., *not later than September 1, 1957.* All discussion will be forwarded to the author, or authors, for reply before being printed in the JOURNAL.

Current Affairs

Annual Report of the Board of Directors of The Electrochemical Society for 1956

During the year 1956 the following awards were made:

Acheson Medal Award—This award was presented to Dr. Robert M. Burns. The award, made in the presence of the Acheson family, was in celebration of the 100th Anniversary of the birth of Edward Goodrich Acheson. Dr. Burns returned the honorarium in the form of common stocks in A.T.&T. with the request that this sum be added to the Society Reserves.

Young Author's Prize—Milton Stern, Metals Research Labs., Electro Metallurgical Co., Niagara Falls, N. Y., for his papers: "The Electrochemical Behavior, including Hydrogen Overvoltage, of Iron in Acid Environments" (November 1955 issue), and "The Effect of Alloying Elements in Iron on Hydrogen Overvoltage and Corrosion Rate in Acid Environments" (December 1955 issue).

Francis Mills Turner Memorial Award—J. G. Jewell, Gulf Research and Development Co., Pittsburgh 30, Pa., for his paper: "A Theoretical Basis for a New Method of Investigating Corrosion Inhibition" (April 1955 issue).

Honorable Mention—D. E. Kinney and S. S. Brenner.

One of the highlights of the year 1956 was the gift of $1,074.40 in Blue Ridge Mutual Stock presented to the Society by Mrs. Colin G. Fink. This gift was given to the Society for general purposes.

During the year 1956 the following monographs were published:

"High Temperature Technology" edited by Dr. I. E. Campbell.

"Stress Corrosion Cracking and Embrittlement" edited by Dr. W. D. Robertson.

At the New York Meeting of the Board of Directors held January 27, 1956 the new Boston Section was chartered with the following officers:

Chairman—F. C. Benner
Vice-Chairman—L. B. Rogers
Secretary-Treasurer—Charles Levy

At the San Francisco Meeting of the Board of Directors, the new Southern California-Nevada Section of the Society was chartered with the following officers:

Chairman—Thomas B. Blair
Vice-Chairman—William Hetherington
Secretary-Treasurer—Lee J. Droege

The final report of the Survey Committee, instituted a year ago, was gratefully accepted by the Board of Directors and its recommendations referred to the Ways and Means Committee for further study and implementation.

One of the first actions taken on the advice of the Survey Committee was the institution of an Investment Advisory Panel.

Hans Thurnauer, *Chairman*

Annual Report of the Secretary for 1956

During the year 1956 the principal operating change was the shift in our fiscal year. Since our accounting is on the cash basis, it has been exceedingly inconvenient to have the fiscal year running January 1-December 31. The Board has authorized changing the fiscal year to April 1-March 31 by means of a 15-month fiscal year starting January 1, 1956 and ending March 31, 1957. This means that our fiscal year ends during a relatively low income period which will make budgeting considerably easier in the future.

Consistent with the former policy the membership count for the year 1956 is contained in the February JOURNAL, Page 38C. This was our best year since the Active Members have increased by 227, which compares with 124 for the year 1955; 1955 was a good year compared with the past history of the membership. Over-all, in all categories, during the year 1956 our membership increased by 264, which amounts to an 11.6% increase, compared with the previous year where the total increase in membership amounted to 129 in all grades, which was a 6.0% increase. So far, 1957 appears to be well on its way toward breaking the 1956 membership record.

During the year 1956 the following companies took our Patron Memberships:

1. Aluminum Co. of Canada Ltd.
2. The International Nickel Co., Inc.
3. Union Carbide & Carbon Corp., Divisions:
   Electro Metallurgical Co.
   National Carbon Co.

The following new Sustaining Members were signed up during the past year:

1. Cramet, Inc. (1 memb.)
2. Westvaco Chlor-Alkali Div., Food Machinery & Chemical Corp. (1 memb.)
3. Boeing Airplane Co. (1 memb.)
4. Titanium Metals Corp. of America (1 memb.)
5. American Zinc, Lead & Smelting Co. (2 additional memb.)
6. Stackpole Carbon Co. (1 additional memb.)
7. Jones & Laughlin Steel Corp. (1 memb.)
8. Bell Telephone Labs. (1 additional memb.)
9. Eppley Lab., Inc. (1 additional memb.)
10. Alloy Steel Products Co. (1 additional memb.)
11. Weirton Steel Co. (1 memb.)
12. Hercules Powder Co. (1 memb.)
13. American Metal Co. Ltd. (1 memb.)
14. Hanson-Van Winkle-Munning Co. (1 additional memb.)
15. The Udylite Corp. (2 additional memb.)
16. Shawinigan Chemicals Ltd. (1 memb.)

17. Michelin Co. (1 memb.)
18. American Potash & Chemical Corp. (1 additional memb.)
19. Reynolds Metals Co. (1 memb.)
20. Wilbur B. Driver Co. (1 additional memb.)
21. Kaiser Aluminum & Chemical Corp., Chemical Research Dept. Library (1 additional memb.)
22. International Minerals & Chemical Corp. (1 memb).
23. General Motors Corp., Brown-Lipe-Chapin Div. (2 memb.)
24. General Motors Corp., Guide Lamp Div. (1 memb.)
25. Stauffer Chemical Co. (1 additional memb.)
26. Gillette Safety Razor Co. (1 memb.)

Report of Tellers of Election

For President: Norman Hackerman, 915; 11 write-ins; 19 abstentions.

For Vice-President: R. A. Schaefer, 420; I. E. Campbell, 308; A. L. Smith, 177; 23 write-ins; 17 abstentions.

Twenty-five ballots were declared invalid because more than one candidate was marked for the same office; three ballots were turned in blank.

Total votes cast as of December 15, 1956, the deadline for casting ballots, was 973.

The ballot tabulations have been placed in a sealed envelope in the charge of the Assistant Secretary at The Electrochemical Society Office.

(Signed) **Attilio L. Bisio,** *Chairman*
A. Venkateswarlu
Emil Schmitt

The Tellers' Report was unanimously accepted and a motion was passed declaring the candidates, Norman Hackerman (President) and R. A. Schaefer (Vice-President) duly elected.

Henry B. Linford, *Secretary*

Section News

Washington-Baltimore Section

The Washington-Baltimore branches of The Electrochemical Society, The National Association of Corrosion Engineers, and The American Electroplaters' Society held a joint meeting on March 26, 1957 at the University of Maryland, College Park, Md. Mr. W. J. Mayer, Chairman of NACE, introduced Mr. B. J. Philibert, who discussed the interrelation of the three societies and NACE's approach to corrosion mitigation. Dr. Jerome Kruger introduced Mr. E. C. Bertucio, Vice-President of AES, who explained the relationship of the AES to the ECS. Mrs. Jeanne Burbank, Chairman of the ECS Section, introduced Dr. Walter J. Hamer, who discussed advances in theoretical electrochemistry and described a symposium on electrolytes to be held in connection with the ECS's 111th Convention in Washington in May.

Left to right, B. J. Philibert, National Association of Corrosion Engineers; Dr. Jerome Kruger, E. C. Bertucio, Vice-President, American Electroplaters' Society; Dean G. F. Corcoran, Dr. Ralph Roberts, the Office of Naval Research, Dr. Walter J. Hamer, W. J. Mayer, Chairman, NACE, and Mrs. Jeanne Burbank, Chairman ECS, at joint meeting of ECS, NACE and AES.

The speaker of the evening was Dr. Ralph Roberts of the Office of Naval Research, who discussed topics related to his recent tour of Europe as Scientific Liaison Officer.

Gwendolyn B. Wood, *Secretary*

Chicago Section

The Chicago Section was privileged to have as its speaker on Extractive Metallurgy Night Mr. Christopher Marzano, Chief Chemist, Amphenol Electronics, whose talk was on "Preparation of Uranium Electrolysis of Fused Salts." The primary purpose of the project, which was performed at Argonne National Lab., was to prepare high purity uranium. Following the talk the nominating committee made its report. Recommendations for nominations are:

Chairman—D. V. Louzos
Vice-Chairman—Ralph Hovey
Treasurer—W. H. Colner
Secretary—J. Kuderna
Program Chairman—J. Miller
Delegate to Council of Local Sections—H. T. Francis

William H. Colner, *Secretary*

India Section

The First Technical Meeting of the India Section for 1956 was held on October 18 jointly with the Indian Institute of Metals, Bangalore Chapter, at the Indian Institute of Science, Bangalore. Dr. T. R. Anantharaman, Assistant Professor of Metallurgy, Indian Institute of Science, spoke on "Metallurgical Education and Research in Europe."

The Second Technical Meeting of the Section for 1956 was held on December 21 at the National Physical Lab., New Delhi, with Dr. D. N. Daruvalla, Director, Shri Ram Institute for Industrial Research, Delhi, as chairman. Mr. G. D. Joglekar, Assistant Director, N.P.L., delivered a lecture on "Carbon Electrodes." The development of the carbon electrode industry, since the discovery by Davy of the carbon arc to the present day, was briefly discussed. The imports of carbon electrodes required for various industries in the country are over Rs.40 lakhs per annum. The present requirements are about 10,000 tons per annum, but this figure is likely to increase to 30,000 tons during the next five years. Carbon products such as dry cell rods, carbon brushes, switch gear contacts, oil seal rings, etc., made in the National Physical Lab. of India were shown. As a result of the work carried out in the N.P.L., a factory is now being established at Patiala for the manufacture of carbon brushes and other carbon products.

The Third Technical Meeting of the Section for 1956 was held on December 26, again jointly with the Indian Institute of Metals, Bangalore Chapter, at the Indian Institute of Science, Bangalore. Mr. L. J. Balasundaram, who recently returned from the United Kingdom, gave a talk on "Metallurgical Applications of X-Rays." After a brief survey of the technological applications of x-rays, such as x-ray crystallography, radiography, and x-ray spectroscopy, the speaker explained the different methods of study of crystal structure. During his talk he referred to measurement of stresses and strains, study of super lattices, investigation of phase diagrams, determination of crystal structure, evaluation of precipitation hardening treatments, industrial radiography for study of casting defects, and microradiography.

The First Technical Meeting of the Section for 1957 was held on February 1, jointly with the Indian Institute of Metals, Bangalore Chapter, at the Indian Institute of Science, Bangalore. Mr. C. V. Sundaram, Dept. of Atomic Energy, Govt. of India, talked on "The Metallurgy of Zirconium." The speaker discussed

the history and the early attempts to prepare ductile zirconium prior to the Kroll process. He then proceeded to describe the importance of zirconium metal in the field of atomic energy. He indicated the uses of the metal and its alloys such as zircalloy. He referred to the need for obtaining hafnium-free reactor-grade zirconium.

T. L. Rama, *Chairman*

Ontario-Quebec Section

The second meeting of the 1956-57 season was held on February 15 at McGill University in Montreal. The speakers for the occasion were Mr. Milton Eaton, Chief Electrical Engineer of Shawinigan Chemicals Ltd., Shawinigan Falls, Quebec, and Mr. C. R. Whittemore, Chief Metallurgist of Deloro Smelting and Refining Co. Ltd., Deloro, Ontario.

Mr. Eaton's paper, "New Electrical Equipment for Electric Furnaces," discussed recent innovations developed primarily for use in connection with calcium carbide furnaces but also applicable to other types of electric furnaces.

H. A. Timm, *Secretary-Treasurer*

Philadelphia Section

The March 6, 1957 meeting of the Philadelphia Section was begun with a social hour and dinner at the Lenape Club. A brief business meeting followed. For the technical feature of the evening Dr. G. E. Evans of National Carbon Co. Research Labs. presented a talk on "Recent Developments in Battery Research." Numerous examples of new battery applications were described to illustrate the increasing demand for special purpose batteries. Several case histories were cited to show how new uses for primary batteries can influence the direction of research and development work.

H. C. Mandell, Jr.

San Francisco Section

A regular Section meeting was held on March 27, 1957 at the University of California Faculty Club. The evening's speaker was Dr. Aaron Wachter, Manager of the Materials Engineering and Corrosion Dept., Shell Development Co., Emeryville, Calif., whose topic was "Electrochemical Aspects of Stress Corrosion Cracking of Metals."

Stress corrosion cracking does not occur in pure metals, but almost any alloy can be subject to stress corrosion provided that it is exposed to the right kind of medium. Dr. Wachter believes that stress corrosion cracking cannot be explained by one simple mechanism, and that it may result from a combination and alternation of electrochemical corrosion and mechanical failures.

Morris Feinleib

Back Volumes Available

Bound Volumes **12** (1907) through **102** (1955) complete, together with the 5 volumes of Indexes from 1902 through 1951, are available. Anyone interested in obtaining back volumes should contact Dr. Oliver W. Storey, 2 Santa Cruz Blvd., Santa Barbara, Calif.

New Members

In April 1956 the following were approved for membership in The Electrochemical Society by the Admissions Committee:

Active Members

Archie Broodo, Research Div., Texas Instruments, Inc., 6000 Lemmon Ave., Dallas 9, Texas (Electronics)

Nelson B. Colton, Electro Metallurgical Co., Niagara Falls, N. Y. (Electrothermics & Metallurgy)

Leland H. Grenell, Frigidaire Div. of General Motors Corp., Dayton, Ohio (Corrosion, Electrodeposition)

Rolf Haberecht, P. R. Mallory & Co., Inc.; Mail add: 6143 Oak Ave., Indianapolis, Ind. (Electronics, Theoretical Electrochemistry)

William James Happel, Westinghouse Electric Corp.; Mail add: 329 Canterbury Drive, Pittsburgh 15, Pa. (Electronics)

Stanley A. Harper, Radio Corp. of America; Mail add: Geneva Drive, East Petersburg, Pa. (Electronics)

Paul George Herold, Radio Corp. of America, New Holland Pike, Lancaster, Pa. (Electronics)

Gilbert G. Kamm, American Can Co.; Mail add: 540 Prairie Ave., Barrington, Ill. (Corrosion)

New Address

for

The Electrochemical Society, Inc.

1860 Broadway New York 23, N. Y.

The Electrochemical Society has moved its offices to new quarters, located on the northeast corner of 61st Street and Broadway. After June 1st, all communications to the Society and the JOURNAL should be addressed to the new address, 1860 Broadway.

Aladar Kelen, Trimont Corp. Ltd.; Mail add: 5842 Plantagenet Place, Montreal, P. Q., Canada (Electrothermics & Metallurgy)

Charles Luner, Applied Research Lab., United States Steel Corp., Monroeville, Pa. (Corrosion, Theoretical Electrochemistry)

Paul J. Melore, Columbian Carbon Co.; Mail add: 1975 West 8th St., Brooklyn 23, N. Y. (Battery)

Samuel M. Polcari, Sylvania Electric Products Inc.; Mail add: 90 Chester Rd., Belmont 78, Mass. (Electronics)

Donald Morgan Smyth, Sprague Electric Co., North Adams, Mass. (Theoretical Electrochemistry)

Rubin Nathan Summergrad, Radio Corp. of America; Mail add: 1042 Homeland Drive, Lancaster, Pa. (Electronics)

Francis C. Todd, Physics Dept., Southwest Research Institute, 8500 Culebra Rd., San Antonio 6, Texas (Electrothermics & Metallurgy)

Klaus J. Vetter, Fritz-Haber-Institut der Max-Planck-Gesellschaft, Berlin-Dahlem, Faradayweg 4-6, Germany (Corrosion, Electronics, Electro-Organic, Theoretical Electrochemistry)

Louis Wilson, Naval Ordnance Lab.; Mail add: 10804 E. Nolcrest Drive, Silver Spring, Md. (Industrial Electrolytic)

Stanley Thaddeus Wlodek, Metals Research Labs., Electro Metallurgical Corp., P. O. Box 580, Niagara Falls, N. Y. (Corrosion, Electrothermics & Metallurgy, Theoretical Electrochemistry)

Herman A. Young, Tel-O-Tube Corp. of America, East Paterson, N. J. (Electronics, Electrothermics & Metallurgy)

Associate Member

William E. Watts, Reynolds Metals Co., P. O. Box 191, Sheffield, Ala. (Industrial Electrolytic)

Reinstatements to Active Membership

Maurice Friedman, General Instrument Corp.; Mail add: 77-11 35th Ave., Jackson Heights 72, N. Y. (Battery, Electronics)

Morton S. Kircher, Hooker Electrochemical Co.; Mail add: 953 Rankine Rd., Niagara Falls, N. Y. (Industrial Electrolytic)

Edmund Clarence Potter, Central Electricity Authority; Mail add: 31 Burnaby Gardens, Chiswick, London W. 4, England (Corrosion, Theoretical Electrochemistry)

Franklin Secord Wartman, Titanium Metals Corp. of America; Mail add: Box 446, Boulder City, Nev. (Electrothermics & Metallurgy)

(Continued on page 129C)

ECS Membership Statistics

The following three tables give breakdown of membership as of April 1, 1957. The Secretary's Office feels that a regular accounting of membership will be very stimulating to membership committee activities. In Table I it should be noted that the totals appearing in the right-hand column are *not* the sums of the figures in that line since members belong to more than one Division and, also, because Sustaining Members are not assigned to Divisions. But the totals listed are the total membership in each Section. In Table I, Sustaining Members have been credited to the various Sections.

Table I. *ECS Membership by Sections and Divisions*

Section	Division: Battery	Corrosion	Electric Insulation	Electro-deposition	Electronics	Electro-Organic	Electrothermics & Met.	Industrial Electrolytic	Theoretical Electrochem.	No Division	Total as of 4/1/57	Total as of 1/1/57
Chicago	13	38	2	44	19	7	12	14	22	13	113	114
Cleveland	55	37	3	47	39	12	22	31	42	15	195	190
Detroit	8	19	5	44	5	8	4	5	21	20	80	85
India	6	3	1	13	3	5	3	11	6	3	27	27
Midland	5	15	0	5	2	2	7	16	9	3	41	41
New York	73	102	21	134	95	32	64	60	91	45	447	460
Niagara Falls	11	21	0	20	3	5	68	58	22	22	156	157
Pacific Northwest	5	16	0	11	1	1	5	11	7	10	47	51
Philadelphia	22	30	3	35	47	14	19	15	44	29	155	156
Pittsburgh	3	42	3	28	20	6	32	16	32	10	117	108
San Francisco	4	13	2	17	12	3	13	22	20	5	60	55
Washington-Baltimore	32	41	7	38	19	3	10	10	28	7	117	115
Ontario-Quebec	8	21	0	14	1	2	29	20	6	15	64	71
U. S. Non-Section	64	120	27	117	70	46	77	80	129	51	486	518
Boston	12	29	4	31	35	8	16	10	22	8	117	119
Southern Calif.-Nevada	15	18	1	21	15	3	9	15	13	9	71	63
Foreign Non-Section	41	53	7	61	25	26	36	60	64	56	212	204
Total as of April 1, 1957	377	618	86	680	411	183	426	454	578	321	2505	
Total as of Jan. 1, 1957	362	600	87	653	395	182	392	425	553	322		2534

Table II. *ECS Membership by Grade*

	Total as of 4/1/57	Total as of 1/1/57	Net Change
Active	2142		
Delinquent	146		
Active Representative Patron Members	8		
Active Representative Sustaining Members	60		
Total Active Members	2356	2240	+116
Life	15	15	0
Emeritus	44	41	+3
Associate	28	38	−10
Student	57	61	−4
Honorary	5	5	0
	2505	2400	+105

The figures pertaining to Patron and Sustaining Member Representatives have been added to reflect reclassifications and changes in membership status.

Table III. *ECS Patron and Sustaining Membership*

	Total as of 4/1/57	Total as of 1/1/57	Net Change
Patron Member Companies	4	3	+1
Sustaining Member Companies	119	120	−1

Transfer from Student to Active Membership

Harold O. Strange, Gulf Research & Development Co.; Mail add: 1805 Penn Ave., Apt. 10, Pittsburgh 21, Pa. (Electro-Organic)

Transfer from Associate to Active Membership

Alan L. McClelland, E. I. du Pont de Nemours & Co., Inc.; Mail add: 2219 W. 17th St., Wilmington, Del. (Electrothermics & Metallurgy, Theoretical Electrochemistry)

By action of the Board of Directors of the Society, all prospective members must include first year's dues with their applications for membership.

Also, please note that, if sponsors sign the application form itself, processing can be expedited considerably.

Personals

F. A. Lowenheim has been appointed Technical Advisor to Dr. C. K. Banks, Vice-President of Research and Development at Metal & Thermit Corp., Rahway, N. J. Dr. Lowenheim has been with Metal & Thermit since 1936 as a research chemist and research supervisor. He is the author of a number of papers and handbook chapters on electroplating.

F. A. Lowenheim

Demetrius Triadis, formerly associated with the International Nickel Co., Bayonne, N. J., is now with Hydrocarbon Research, Inc., New York, N. Y.

K. S. G. Doss has taken charge of the Central Electrochemical Research Institute, Karaikudi, India, on the retirement of Dr. B. B. Dey. Dr. Doss, formerly Professor of Sugar Chemistry at the Indian Institute of Sugar Technology, Kanpur, is a well-known physical chemist whose research work has included colloids, surface chemistry, and electrochemistry.

S. Sathyanarayana has left the Indian Institute of Science, Bangalore, to join the Central Electrochemical Research Institute, Karaikudi.

M. S. Thacker participated in the ninth UNESCO conference held at New Delhi, India, in November, 1956, as a member of the Indian Delegation. He has been nominated as a member of the University Grants Commission, India, and the Defense Research and Development Committee, Ministry of Defense.

L. J. Balasundaram has returned to India from the United Kingdom and is now with the Dept. of Metallurgy, Indian Institute of Science. He has been awarded the degree of Master of Metallurgy by the University of Sheffield.

K. Seshadri has left the National Chemical Lab., Poona, India, and joined the Central Salt Research Institute, Bhavnagar, as Junior Scientific Officer.

J. Balachandra has been nominated an alternate member of the Precious Metals Section Committee of the Indian Standards Institution.

A. N. Kappanna has joined the Central Electrochemical Research Institute, Karaikudi, as Assistant Director.

J. Vaid has been appointed Assistant Engineer, Plating Section, Indian Telephone Industries, Bangalore.

Pioneer Scientist Honored

Dr. Gorton R. Fonda (*left*), of the General Electric Co., was presented with a commemorative certificate recently by Richard S. Mackie, manager of engineering for GE's Chemical Products Works, Lamp Div. Dr. Fonda, internationally known authority on incandescent lamps and luminescence, completed 40 years of service with the G.E. Research Lab. in 1950. Since that time he has been a consultant to the company's Lamp Div.

News Items

International Symposium on Passivity

The Electrochemical Society, the Bunsen Gesellschaft, and the Faraday Society are jointly sponsoring discussions on the subject of passivity in metals to be held near Darmstadt, Germany, during the week of September 2-7, 1957. This is probably the first international symposium on this subject since a similar meeting was arranged by the Faraday Society in 1914.

The program calls for invited and submitted papers from representatives of many countries including the United States, Canada, Germany, England, Switzerland, Italy, France, Japan, and Russia. Papers and discussion will appear in a special issue of the *Z. Elektrochem.*

Members of the committee arranging the Symposium are Professor K. F. Bonhoeffer, representing the Bunsen Gesellschaft, Dr. T. P. Hoar, representing the Faraday Society, and Professor H. H. Uhlig, repre-

WILEY BOOKS

bring you up to date

1. AN INTRODUCTION TO SEMICONDUCTORS

By W. CRAWFORD DUNLAP, JR., Bendix Aviation Corp.

A comprehensive survey of *all* the important aspects of semiconductors, from research to devices. Covers basic concepts, properties of materials, methods of measurement, and applications. Written in easy-to-understand, non-technical language, this new book presents the most recent developments in semiconductors. A thoroughly practical and informative work. 1957.

417 pages. 268 illus. $11.75.

2. THE CHEMISTRY OF ORGANO-METALLIC COMPOUNDS

By EUGENE G. ROCHOW, Harvard University; DALLAS T. HURD, General Electric Company; and RICHARD N. LEWIS, Olin Mathieson Chemical Corp.

A fresh, readable discussion of the theoretical, factual, and practical aspects of organometallic compounds: their structure and physical properties, preparation, chemical reactions, and application. The subject is not covered in any recent book, despite current interest in this important branch of chemistry. 1957.

344 pages. Illus. $8.50.

3. PROGRESS IN SEMICONDUCTORS Volume I

Edited by ALAN F. GIBSON, Radar Research Establishment, Malvern, U.K.; P. AIGRAIN, Université de Paris; and R. E. BURGESS, University of British Colombia.

The very latest information on semiconductors brought to you by eight specialists in the field, in the first volume of an important new series. 1956.

220 pages. Illus. $8.00.

4. ORGANO-METALLIC COMPOUNDS

By G. E. COATES, One of the Methuen Monographs. 1956. 197 pages. $2.50

Send for ON-APPROVAL copies of these useful books TODAY!

JOHN WILEY & SONS, Inc. JES-67
440 Fourth Avenue, New York 16, N. Y.

Please send me the book(s) checked below to read and examine ON APPROVAL. Within 10 days I will return the book(s) and owe nothing, or I will remit the full purchase price, plus postage.

1 2 3 4

Name .....

Address .....

City ..... Zone ..... State .....

( ) SAVE POSTAGE! Check here if you ENCLOSE payment, in which case we will pay the postage. Same return privilege, of course.

sented The Electrochemical Society. Accommodations at the meeting are limited, but it is hoped that a few places can be kept open for active research workers in the field of passivity who feel that they would benefit by attending the discussions.

Inquiries in the United States should be addressed to Professor H. H. Uhlig, 8-202 Massachusetts Institute of Technology, Cambridge 39, Mass.

Paper on Oxide Films Wins NACE Young Author Award

"Oxide Films on Stainless Steels," a paper by Thor N. Rhodin, Du Pont research engineer, in the March 1956 issue of *Corrosion* was judged to be the best published during the year by an author under 35 years of age. The award, which consists of a certificate and an honorarium, was presented at the annual banquet of the National Association of Corrosion Engineers in St. Louis in March.

TISCO Ferromanganese Plant

The Tata Iron & Steel Co., Jamshedpur, India, has undertaken a RS. 2-crore project for the production of ferromanganese. The plant, to be located in Orissa, will consist of two electric rotating furnaces of the latest design (Norwegian supply) with an initial capacity of 30,000 tons of standard grade alloy. It is designed and laid out for future expansion up to 100,000 tons per year.

Arthur T. Hinckley Retires from Hooker

Arthur T. Hinckley, Niagara Falls, N. Y., was honored recently at a luncheon at the Niagara Falls Country Club attended by officers, directors, and other company friends of Hooker Electrochemical Co. The occasion was Mr. Hinckley's retirement March 31 as manager of development of Oldbury Products, now consolidated with Hooker Electrochemical Co., which position he has held since 1939. Mr. Klaussen, president, stated that Mr. Hinckley would be retained by Hooker as consultant.

A native of Boston, Mr. Hinckley has lived in Niagara Falls since 1909 when he was graduated from Massachusetts Institute of Technology with degrees of bachelor and master of science. He has been an electrochemist at National Carbon Co., manager of the primary battery division of U.S.L. Battery Corp., and

(Continued on page 131C)

Letter to the Editor

Voltage Dependence of Electroluminescence

Dear Sir:

Recently Lehmann[1] in discussing the voltage dependence of electroluminescence stated that a brightness law[2-5] proportional to $\exp - b/V^{1/2}$ gives a remarkably good fit with his experiments. In replotting Lehmann's experimental results[1] (his Fig. 1) we found the fit even more remarkable than he suggested in his Fig. 5 (over 8 decades instead of 4 decades, in agreement with our own measurements[4,5]). Admittedly, at the highest brightness levels one is so near to breakdown of the dielectric that some deviations may occur. The theoretical derivation of the $\exp - b/V^{1/2}$ law takes account of the inhomogeneities in the fieldstrength due to space charge. In a discussion of other factors that may influence the voltage dependence[4,5] we have shown that generally they do not alter the $\exp - b/V^{1/2}$ law significantly.

G. Diemer
H. A. Klasens
P. Zalm
Philips Research Labs.
Eindhoven, Netherlands

[1] W. Lehmann, *This Journal*, **103**, 667 (1956).

[2] G. F. Alfrey, *Brit. J. Appl. Phys., Suppl.* 4, p. 44 (1955).

[3] J. B. Taylor, *ibid.* p. 45 (1955).

[4] P. Zalm, G. Diemer and H. A. Klasens, *Philips Research Repts.* **10**, 205 (1955).

[5] P. Zalm, *ibid.*, **11**, 353, 417 (1956).

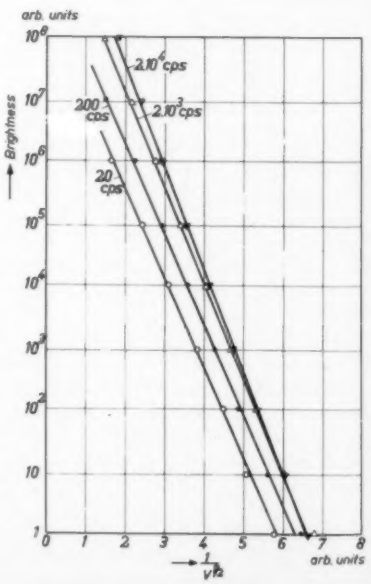

Lehmann's experimental data replotted

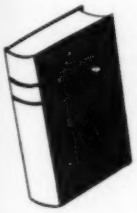

READY NOW

SEMICONDUCTOR ABSTRACTS

Volume III — 1955 Issue

Abstracts of the Literature on Semiconducting and Luminescent Materials and Their Applications.

Edited by E. Paskell, Battelle Memorial Institute

1258 abstracted articles — in hard cover binding

Here's your handy guide to all the important literature that appeared throughout the world in 1955. This is the biggest *Abstracts* book yet—and it comes now in hard cover to take the heavy reference use of men in the electronic components fields—covers all phases of semiconductor activity.

This year's volume reflects the growing use of semiconductor and luminescent materials in new products like transistors, rectifiers, colored television screens. It shows you what's being written as a result of the developing interest in new electronic functional materials throughout the whole electronic industry. New work is covered on the purification of silicon and development of material processing techniques to give practical silicon devices. The wider use of intermetallic compounds as supplemental or substitute materials for germanium and silicon is also covered.

Materials are the keynote of the *Abstracts*' organization. (See Contents). Articles are carefully cross referenced. There's both a subject index and an author index to help you locate information in seconds.

1955 Issue: Just out. 322 pages. 8⅝ x 11¼. $10.00

Headings: Germanium. Silicon. Carbon, selenium, and other elemental semiconductors. Intermetallics. Sulfides, selenides, and Tellurides. Oxides. Halides. Arsenates, phosphates, and tungstates. Organics. Theory.

Do you have the earlier two volumes in The Electrochemical Society Abstracts Series?

1954 Issue: 1955. 200 pages. $5.00
1953 Issue: 1955. 169 pages. $5.00

Order all three now. Mail Coupon below.

JOHN WILEY & SONS, Inc. JS-67
440 Fourth Ave., New York 16, N. Y.

Please send me the following volumes of SEMICONDUCTOR ABSTRACTS to read and examine. Within 10 days I will return the book(s) and owe nothing, or I will remit the full purchase price(s) plus postage.

☐ **1955 Issue, Volume III, $10.00**
☐ **1954 Issue, Volume II, $ 5.00**
☐ **1953 Issue, Volume I, $ 5.00**

Name .....

Address .....

City ..... Zone ..... State .....

☐ SAVE POSTAGE! Check here if you ENCLOSE payment in which case we pay the postage: Same return privilege, of course.

consultant for the Bureau of Mines in connection with a survey of mineral deposits in the southern and western states. Mr. Hinckley is a member of the American Chemical Society, American Ceramic Society and a member and Past President of The Electrochemical Society.

N.S.F. Science Awards

The National Science Foundation has announced the award of 100 Science Faculty Fellowships for the academic year 1957-58. Awarded this year for the first time, the fellowships are offered as an opportunity for college and university science teachers to enhance their effectiveness.

The Foundation has also announced the award of 30 Senior Postdoctoral Fellowships in the sciences for the academic year 1957-58. Science Faculty and Senior Postdoctoral Fellowships carry stipends adjusted to approximate the regular salaries of award recipients. These stipends may be applied toward study or research in an accredited nonprofit institution of higher learning in the United States and abroad.

N.S.F. Invites Proposals for Science Institutes

The National Science Foundation is accepting proposals for support of summer institutes in 1958 and academic-year institutes during 1958-59. The institute program of the Foundation is designed to help teachers of science and mathematics improve their subject matter knowledge and their teaching capabilities. The current Foundation program will support a total of 96 summer institutes this year, and 16 academic-year (1957-58) institutes in colleges and universities throughout the nation.

Academic-year institutes will offer full-time work during the regular school year 1958-59 in the subject matter of the sciences and mathematics, designed especially for the needs of secondary-school teachers in those fields. The Foundation will support attendance of secondary-school teachers as well as dependency, book, and travel allowances. Tuition and fees and support of other operating costs of the institute may also be requested in the proposals submitted. Summer institutes also offer work in the subject matter of the sciences and mathematics especially designed for teachers.

Directions for preparing proposals, and forms to be used in making application, may be obtained by interested institutions of higher education from the Div. of Scientific Personnel and Education, National Science Foundation, Washington 25, D. C. Deadlines are August 1, 1957, for submission of proposals for institutes to be held in the summer of 1958; September 1, 1957, for proposals for support of academic-year institutes during 1958-59.

Bell Labs Announces Winners of University Graduate Fellowships

Bell Telephone Labs., research and development organization of the Bell System, has announced the names of 20 recipients of its 1957-58 college fellowships. Established in 1955, the grants go to outstanding students pursuing graduate studies leading to Ph.D. degrees in engineering and physical sciences. Each fellowship carries a grant of $2000 to the fellow and an additional $2000 to cover tuition, fees, and other costs to the institution where he elects to study.

Announcements from Publishers

The Study of Properties of Single Crystals for Use as Detectors and Crystal Counters, S. J. Czyzak and others, University of Detroit, for Office of Naval Research, Oct. 1955. Report PB 121537,* 42 pages, $1.25.

Development of Ferroelectric Ceramics, J. D. Wallace and M. F. Pressler, U. S. Naval Air Development Center, Feb. 1953. Report PB 121418,* 59 pages, $1.50.

Electrodeposition of Titanium: Part 3, W. E. Reid, Jr., J. H. Connor, and A. Brenner, National Bureau of Standards, for Wright Air Development Center, Sept. 1956. Report PB 121721,* 18 pages, 50 cents.

Development of Subminiature High Temperature Capacitors, Balco Research Labs., for Wright Air Development Center, Mar. 1955. Report PB 111729,* 79 pages, $2.00.

Teflon, best known as the revolutionary dry lubricant and preservative for metals, met or exceeded all requirements for replacement of mica capacitors (specification MIL-C-5A) under temperatures from minus 60° to 200°C. The single exception was r-f current rating, which could not be applied to metal-cased units because of overheating.

A Sintered-Plate Nickel-Cadmium Cell, G. W. Work, Naval Research Lab., Oct. 1956. Report PB 121533,* 15 pages, 50 cents.

Annual Report 1956: National Bureau of Standards, National Bureau of Standards Miscellaneous Publication 220, 158 pages, 60 cents. (Order from Superintendent of Documents, U. S. Government Printing Office, Washington 25, D. C.)

This report summarizes the research and development activities of the National Bureau of Standards during the fiscal year 1956, such as maintenance of basic standards, determination of physical constants and properties of matter, development of methods and instruments of measurement, and the provision of calibration, testing, and scientific advisory services. During the past year a new high-speed computer which gives the geographic fallout pattern after a nuclear explosion was developed for the Atomic Energy Commission. A microimage date storage and retrieval device provides rapid access to any one of 10,000 microfilmed images located on a 10-inch-square sheet of film. The Bureau also developed a technique for capturing and storing large numbers of free radicals—highly reactive molecular fragments—at temperatures near absolute zero, and, in the field of optics and metrology, the Bureau completed a comprehensive dictionary of color names, which lists some 7500 individual color names and defines them in simple accurate terms easily understood by workers in different fields. A study of the effect of crystal orientation of fatigue crack initiation in metal was also completed.

A Review of the Air Force Materials Research and Development Program, H. E. Hines and R. F. Walden, Wright Air Development Center, U. S. Air Force, Oct. 1956. Report PB 111648-S2,* 94 pages, $2.50.

One hundred and forty-five reports of research conducted under the Air Force's materials research and development program from July 1, 1955 to June 30, 1956 are abstracted in this report. Included are abstracts of research in adhesives, metallurgy, analysis and measurement, biochemistry, textiles, petroleum products, plastics, packaging, protective treatments, and rubber. This publication is supplementary to three other volumes of the same title. One is Report PB 111648-S,* covering Air Force materials research from July 1, 1954 to June 30, 1955, $3.50; another is Report PB 111648,* covering July 1, 1953 to June 30, 1954, $2.75; the third is Report PB 111537,* covering the 10 years of research prior to July 1, 1953, $3.75.

* Order from Office of Technical Services, U. S. Dept. of Commerce, Washington 25, D. C.

"Plus-4" Anodes make better boot molds too!

A copper mold and one of the U. S. Rubber Co. Gaytees produced in it. Mold thicknesses vary from .035" to .090", depending on size and type of boot.

Each electroforming tank can plate 10 molds —uses standard acid-plating solution and 33 "Plus-4" Rolled Anodes, ½" x 8" x 20" —300 amps power input.

IN ELECTROFORMING—as in acid electroplating and electrotyping—ANACONDA "Plus-4" (Phosphorized Copper) Anodes are turning in superior performance records.

The Shoe Hardware Div. of U. S. Rubber Co. electroforms the copper molds used in the production of rubber and plastic rainwear known as Gaytees®. With ordinary anodes, they had been troubled with porosity and "treeing."

Nearly two years ago, they turned to "Plus-4" Anodes and report the following advantages: 1. Extremely smooth plating, without "treeing." 2. Good grain build-up. 3. No porosity. 4. Uniform anode corrosion with consequent scrap reduction. 5. Savings in solution correction due to reduction of sludge and copper build-up. 6. All-round cleaner plate.

You have everything to gain and nothing to lose by setting up one acid-copperplating tank to test "Plus-4" Anodes. Send in the coupon today. 5814

The American Brass Co., Waterbury 20, Conn.
In Canada: Anaconda American Brass Ltd., New Toronto, Ont.

Give me details on how I can get a test supply of "Plus-4" Anodes sufficient to fill one tank.

NAME.....
COMPANY.....
ADDRESS.....
CITY.....ZONE....STATE.....

"Plus-4" Anodes
(Phosphorized Copper)
A product of
ANACONDA
Made by The American Brass Company
For use under Pat. No. 2,689,216

Automation: Its Purpose and Future, by Magnus Pyke. Philosophical Library, New York, 1957. 191 pages, $10.00.

Foundations of Radio, 6th Edition, by M. G. Scroggie. Philosophical Library, New York, 1957. 349 pages, $10.00.

Ernest Rutherford—Atom Pioneer, by John Rowland. Philosophical Library, New York, 1957. 160 pages, $4.75.

The First One Hundred and Fifty Years, a history of John Wiley and Sons, Inc., 241 pages, $7.50.

Lists many famous titles in Science and Engineering, published by Wiley through the years.

Contributions to Titanium Metallurgy, a 44-page multigraph pamphlet, by R. S. Dean and staff, Chicago Development Corp., Riverdale, Md., Feb. 1957.

Three papers of electrodeposition of titanium, with photographs of crystals obtained. Available without charge to those interested.

Book Reviews

Organic Synthesis by Vartkes Migrdichian. Reinhold Publishing Corp., New York, 1957. Two volumes, 38 + 1822 pages, $35.00.

The author has written this text with the primary objective of meeting the requirements of the serious organic chemical research worker. It is an excellent, comprehensive survey of the syntheses and reactions of organic compounds. Several thousand literature references are given.

Volume I deals with open-chain saturated compounds, and is of particular interest to those working in the field of organometallics, organonon metals, and metalloids. For example, the properties, reactions, and syntheses of uncommon organic compounds containing gold, silver, and berylium are described and pertinent references given.

Volume II deals with open-chain unsaturated compounds, alicyclics, and aromatics. The chapter on quinones and their preparations is an excellent source of information to those interested in antioxidants and "redox" indicators.

One is impressed, in this comprehensive survey, by the almost complete lack of reference to electrochemical synthesis.

Albert Meyers

Progress in Semiconductors I, A. F. Gibson, P. Aigrain, and R. E. Burgess, Editors. John Wiley & Sons, Inc., New York, 1956. vii + 220 pages, $8.00.

This volume, the first in what is promised to be an annual series, undertakes to offer "critical reviews of the present state of knowledge," together with a certain amount of original work. Unfortunately, the word "present" is a little inappropriate, since it is clear that most of the articles were written somewhere about the middle of 1955. The editors have had to cope with the usual chronic problem—delay in publication—which anyone encounters who tries to produce a book serving some useful purpose in a rapidly changing field. Even allowing for this, however, the choice of topics has a curiously antique flavor. Reading the book, one receives little intimation that anything particularly revolutionary was happening in the years 1954 and 1955. But what years they were! Cyclotron resonance . . . electron spin resonance on donors in

Opening for ELECTROCHEMIST

Interested In Development Work in aqueous and fused salt electrolysis, including all aspects of cell operation

A program is being established in a new laboratory devoted to these fields of investigation, and contacts will be had with Management, Research, Sales, Production, and Customer organizations.

The man we want should be well grounded in theoretical and applied electrochemistry and preferably should have had one or more years experience in the electrolysis of alkali halides and metal compounds. Emphasis will be placed on the commercial application of the work.

This is a challenging opportunity to establish yourself with a Development program in electrolysis where the future is practically unlimited.

Please submit full details of qualifications to:

NATIONAL CARBON COMPANY

Division of Union Carbide Corporation • Development Laboratory
3625 Highland Avenue, Niagara Falls, New York—Attention: Dr. N. J. Johnson

RESEARCH AND DEVELOPMENT

Research program requires experienced electrochemists to work in electrolytic process development. Excellent laboratory facilities located twenty miles East of Los Angeles.

GROUP LEADER

Electrochemical engineer, three to four years experience desired. The man we are seeking need not be acting in this capacity at the present time, but desires more responsibility based on successful performance in electrochemical research and process development.

ELECTROCHEMIST

Position open in electrochemical process development. Degree in chemistry or chemical engineering with two to three years experience required. Salary commensurate with experience.

Send resume to: Personnel Manager

American Potash & Chemical Corporation

3030 W. 6th St., Los Angeles 54, Calif.

silicon . . . the infra-red excitation of impurity levels . . . the theory of band structure in germanium and silicon . . . avalanche breakdown . . . the first quantitative work on surface properties . . . diffusion of impurities. Accounts of all of these appeared in print during these two years, most of them in time to be considered for inclusion in this volume. Yet none of them receives more than passing mention.

Turning to the articles themselves, this reviewer finds a rather wide spread of merit. There is an excellent review article by Hannay, which covers in a thorough manner the physics, chemistry, and metallurgy of silicon as they were about two years ago, together with a useful summary of the device art as it then was. The article on the photo-magneto-electric effect, by Garreta and Grosvalet, is a competent and readable account of one of the less rapidly moving sidelines of semiconductor physics, written, unfortunately, too soon to include a discussion of the comprehensive theory of van Roosbroeck. The articles by Garlick on the electrical properties of phosphors, and by Evans on the design of transistors to operate at high frequencies, are interesting, although in both cases the field has since advanced so rapidly that the treatment given is rather out of date. There are also articles by Johnson on the Seebeck effect, by Hogarth on "the germanium filament," and by Godefroy on the field effect experiment.

Perhaps it is not inappropriate to suggest that the editors must make up their minds as to what it is that they are trying to do. Do they aim to present reasonably up-to-date snapshots of the changing scene? Then they should start a new journal, with a publication lag of not more than four to six months. Or do they wish to offer something more scholarly and comprehensive, possibly along the lines of the articles in the old "Handbuch der Physik"? As it stands, this book seems to fall awkwardly between three stools—the classic English research monograph, the encyclopaedic German tome, and the current American fashion of publishing, in book form, a series of original papers in some fairly narrow field, as first presented at a special conference arranged for the purpose.

C. G. B. Garrett

Meetings of Other Organizations

June 9-12—American Institute of Chemical Engineers, Regional Meeting, Olympic Hotel, Seattle, Wash.

June 17-21—American Society for Engineering Education, Annual Meeting, Cornell University, Ithaca, N. Y.

June 20-22—American Physical Society, Regional Meeting, Notre Dame, Ind.

Sept. 8-13—American Chemical Society, National Meeting, New York, N. Y.

Sept. 15-18—American Institute of Chemical Engineers, Regional Meeting, Lord Baltimore Hotel, Baltimore, Md.

Employment Situations

Please address replies to box shown, c/o The Electrochemical Society, Inc., 1860 Broadway, New York 23, N. Y.

Positions Wanted

Chemist, 15 years' creative and responsible work in metal finishing, corrosion, with experience in the continuous anodizing and dyeing of aluminum, seeks position in or near Metropolitan New York. *Reply to Box 361.*

Storage Battery Chemist is interested in a responsible position in research and development. Has a long and successful record in lead-acid battery field, and a good understanding of problems facing the industry, coupled with imagination and a scientific approach to practical problems. Publications and patents. *Reply to Box 362.*

CORROSION RESEARCH

For long range and fundamental research work in container corrosion problems, encompassing practically all types of corrosion principles and investigational techniques. Good understanding of electrochemical fundamentals required. Applicant must have Ph.D. degree or equivalent ability.

Excellent working conditions in well-equipped laboratory with high-caliber associates. Company has liberal benefit plans and will pay salary commensurate with abilities. Write to:

Director, Electrochemical Metallurgy Laboratory
Central Research and Engineering Division

Continental Can Company, Inc.

7622 South Racine Avenue
Chicago 20, Illinois

Advertisers' Index
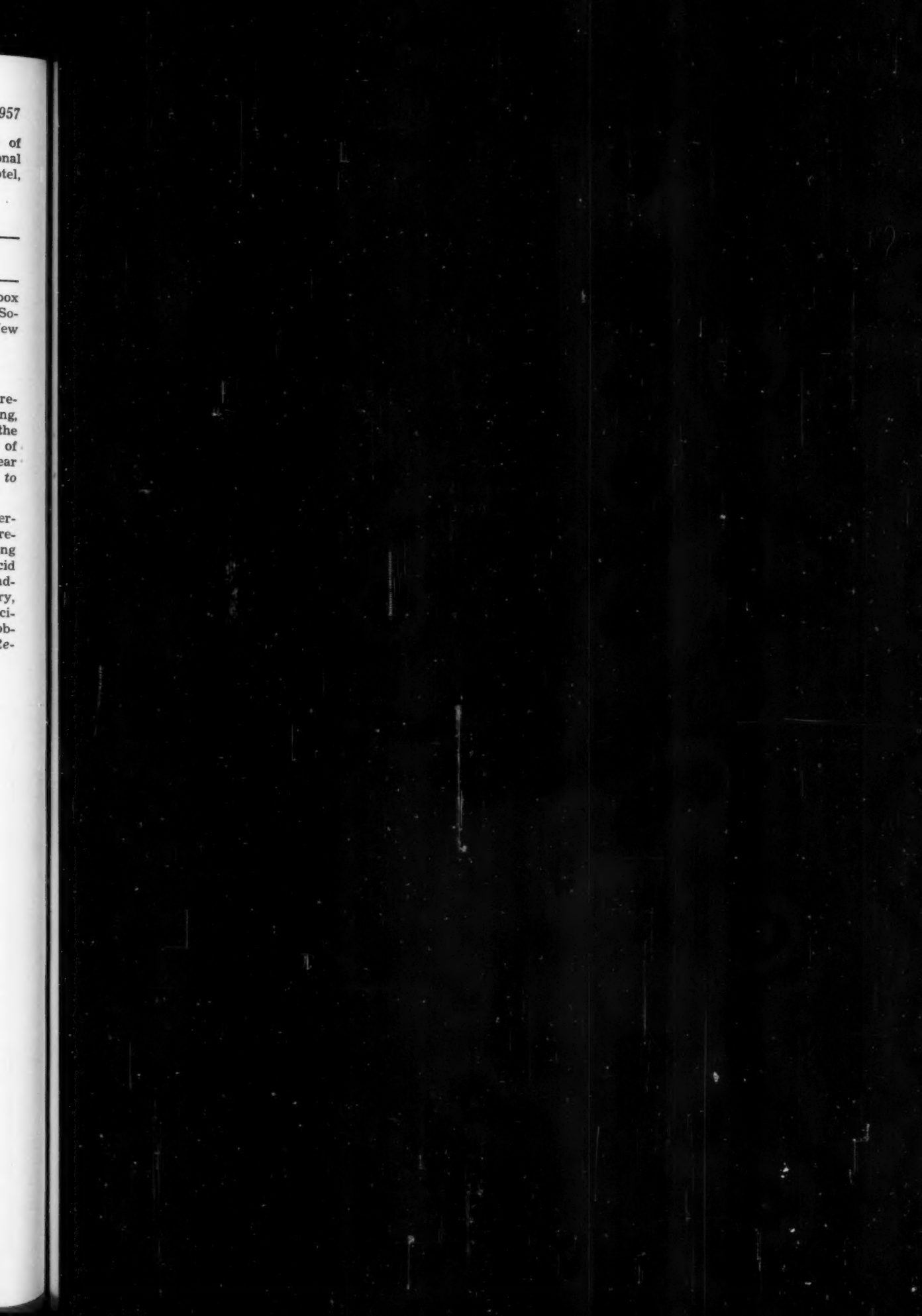
American Brass Company 132C
American Potash & Chemical Corporation 133C
Continental Can Company, Inc. 134C
Dow Chemical Company 124C
Enthone, Incorporated ..... Cover 4
Great Lakes Carbon Corporation ..... Cover 2
National Carbon Company 133C
John Wiley & Sons, Inc. 130C, 131C